

1988

# The crystal and molecular structures of rosebengal derivatives and organometallic compounds containing mercury, rhodium, silver and silicon

Musiri N. Janakiraman  
*Iowa State University*

Follow this and additional works at: <https://lib.dr.iastate.edu/rtd>

 Part of the [Physical Chemistry Commons](#)

## Recommended Citation

Janakiraman, Musiri N., "The crystal and molecular structures of rosebengal derivatives and organometallic compounds containing mercury, rhodium, silver and silicon " (1988). *Retrospective Theses and Dissertations*. 9355.  
<https://lib.dr.iastate.edu/rtd/9355>

This Dissertation is brought to you for free and open access by the Iowa State University Capstones, Theses and Dissertations at Iowa State University Digital Repository. It has been accepted for inclusion in Retrospective Theses and Dissertations by an authorized administrator of Iowa State University Digital Repository. For more information, please contact [digirep@iastate.edu](mailto:digirep@iastate.edu).

## **INFORMATION TO USERS**

The most advanced technology has been used to photograph and reproduce this manuscript from the microfilm master. UMI films the original text directly from the copy submitted. Thus, some dissertation copies are in typewriter face, while others may be from a computer printer.

In the unlikely event that the author did not send UMI a complete manuscript and there are missing pages, these will be noted. Also, if unauthorized copyrighted material had to be removed, a note will indicate the deletion.

Oversize materials (e.g., maps, drawings, charts) are reproduced by sectioning the original, beginning at the upper left-hand corner and continuing from left to right in equal sections with small overlaps. Each oversize page is available as one exposure on a standard 35 mm slide or as a 17" × 23" black and white photographic print for an additional charge.

Photographs included in the original manuscript have been reproduced xerographically in this copy. 35 mm slides or 6" × 9" black and white photographic prints are available for any photographs or illustrations appearing in this copy for an additional charge. Contact UMI directly to order.



300 North Zeeb Road, Ann Arbor, MI 48106-1346 USA



Order Number 8825405

**The crystal and molecular structures of rosebengal derivatives  
and organometallic compounds containing mercury, rhodium,  
silver and silicon**

Janakiraman, Musiri N., Ph.D.

Iowa State University, 1988

**U·M·I**  
300 N. Zeeb Rd.  
Ann Arbor, MI 48106



**PLEASE NOTE:**

In all cases this material has been filmed in the best possible way from the available copy. Problems encountered with this document have been identified here with a check mark .

1. Glossy photographs or pages \_\_\_\_\_
2. Colored illustrations, paper or print \_\_\_\_\_
3. Photographs with dark background \_\_\_\_\_
4. illustrations are poor copy \_\_\_\_\_
5. Pages with black marks, not original copy \_\_\_\_\_
6. Print shows through as there is text on both sides of page \_\_\_\_\_
7. Indistinct, broken or small print on several pages
8. Print exceeds margin requirements \_\_\_\_\_
9. Tightly bound copy with print lost in spine \_\_\_\_\_
10. Computer printout pages with indistinct print \_\_\_\_\_
11. Page(s) \_\_\_\_\_ lacking when material received, and not available from school or author.
12. Page(s) \_\_\_\_\_ seem to be missing in numbering only as text follows.
13. Two pages numbered \_\_\_\_\_. Text follows.
14. Curling and wrinkled pages \_\_\_\_\_
15. Dissertation contains pages with print at a slant, filmed as received \_\_\_\_\_
16. Other \_\_\_\_\_

---

---

---

**U·M·I**



The crystal and molecular structures of  
rosebengal derivatives and organometallic compounds  
containing mercury, rhodium, silver and silicon

by

Musiri N. Janakiraman

A Dissertation Submitted to the  
Graduate Faculty in Partial Fulfillment of the  
Requirements for the Degree of  
DOCTOR OF PHILOSOPHY

Department: Chemistry

Major: Physical Chemistry

**Approved:**

Signature was redacted for privacy.

In Charge of Major Work

Signature was redacted for privacy.

For the Major Department

Signature was redacted for privacy.

For the Graduate College

Iowa State University  
Ames, Iowa

1988



## TABLE OF CONTENTS

	Page
GENERAL INTRODUCTION	1
Explanation of Dissertation Format	2
CRYSTAL AND MOLECULAR STRUCTURES OF ROSEBENGAL DERIVATIVES	3
Introduction	3
Experimental	5
Data collection	6
Reduction of x-ray intensity data	6
Structure Determination and Refinement	10
Discussion of the Structures	12
Structure of $C_{20}H_4Cl_4I_4O_5 \cdot 1\frac{1}{2}C_4H_8O_2$ (1)	12
Structure of $C_{34}H_{16}Cl_4I_4O_5$ (2)	27
Structure of $C_{32}H_{34}Cl_4I_4N_2O_5$ (3)	41
Conclusion	62
CRYSTAL STRUCTURE OF [N-(E-3-CHLOROMERCURIOBUT-2-ENYL)- N,N-DIMETHYLAMMONIUM]TRICHLOROMERCURATE(II) (4)	63
Introduction	63
Experimental	64
Data collection	64
Reduction of x-ray intensity data	65
Structure Determination and Refinement	67
Discussion of the Structure	70
Conclusion	86

	Page
CRYSTAL STRUCTURE OF BIS(TRIPHENYLPHOSPHINE)CHLORO( $\eta^2$ -1,2,3-CYCLONONATRIENE)RHODIUM(I) (5)	88
Introduction	88
Experimental	90
Data collection	90
Reduction of x-ray intensity data	90
Structure Determination and Refinement	92
Discussion of the Structure	93
Conclusion	110
CRYSTAL STRUCTURE OF TRI( $\mu$ -CARBONYL- $\mu$ -THIOCARBONYLBIS [CARBONYL- $\eta^5$ -CYCLOPENTADIENYL IRON(II)])SILVER(I) TETRAFLUOROBORATE (6)	112
Introduction	112
Experimental	113
Data collection	113
Reduction of x-ray intensity data	115
Structure Determination and Refinement	115
Discussion of the Structure	117
Conclusion	135
CRYSTAL STRUCTURE OF 1-ETHOXYSILATRANE (7)	136
Introduction	136
Experimental	137
Data collection	137
Reduction of x-ray intensity data	139
Structure Determination and Refinement	139

Discussion of the Structure	Page 140
Conclusion	153
APPENDIX: LOW TEMPERATURE APPARATUS FOR SINGLE CRYSTAL DATA COLLECTION	154
REFERENCES	159
ACKNOWLEDGEMENTS	165

## GENERAL INTRODUCTION

This dissertation reports the single crystal X-ray structure determinations of seven compounds. These were performed to unequivocally unravel molecular structures and to provide other information at the molecular level which would help explain their properties.

Rose bengal, like any other xanthene dye, can exist in at least three different structural forms. These are the lactone form, the zwitterionic form and the quinoidal form. In order to fully characterize two of these forms (the lactone and the quinoid forms) three rosebengal derivatives were investigated by the single crystal X-ray method.

Chloromercuration of acetylenes can result in cis- or transvinyl mercurials. Apart from these stereo isomers, regio isomers can also result. Mercuration of propargylic amines with  $\text{HgCl}_2/\text{HCl}$  results in chloromercurate salts of different compositions depending on the nature of the propargylic amine and the reaction conditions. The Crystal and molecular structure of the chloromercurate with the composition  $[\text{ClC}_6\text{H}_{12}\text{NHgCl}]\text{HgCl}_3$  was determined in order to establish the stereo- and regio- chemistry in the organomercurate portion and to establish the nature of the chloromercurate anion.

Very little is known about the structure and chemistry of cyclic butatrienes. In order to fully characterize 1,2,3-cyclonatriene (the smallest isolable cyclic butatriene), a stable rhodium complex containing the triene as a ligand was subjected to crystal structure analysis; the free triene molecule can otherwise be stabilized only in dilute solutions

and in the absence of oxygen and hence a full characterization of the free triene is made impossible.

Analogous to organic compounds containing C=S double bond, thiocarbonyl complexes containing bridging C=S group can be expected to undergo oxidative dimerization to yield dithiocarbenium salts containing disulfide linkage. Oxidation of one such thiocarbonyl complex, ( $\eta^5$ -C<sub>5</sub>H<sub>5</sub>)<sub>2</sub>Fe<sub>2</sub>(CO)<sub>3</sub>CS with AgBF<sub>4</sub> gave a dark red compound the structure of which could not be assigned based on spectroscopic data. Thus the structure of this compound was determined to see if indeed a dithiocarbenium salt was the oxidation product.

1-Ethoxysilatrane forms an onium salt upon reaction with trifluoroacetic acid. The crystal structure of the silatrane was initially carried out in order to correlate the the strength of N→Si bond in the silatrane with that in its onium salt. The X-ray experiment could not be carried out on 1-ethoxysilatronium trifluoroacetate because it turned out to be highly hygroscopic.

#### Explanation of Dissertation Format

In this dissertation, the crystal and molecular structures of the rosebengal derivatives are discussed in one section while those of the organometallic compounds are discussed in separate sections. The appendix deals with the design and assembly of low temperature apparatus for one of our four-circle diffractometers. All tables, figures, schemes and references are numbered consecutively throughout this dissertation.

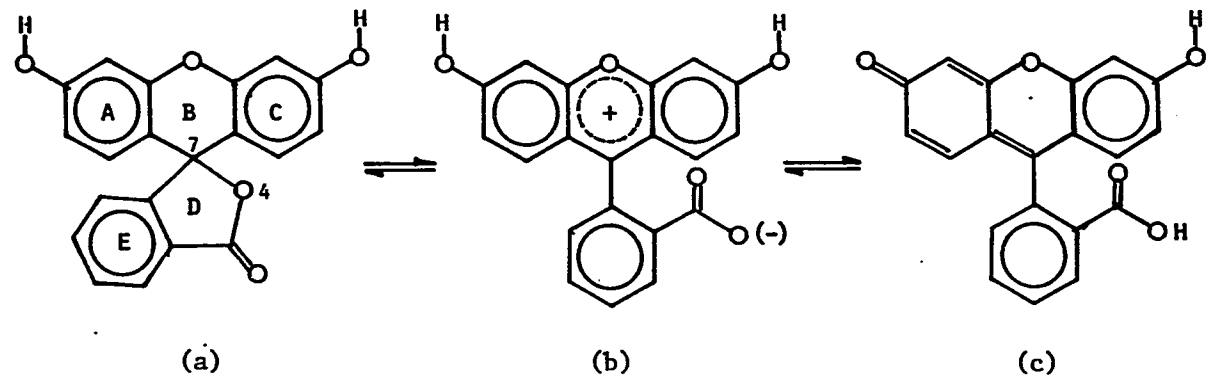
## CRYSTAL AND MOLECULAR STRUCTURES OF ROSE BENGAL DERIVATIVES

## Introduction

The xanthene dyes such as fluorescein, eosin and rose bengal are used in a variety of ways including as indicators, photosensitizers, to stain microscopic slides and in a number of biochemical applications.

There are at least three different structural forms in which each of these dyes can exist. These are the lactone form (which is generally colorless), the zwitterionic form (which is yellow in the case of fluorescein and almost orange in the case of rose bengal) and the quinoidal form (which is always intensely colored - red for both rose bengal and fluorescein). In principle, in acid solution a pyrrillium salt can also exist, but this just derives from protonation of the zwitterion. These are shown in Scheme 1 for the dye fluorescein. The forms all have different spectral properties and one form can be converted to the other depending on solvent polarity and pH of the solution.

Osborn and Rogers,<sup>1</sup> Polyakova et al.<sup>2</sup> presented the crystal structure of the lactonoid form of fluorescein in which they report an exceptionally long (1.525, 1.514 Å), hence severely weak, lactonic C(7)-O(4) bond; such weakness is characteristic of the behavior of fluorescein in solution, where increasing solvent polarity shifts the equilibrium towards the zwitterion. Markuzewski and Diehl<sup>3</sup> assigned the structures of the three forms of fluorescein principally based on the infrared spectra of the solids. Dubost et al.<sup>4</sup> published the crystal structure of the pyrrillium perchlorate of fluorescein. Erythrosin is the only



Scheme 1. Lactone (a), zwitterion (b) and quinoid (c) forms of fluorescein

substituted fluorescein (2,4,5,7-tetraiodofluorescein) for which x-ray crystal structure has been reported.<sup>5</sup>

The studies so far undertaken show that the color of the fluorescein samples does not correspond unequivocally to the molecular forms and that only through x-ray crystal structural studies can one establish the correct structure of the three possible forms.

Rose bengal, 3',4',5',6'-tetrachloro-2,4,5,7-tetraiodofluorescein, shows similar solution behavior. Like erythrosin, it has been shown to exert a wide range of pharmacological effects including inhibition of thyroid hormones.<sup>5</sup> In order to fully characterize the three forms of rose bengal, x-ray single crystal investigations of three rose bengal derivatives were carried out. Samples were obtained from Prof. D. C. Neckers, Bowling Green State University, Ohio.

### Experimental

Samples as obtained from Prof. Neckers contained single crystals which were too small to study by single crystal methods; thus they were recrystallized appropriately. Well-formed crystals of almost colorless sample of rose bengal (1) were grown from a dioxane-methylenechloride mixture by slow evaporation. The sample of 6-O-benzyl rose bengal (2) was expected to be either a free carboxylic acid or a sodium carboxylate. Thus in the hope of converting all the sample to the free carboxylic acid form, two drops of 50% aqueous hydrochloric acid were added to the acetone-methylenechloride solution from which rosy red crystals were obtained. The third sample of the dianion of rose bengal (3) (with triethylammonium ions as counterions) was recrystallized from an



ethylacetate-THF mixture.

Data collection Single crystals of compounds 1,2 and 3 with approximate dimensions  $0.22 \times 0.24 \times 0.08$  mm,  $0.20 \times 0.15 \times 0.10$ mm, and  $0.25 \times 0.15 \times 0.08$ mm respectively were adhered to glass fibers (inside a Lindeman glass capillary for compound 1) and mounted on goniometer heads. Data were collected at room temperature in all cases on a four-circle diffractometer designed and built in the Ames Laboratory<sup>6</sup> using monochromated Mo  $K_{\alpha}$  radiation. Several  $\omega$ -oscillation photographs at various  $\phi$ -settings were taken for each crystal. From these photographs, the settings for 12 reflections each were obtained and input into a automatic indexing algorithm.<sup>7</sup> The resulting reduced cells and reduced cell scalars revealed triclinic symmetry for all three crystals. Crystal data are summarized in Tables 1, 2 and 3. One hemisphere of data (unique) were collected for each crystal. In each case, the intensities of three standard reflections were measured every 75 reflections during data collection to monitor any crystal decay.

Reduction of intensity data In all three cases no significant decay was observed. A statistical test<sup>8</sup> in each case indicated P $\bar{1}$  as the space group. Empirical absorption corrections<sup>9</sup> were made based on observed variations in the intensity distribution as a function of the orientation of the crystal reflections near  $\chi = 90^{\circ}$ . Data were corrected for Lorentz and polarization effects and appropriately averaged. The estimated variance in each intensity was calculated by

$$\sigma_I^2 = C_T + K_T^2 C_B + (0.03C_T)^2 + (0.03C_B)^2 + (0.03C_N)^2$$

where  $C_T, C_B, C_N$  and  $K_T$  represent total count, background count, net count

Table 1. Crystal data for  $C_{20}H_4Cl_4I_4O_5 \cdot 1\frac{1}{2}C_4H_8O_2$  (1)

---

F.W.	: 1105.83
Space Group	: $P\bar{1}$
a, Å	: 12.669(6) <sup>a</sup>
b, Å	: 12.989(2)
c, Å	: 10.693(4)
$\alpha$ , °	: 92.60(4)
$\beta$ , °	: 111.04(5)
$\gamma$ , °	: 102.32(5)
V, Å <sup>3</sup>	: 1590.1(8)
$\rho_{calc}$ , g/cm <sup>3</sup>	: 2.309
Z	: 2
Temperature, °K	: 298
Radiation, Å	: Mo $K_{\alpha}$
$\lambda$ , Å	: 0.70964 (graphite monochromator)
$\mu$ , cm <sup>-1</sup>	: 42.63 (correction applied)
$2\theta_{max}$ , °	: 50.0
Number of reflections collected	: 6552
Number of reflections observed	: 4546
Min of I/ $\sigma$ (I)	: 3.0
Number of variables	: 422
Observations/Variables	: 10.8
R, % <sup>b</sup>	: 4.8
$R_{\omega}$ , %	: 6.8

---

<sup>a</sup>Estimated standard deviations shown in parentheses are for the least significant digits.

$$R = \frac{\sum ||F_o| - |F_c||}{\sum |F_o|}$$

$$R_{\omega} = [\sum \omega (|F_o| - |F_c|)^2 / \sum \omega |F_o|^2]^{1/2}, \text{ where } \omega = 1/\sigma^2(F).$$

Table 2. Crystal data for  $C_{34}H_{16}Cl_4I_4O_5$  (2)

---

F.W.	: 1153.43
Space Group	: $P\bar{1}$
a, Å	: 13.637(5) <sup>a</sup>
b, Å	: 15.284(6)
c, Å	: 9.021(3)
$\alpha$ , °	: 102.38(3)
$\beta$ , °	: 96.59(3)
$\gamma$ , °	: 108.11(4)
V, Å <sup>3</sup>	: 1711.7(9)
$\rho_{\text{calc}}$ , g/cm <sup>3</sup>	: 2.239
Z	: 2
Temperature, °K	: 298
Radiation, Å	: Mo $K_{\alpha}$
$\lambda$ , Å	: 0.70964 (graphite monochromator)
$\mu$ , cm <sup>-1</sup>	: 39.60 (correction applied)
$2\theta_{\text{max}}$ , °	: 50.0
Number of reflections collected	: 3816
Number of reflections observed	: 1416
Min of I/ $\sigma$ (I)	: 3.0
Number of variables	: 295
Observations/Variables	: 5.0
R, % <sup>b</sup>	: 12.3
$R_{\omega}$ , %	: 14.7

---

<sup>a</sup>Estimated standard deviations shown in parentheses are for the least significant digits.

$$R = \frac{\sum ||F_o| - |F_c||}{\sum |F_o|}$$

$$R_{\omega} = [\sum \omega (|F_o| - |F_c|)^2 / \sum \omega |F_o|^2]^{1/2}, \text{ where } \omega = 1/\sigma^2(F).$$

Table 3. Crystal Data for  $C_{32}H_{34}Cl_4I_4N_2O_5$  (3)

---

F.W.	: 1176.06
Space Group	: $P\bar{1}$
a, Å	: 18.293(8) <sup>a</sup>
b, Å	: 18.907(6)
c, Å	: 13.534(3)
$\alpha$ , °	: 95.76(3)
$\beta$ , °	: 90.99(3)
$\gamma$ , °	: 61.32(3)
V, Å <sup>3</sup>	: 4083.4(2.0)
$\rho_{calc}$ , g/cm <sup>3</sup>	: 1.913
Z	: 4(two independent units)
Temperature, °K	: 298
Radiation, Å	: Mo $K_{\alpha}$
$\lambda$ , Å	: 0.70964 (graphite monochromator)
$\mu$ , cm <sup>-1</sup>	: 33.219 (correction applied)
$2\theta_{max}$ , °	: 50.0
Number of reflections collected	: 13275 (one hemisphere)
Number of reflections observed	: 3588
Min of I/ $\sigma$ (I)	: 3.0
Number of variables	: 633
Observations/Variables	: 5.7
R, % <sup>b</sup>	: 6.9
$R_{\omega}$ , %	: 8.0

---

<sup>a</sup>Estimated standard deviations shown in parentheses are for the least significant digits.

$$R = \frac{\sum (|F_o| - |F_c|)}{\sum |F_o|}$$

$$R_{\omega} = \left[ \frac{\sum \omega (|F_o| - |F_c|)^2}{\sum \omega |F_o|^2} \right]^{1/2}, \text{ where } \omega = 1/\sigma^2(F).$$

and counting time factor respectively while the factor 0.03 represents an estimate of non-statistical errors. The estimated deviations in the structure factors were calculated by the finite difference method.<sup>10</sup> The final unit cell parameters and their standard deviations were obtained by a least-squares fit to the tuned  $2\theta$  values of 21 (1), 18 (2) and 12 (3) independent high angle reflections ( $15 \leq 2\theta \leq 35^\circ$ ).

### Structure Determination and Refinement

The positions of the iodine atoms were readily obtained from analyses of sharpened three-dimensional Patterson maps in all three cases. All other non-hydrogen atoms were found by successive structure factor and electron density map calculations.<sup>11</sup>

In the case of compound 1, the hydrogen atom positions were calculated with an O-H or C-H distance set to 1.05 Å. Two molecules of 1,4-dioxane solvent-of-crystallization were located in a final difference electron density map; the identification of the solvent atoms as either oxygen or carbon was based on initially treating these atoms as nitrogens and then varying their occupancies; further evidence comes from possible hydrogen bonding (see later). All positional parameters were initially refined using a block-matrix<sup>12</sup> least squares procedure. All non-hydrogen atoms were refined anisotropically, while the hydrogen atoms were not refined. A final full-matrix least squares procedure minimizing the function  $\sum \omega (|F_o| - |F_c|)^2$ , where  $\omega = 1/\sigma^2(F)$ , yielded a final crystallographic residual factor of 4.8%.

In the case of compound 2, the nature of the substituents attached to O(1) and O(5) appear to be benzyl groups as was seen from a difference

electron density map. The refinement could be carried out to a point where only the iodine atoms and chlorine atoms could be refined anisotropically, while the rest of the atoms could only be refined isotropically. Furthermore, since the temperature factors for the benzylic carbon atoms (C(21) through C(34)) individually refined to high thermal parameters (as high as  $17 \text{ \AA}^2$ ), these were all forced to have a fixed temperature factor of  $10 \text{ \AA}^2$ ; even so many of these atoms showed little sign of "settling down". At this stage the crystallographic residual factor was 12.3%. The low ratio (3.3) of number of observations to the maximum number of variables possible (424, excluding those of the hydrogens) would make it doubtful that statistically significant results could be obtained for anisotropic refinement for all the atoms. Indeed any attempt to anisotropically vary even the oxygen atoms led to non-positive definite temperature factors for these atoms. Thus the refinement had to be stopped at this stage with a residual of 12.3%. Inclusion of the hydrogen atoms did not improve the results, and hence were not included.

As for compound 3, hydrogen atom positions were calculated as in the case of 1. There are 94 non-hydrogen atoms in the asymmetric unit. As in the case of 2, the rather low ratio (4.47) of the number of observations to number of maximum possible variables (847, excluding those of hydrogen) would again make it uncertain that statistically significant results could be obtained for anisotropically refining all the atoms. Attempts at such refinements led to non-positive definite temperature factors for the nitrogen atoms and many of the carbon atoms. Thus in a full-matrix least squares procedure the carbon atoms and the nitrogen atoms were refined only isotropically and all the hydrogen atoms

were simply assigned an isotropic thermal parameter of  $6.0 \text{ \AA}^2$ ; this yielded a final crystallographic residual factor of 6.9%.

The atomic scattering factors were those from reference 13; those of iodine atoms and chlorine atoms were modified for anomalous dispersion effects.<sup>14</sup>

### Discussion of the Structures

Structure of  $C_{20}H_4Cl_4I_4O_5 \cdot 1\frac{1}{2}C_4H_8O_2$  (1)      The final atomic positional and anisotropic thermal parameters are listed in Tables 4 and 5 respectively while the refined bond distances and bond angles are listed in Tables 6 and 7 respectively. Table 8 furnishes details about some least squares planes. Figure 1 shows the ORTEP<sup>15</sup> drawing of the main molecule (omitting the hydrogen atoms and solvent molecule 1,4-dioxan for clarity) whereas Figure 2 shows the unit cell drawing (the hydrogen atoms of the dioxane molecule are omitted for clarity).

An x-ray structure determination of compound 1 clearly reveals that it is in the lactoid form with the lactone-tetrachlorobenzene group nearly perpendicular to the xanthene ring system (Fig. 1 and Table 8). The whole group appears to be kind of 'nodding' in its own plane about the spiro atom C(7), the amplitude of this 'nodding' motion is roughly proportional to the distance from C(7). Column 4 of Table 4 indicates that the isotropic equivalent thermal parameter ( $U_{iso}$ ) for the carbon atoms in this group are comparable to those of carbon atoms in the rest of the main molecule. This can be taken to mean that the lactone-tetrachlorobenzene group hardly shows any 'flapping' motion even though large voids surround them. The bond distances and bond angles of the

Table 4. Positional parameters<sup>a</sup> ( $\times 10^4$ ) for  $C_{20}H_4Cl_4I_4O_5 \cdot 1\frac{1}{2}C_4H_8O_2$  (1)

Atom	x	y	z	$U_{iso}^b$
I(1)	3393.5(6)	0916.2(6)	-3576.0(6)	64.2(3)
I(2)	3483.9(5)	0517.8(5)	2041.7(7)	56.8(3)
I(3)	6611.1(6)	1852.6(5)	5717.8(6)	57.2(3)
I(4)	11294.5(5)	3968.7(5)	5552.0(6)	56.1(2)
CL(1)	6042(2)	4456(2)	1964(2)	49.5(8)
CL(2)	6525(3)	6648(2)	0945(3)	79(1)
CL(3)	7848(4)	6987(2)	-0998(3)	106(2)
CL(4)	8814(3)	5149(2)	-1845(3)	85(1)
O(1)	2651(6)	0144(5)	-1203(8)	74(3)
O(2)	5980(4)	1900(4)	2679(5)	40(2)
O(3)	9398(5)	3057(5)	6706(5)	51(2)
O(4)	7949(4)	2370(4)	0365(5)	34(2)
O(5)	8891(5)	2869(5)	-0988(6)	55(3)
C(1)	5468(7)	1679(6)	1291(8)	35(3)
C(2)	4335(7)	1053(6)	0757(9)	41(3)
C(3)	3741(7)	0793(6)	-0638(9)	42(3)
C(4)	4302(7)	1196(6)	-1476(8)	39(3)
C(5)	5418(6)	1824(6)	-0957(8)	36(3)
C(6)	6016(6)	2070(6)	0437(7)	31(3)
C(7)	7249(6)	2785(5)	1010(7)	29(2)
C(8)	7814(6)	2785(5)	2523(7)	31(3)
C(9)	8998(7)	3239(6)	3199(7)	35(3)
C(10)	9501(7)	3291(6)	4582(7)	37(3)
C(11)	8834(7)	2948(6)	5327(7)	40(3)
C(12)	7662(7)	2469(6)	4653(8)	38(3)
C(13)	7153(7)	2384(6)	3265(8)	34(3)
C(14)	8321(7)	3069(6)	-0371(7)	37(3)
C(15)	7916(7)	4042(6)	-0230(7)	35(3)
C(16)	8080(8)	4999(7)	-0759(8)	49(3)
C(17)	7635(9)	5789(7)	-0393(9)	58(4)
C(18)	7038(8)	5640(6)	0468(8)	51(3)
C(19)	6838(7)	4673(6)	0956(8)	38(3)
C(20)	7308(6)	3881(5)	0598(7)	30(3)

<sup>a</sup>The estimated standard deviations in the parentheses are for the least significant digits. Parameters for hydrogen atoms are multiplied by  $10^3$ .

<sup>b</sup>For anisotropically refined atoms,  $U_{iso} \equiv 10^3/3 \sum_{ij} a_i^* a_j^* \vec{a}_i \cdot \vec{a}_j$ , where the temperature factors are defined as  $\exp(-2\pi^2 \sum_{h,j} h_j a_j^* U_{ij})$ .

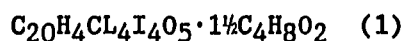


Table 4. (continued)

---

Atom	x	y	z	U <sub>iso</sub>
C(21)	9749(18)	9057(13)	8426(25)	163(13)
C(22)	9275(22)	8705(13)	7047(17)	159(14)
O(6)	10618(9)	10089(10)	8859(13)	138(7)
O(7)	8701(13)	9493(9)	6483(12)	161(8)
C(23)	9677(22)	10454(13)	6577(17)	161(13)
C(24)	10043(18)	10835(12)	7939(21)	149(11)
C(25)	4400(16)	3943(12)	4565(19)	120(10)
C(26)	5223(20)	4301(12)	5948(19)	133(12)
O(8)	5361(10)	5368(8)	6371(11)	116(6)
H(1)	183	12	-118	51
H(3)	921	299	758	51
H(5)	586	213	-158	51
H(9)	950	354	266	51

---

Table 5. Anisotropic thermal parameters<sup>a</sup> ( $\times 10^3$ ) for

Atom	U <sub>11</sub>	U <sub>22</sub>	U <sub>33</sub>	U <sub>23</sub>	U <sub>13</sub>	U <sub>12</sub>
I(1)	54.3(4)	71.7(4)	43.1(3)	-08.5(3)	03.0(3)	-01.8(3)
I(2)	42.4(3)	62.8(4)	70.8(4)	21.6(3)	32.1(3)	02.8(3)
I(3)	60.7(4)	74.6(4)	42.2(3)	11.4(3)	33.6(3)	02.8(3)
I(4)	36.3(3)	79.1(4)	38.6(3)	-01.3(3)	06.4(2)	00.6(3)
CL(1)	39(1)	54(1)	55(1)	-06(1)	19(1)	11.8(9)
CL(2)	92(2)	45(1)	80(2)	-02(1)	01(2)	33(1)
CL(3)	157(3)	45(1)	85(2)	33(1)	22(2)	-02(2)
CL(4)	105(2)	85(2)	64(2)	24(1)	50(2)	-15(2)
O(1)	41(4)	62(4)	89(5)	04(4)	06(4)	-15(3)
O(2)	30(3)	50(3)	40(3)	08(2)	20(2)	01(2)
O(3)	49(4)	71(4)	29(3)	04(3)	14(3)	07(3)
O(4)	36(3)	39(3)	33(3)	04(2)	18(2)	10(2)
O(5)	52(4)	82(4)	45(3)	07(3)	33(3)	18(3)
O(6)	75(7)	164(11)	142(10)	04(8)	14(7)	14(7)
O(7)	181(13)	111(9)	106(9)	14(7)	-17(8)	-12(8)
O(8)	129(9)	112(8)	111(8)	-09(6)	62(7)	08(6)
C(1)	33(4)	30(4)	40(4)	08(3)	11(3)	09(3)
C(2)	28(4)	38(4)	57(5)	11(4)	17(4)	04(3)
C(3)	28(4)	34(4)	55(5)	07(4)	08(4)	03(3)
C(4)	35(4)	34(4)	43(4)	-02(3)	10(4)	09(3)
C(5)	30(4)	34(4)	34(4)	03(3)	05(3)	03(3)
C(6)	27(4)	34(4)	34(4)	07(3)	12(3)	09(3)
C(7)	23(3)	32(3)	26(3)	01(3)	06(3)	00(3)
C(8)	30(4)	30(4)	32(4)	06(3)	13(3)	08(3)
C(9)	36(4)	37(4)	35(4)	08(3)	17(3)	06(3)
C(10)	38(4)	43(4)	30(4)	03(3)	16(3)	06(3)
C(11)	48(5)	48(4)	27(4)	08(3)	17(4)	15(4)
C(12)	43(4)	44(4)	34(4)	12(3)	24(4)	06(3)
C(13)	36(4)	36(4)	37(4)	07(3)	18(3)	12(3)
C(14)	30(4)	48(4)	28(4)	02(3)	09(3)	03(3)
C(15)	37(4)	36(4)	27(4)	04(3)	10(3)	01(3)
C(16)	61(6)	48(5)	27(4)	15(3)	13(4)	-02(4)
C(17)	74(6)	35(4)	38(5)	16(4)	-02(4)	-04(4)
C(18)	60(6)	37(4)	34(4)	05(3)	-06(4)	12(4)
C(19)	35(4)	36(4)	36(4)	01(3)	07(3)	06(3)

<sup>a</sup>The estimated standard deviations in the parentheses are for the least significant digits. The anisotropic temperature factors are defined as  $\exp(-2\pi^2 \sum h_j a_j^* a_j^* U_{ij})$ .

Table 5. (continued)

Atom	U <sub>11</sub>	U <sub>22</sub>	U <sub>33</sub>	U <sub>23</sub>	U <sub>13</sub>	U <sub>12</sub>
C(20)	24(3)	35(4)	25(3)	04(3)	05(3)	03(3)
C(21)	126(15)	83(10)	256(24)	67(13)	38(16)	26(10)
C(22)	288(28)	95(11)	83(11)	05(8)	36(14)	87(14)
C(23)	256(26)	86(10)	83(11)	17(8)	19(13)	04(13)
C(24)	157(18)	80(10)	175(18)	21(11)	05(14)	57(11)
C(25)	133(14)	92(10)	138(14)	07(9)	68(12)	02(10)
C(26)	199(20)	88(10)	130(15)	10(9)	81(15)	39(12)

Table 6. Refined bond distances<sup>a</sup> (Å) for C<sub>20</sub>H<sub>4</sub>Cl<sub>4</sub>I<sub>4</sub>O<sub>5</sub>·1½C<sub>4</sub>H<sub>8</sub>O<sub>2</sub> (1)

Atoms	Distance	Atoms	Distance
I(1) - C(4)	2.096( 6)	C(7) - C(20)	1.504( 8)
I(2) - C(2)	2.088( 7)	C(8) - C(9)	1.388( 8)
I(3) - C(12)	2.104( 6)	C(8) - C(13)	1.390( 8)
I(4) - C(10)	2.094( 6)	C(9) - C(10)	1.376( 9)
CL(1) - C(19)	1.716( 6)	C(10) - C(11)	1.379( 9)
CL(2) - C(18)	1.714( 7)	C(11) - C(12)	1.381( 9)
CL(3) - C(17)	1.717( 8)	C(12) - C(13)	1.378( 9)
CL(4) - C(16)	1.722( 7)	C(14) - C(15)	1.482( 9)
O(1) - C(3)	1.358( 9)	C(15) - C(16)	1.396( 9)
O(2) - C(1)	1.377( 7)	C(15) - C(20)	1.363( 8)
O(2) - C(13)	1.376( 7)	C(16) - C(17)	1.376(10)
O(3) - C(11)	1.374( 8)	C(17) - C(18)	1.383(10)
O(4) - C(7)	1.469( 7)	C(18) - C(19)	1.390( 9)
O(4) - C(14)	1.348( 7)	C(19) - C(20)	1.395( 8)
O(5) - C(14)	1.196( 8)	O(6) - C(21)	1.474(20)
C(1) - C(2)	1.386( 9)	O(6) - C(24)	1.519(19)
C(1) - C(6)	1.386( 8)	O(7) - C(22)	1.414(19)
C(2) - C(3)	1.395( 9)	O(7) - C(23)	1.528(19)
C(3) - C(4)	1.387( 9)	O(8) - C(26)	1.393(18)
C(4) - C(5)	1.369( 9)	C(21) - C(22)	1.389(23)
C(5) - C(6)	1.394( 8)	C(23) - C(24)	1.391(22)
C(6) - C(7)	1.523( 8)	C(25) - C(26)	1.454(21)
C(7) - C(8)	1.516( 8)		
O(1) - O(6') <sup>b</sup>	2.586(12)	O(3) - O(5')	2.771( 7)

<sup>a</sup>The estimated standard deviations in the parentheses are for the least significant digits.

<sup>b</sup>The O - O distances are non-bonding distances and these are the lengths of hydrogen-bonds. O(6') is symmetry related to O(6) by the operation (x-1,y-1,z-1). O(5') is symmetry related to O(5) by the operation (x,y,z+1).

Table 7. Refined angles<sup>a</sup> (°) for C<sub>20</sub>H<sub>4</sub>Cl<sub>4</sub>I<sub>4</sub>O<sub>5</sub>·1½C<sub>4</sub>H<sub>8</sub>O<sub>2</sub> (1)

Atoms	Angle	Atoms	Angle
C(1) - O(2) - C(13)	118.7( 5)	I(3) - C(12)- C(11)	120.9( 5)
C(7) - O(4) - C(14)	111.7( 4)	I(3) - C(12)- C(13)	118.4( 5)
O(2) - C(1) - C(2)	116.5( 5)	C(11)- C(12)- C(13)	120.7( 6)
O(2) - C(1) - C(6)	123.4( 5)	O(2) - C(13)- C(8)	122.9( 5)
C(2) - C(1) - C(6)	120.0( 6)	O(2) - C(13)- C(12)	116.8( 5)
I(2) - C(2) - C(1)	120.0( 5)	C(8) - C(13)- C(12)	120.2( 6)
I(2) - C(2) - C(3)	119.3( 5)	O(4) - C(14)- O(5)	121.5( 6)
C(1) - C(2) - C(3)	120.6( 6)	O(4) - C(14)- C(15)	108.3( 5)
O(1) - C(3) - C(2)	122.6( 6)	O(5) - C(14)- C(15)	130.2( 6)
O(1) - C(3) - C(4)	118.9( 6)	C(14)- C(15)- C(16)	131.3( 6)
C(2) - C(3) - C(4)	118.4( 6)	C(14)- C(15)- C(20)	107.4( 5)
I(1) - C(4) - C(3)	119.4( 5)	C(16)- C(15)- C(20)	121.2( 6)
I(1) - C(4) - C(5)	119.2( 5)	CL(4)- C(16)- C(15)	119.5( 5)
C(3) - C(4) - C(5)	121.3( 6)	CL(4)- C(16)- C(17)	122.5( 6)
C(4) - C(5) - C(6)	120.2( 6)	C(15)- C(16)- C(17)	118.0( 6)
C(1) - C(6) - C(5)	119.3( 5)	CL(3)- C(17)- C(16)	119.2( 6)
C(1) - C(6) - C(7)	120.6( 5)	CL(3)- C(17)- C(18)	119.6( 6)
C(5) - C(6) - C(7)	120.1( 5)	C(16)- C(17)- C(18)	121.1( 7)
O(4) - C(7) - C(6)	108.3( 4)	CL(2)- C(18)- C(17)	120.3( 6)
O(4) - C(7) - C(8)	108.2( 4)	CL(2)- C(18)- C(19)	118.9( 5)
O(4) - C(7) - C(20)	102.2( 4)	C(17)- C(18)- C(19)	120.8( 6)
C(6) - C(7) - C(8)	111.2( 5)	CL(1)- C(19)- C(18)	121.3( 5)
C(6) - C(7) - C(20)	112.8( 5)	CL(1)- C(19)- C(20)	121.0( 5)
C(8) - C(7) - C(20)	113.6( 5)	C(18)- C(19)- C(20)	117.7( 6)
C(7) - C(8) - C(9)	120.0( 5)	C(7) - C(20)- C(15)	110.4( 5)
C(7) - C(8) - C(13)	121.0( 5)	C(7) - C(20)- C(19)	128.6( 5)
C(9) - C(8) - C(13)	118.9( 5)	C(15)- C(20)- C(19)	121.1( 5)
C(8) - C(9) - C(10)	120.2( 6)	C(22)- C(21)- O(6)	115.9(14)
I(4) - C(10)- C(9)	118.7( 4)	C(21)- C(22)- O(7)	103.5(13)
I(4) - C(10)- C(11)	120.3( 5)	C(21)- O(6) - C(24)	104.8(11)
C(9) - C(10)- C(11)	120.9( 6)	C(22)- O(7) - C(23)	105.2(11)
O(3) - C(11)- C(10)	117.3( 6)	O(7) - C(23)- C(24)	99.1(12)
O(3) - C(11)- C(12)	123.8( 6)	O(6) - C(24)- C(23)	112.5(13)
C(10)- C(11)- C(12)	118.8( 6)	C(25)- C(26)- O(8)	113.4(12)
C(3) - O(1) - O(6') <sup>b</sup>	137.0( 6)	C(11)- O(3) - O(5')	139.8( 5)

<sup>a</sup>The estimated standard deviations in the parentheses are for the least significant digits.

<sup>b</sup>Notation same as in Table 6.

Table 8. Equations of least squares planes (in the triclinic coordinate system) and interplanar angles for 1

Atom	Distance from Plane(Å)	Atom	Distance from Plane(Å) <sup>a</sup>
Plane I fitting I(1)-I(2)-O(1)-C(1)-C(2)-C(3)-C(4)-C(5)-C(6)			
$-7.1162*X + 12.0548*Y + 0.9526*Z + 1.7386 = 0.0$			
I(1)	0.0875	C(3)	-0.0288
I(2)	0.0779	C(4)	-0.0217
O(1)	-0.0891	C(5)	-0.0094
C(1)	-0.0050	C(6)	-0.0062
C(2)	-0.0051	O(6')	1.2981*
		H(1)	0.4742*
Plane II fitting I(3)-I(4)-O(3)-C(8)-C(9)-C(10)-C(11)-C(12)-C(13)			
$-5.6316*X + 12.5453*Y + 1.3784*Z + 0.5755 = 0.0$			
I(3)	-0.0353	C(10)	-0.0144
I(4)	-0.0423	C(11)	0.0332
O(3)	0.0423	C(12)	-0.0012
C(8)	0.0160	C(13)	-0.0118
C(9)	0.0122	O(5')	0.4096*
		H(3)	0.1815*
Plane III fitting O(2)-C(1)-C(6)-C(7)-C(8)-C(13)			
$-6.6039*X + 12.2536*Y + 1.3833*Z + 1.3311 = 0.0$			
O(2)	0.0809	C(7)	0.0958
C(1)	-0.0434	C(8)	-0.0683
C(6)	-0.0454	C(13)	-0.0196
Plane IV fitting CL(1) through CL(4)-O(4)-O(5)-C(7)-C(14) through C(20)			
$6.9746*X + 1.6847*Y + 5.4173*Z - 6.0938 = 0.0$			
CL(1)	-0.0648	C(14)	0.0255
CL(2)	0.0889	C(15)	-0.0165
CL(3)	0.0165	C(16)	-0.0274
CL(4)	-0.0783	C(17)	-0.0061
O(4)	0.0473	C(18)	0.0186
O(5)	0.0558	C(19)	-0.0195
C(7)	-0.0213	C(20)	-0.0188

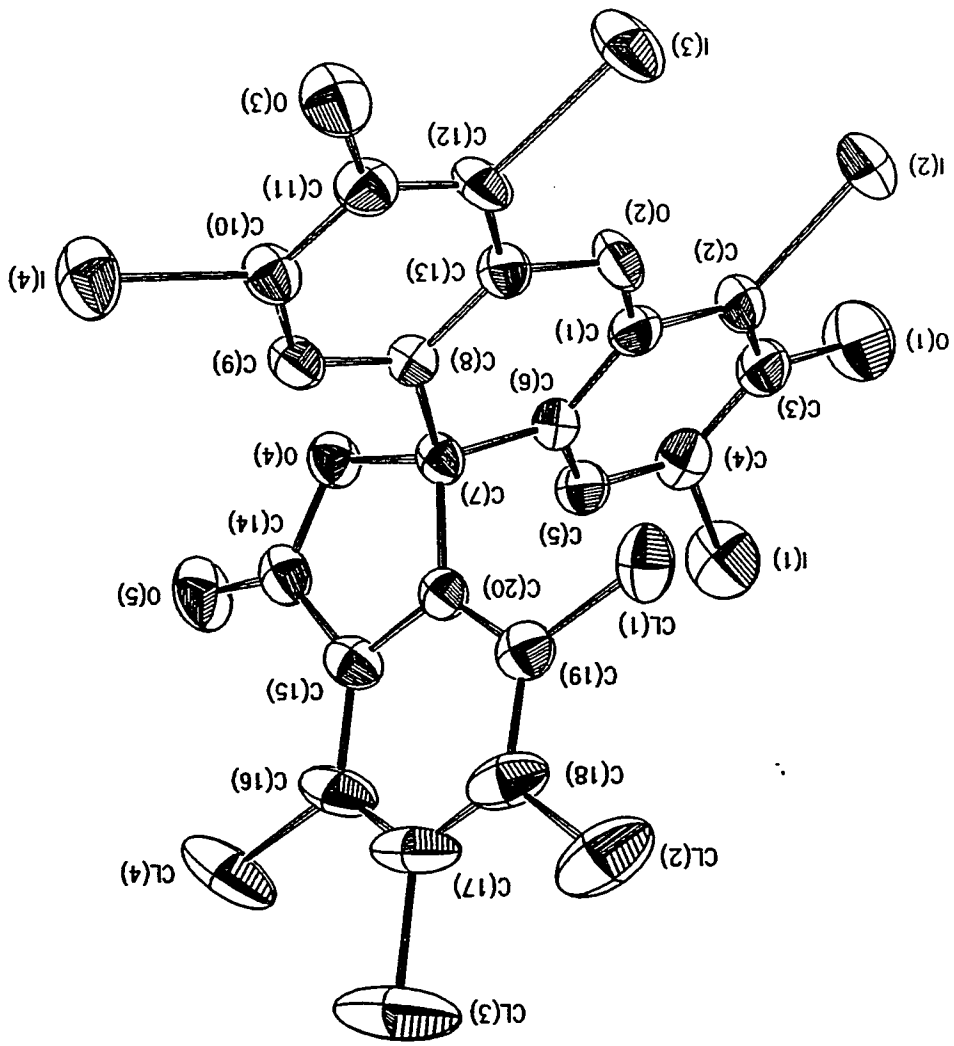
<sup>a</sup>The distances marked with a \* are those for atoms not included in the calculation of the planes. Notation same as in Table 6 for atoms associated with atoms O(5') and O(6').

Table 8. (continued)

Atom	Distance from Plane(Å)	Atom	Distance from Plane(Å)
Plane V fitting O(4')-O(5')-C(14')-C(15')			
$6.7570*X + 2.0813*Y + 5.4709*Z - 11.5338 = 0.0$			
O(4')	0.0013	O(5')	0.0018
C(14')	-0.0043	C(15')	0.0013
Plane VI fitting C(11)-O(3)-H(3)-O(5')			
$3.3060*X - 12.9481*Y - 0.3297*Z + 1.0722 = 0.0$			
C(11)	0.0000	O(3)	0.0000
H(3)	0.0000	O(5')	0.0000
Plane VII fitting C(3)-O(1)-H(1)-O(6')			
$0.4684*X - 8.0768*Y + 8.3819*Z + 0.9999 = 0.0$			
C(3)	0.0000	O(1)	0.0000
H(1)	0.0000	O(6')	0.0000
Plane VIII fitting O(6')-C(21')-C(24')			
$9.3411*X - 4.0456*Y - 9.1166*Z - 1.5814 = 0.0$			
Interplanar Angles(°)			
<u>Plane</u>		<u>Plane</u>	<u>Angle</u>
I		II	170.52
III		IV	91.70
V		VI	79.60
VII		VIII	112.58

Figure 1. ORTEP drawing of  $C_{20}H_4Cl_4I_4O_5 \cdot \frac{1}{2}C_4H_8O_2$  (1)  
excluding the hydrogen atoms and dioxane





tetrachlorobenzene part are well within expected values.

The main geometrical feature of interest in compound 1 occurs in ring D; this ring forms in the relatively less polar solvent 1,4-dioxane (relative to acetone or methanol, the latter being less polar than the former). The C(7)-O(4) bond, the lactonic bond, has a distance of 1.469(7) Å. This distance is shorter than those reported earlier: in the fluorescein-acetone (F·A) complex<sup>1</sup> it is 1.525(3) Å, and in the fluorescein-methanol (F·M) complex<sup>2</sup> it is 1.514 Å. In fact it is nearly the same as the C-O bond distance of 1.48 Å noted in a six-membered lactone ring<sup>16</sup> and in epoxides<sup>17</sup> (1.47 Å); it is however 0.4 Å longer than a typical C-O single bond as one would expect. Thus we have a lactonic bond whose strength is comparable to the ones in epoxides. Although very much less strained than the ones in either F·A or F·M complexes, the lability of the C(7)-O(4) bond is responsible for the behavior of 1 in solution.

The bond lengths in the aromatic ring A range from 1.369 to 1.395 Å (with an average of 1.386 Å) while those in ring C range from 1.376 to 1.390 Å (with an average of 1.382 Å); these agree well with each other and one can note that there appears to be marked local symmetry about the line C(7)-O(2) even though it is not required by the triclinic symmetry. The bonds C(6)-C(7) and C(8)-C(7) in the ring B and the bond C(20)-C(7) in ring D are shorter than a regular C-C single bond (1.541 Å) and are typical C-C sp<sup>2</sup>-sp<sup>3</sup> bonds even though there are no special electronic effects, such as hyperconjugation which tend to shorten bonds between such atoms, found at the spiro atom C(7). Perhaps the spiro nature of the atom C(7) itself together with a strong lactonic bond C(7)-O(4) (see earlier) is responsible for such observed shortening: In other words, we

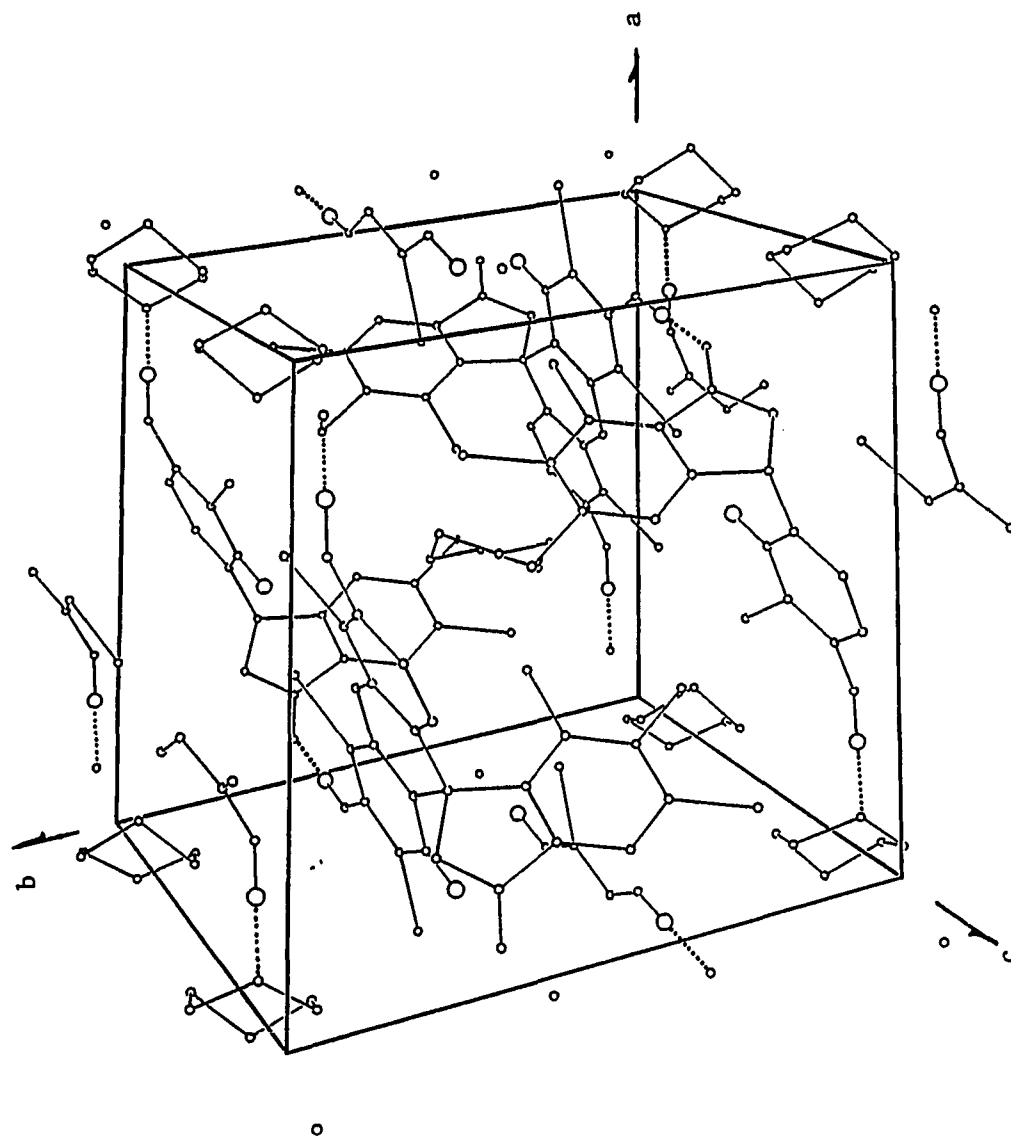
are dealing with steric effects and not any electronic effects.

The angle of  $118.7(5)^\circ$  about the oxygen O(2) suggests that this oxygen has  $sp^2$  hybridization. The O(2)-C(1) and O(2)-C(13) distances of 1.377(7) and 1.376(7) Å are very much the same as those found for F·A (1.377(3), 1.378(3) Å) and F·M (1.375(2), 1.378(2) Å) complexes. Here we see the electronic effect dominating. If one lone pair on O(2) is assumed to be in a  $sp^2$  orbital and the second is in a p type, the latter is nearly in the right orientation to efficiently overlap with the two aromatic  $\pi$ -ring systems flanking O(2). However this overlap is not as complete as is found in the case of the pyrrillium perchlorate of fluorescein<sup>4</sup> where this is manifested by a still shorter C-O(2) distances of 1.32 Å each. This lack of completeness of p- $\pi$  overlap results from the B ring being strained into a deformed boat conformation by the steric strain at the spiro atom C(7) (see Table 8).

In the crystal, compound 1 stacks up with large voids filled with 1,4-dioxane solvent molecules at two sites (Figure 2). One of these molecules sits with its center at the inversion center (1/2, 1/2, 1/2). This solvent molecule does not participate in any hydrogen bonding and it just appears to occupy a large cavity about the aforementioned inversion center. The second dioxane molecule with all its atoms in general positions hydrogen bonds to the main molecule; again it also occupies a large cavity not far from the cell corner(s). In both cases, the atoms of these solvent molecules show very high isotropic temperature factors (see Table 4). It is interesting to note that both of these are in present in the more stable (but perhaps distorted) chair conformation.

Finally, mention must be made of the two kinds of hydrogen bonds in the crystal lattice. One of these, mentioned earlier, is between O(1) of

Figure 2. Unit cell drawing of  $C_{20}H_4Cl_4I_4O_5 \cdot \frac{1}{2}C_4H_8O_2$  (1) omitting the hydrogen atoms of the dioxane molecule. Big circles are the hydrogen atoms. Hydrogen bonds are indicated by the dotted lines



the hydroxyl oxygen and O(6') of the solvent molecule via H(1); the other hydrogen bond is between O(3) of the other hydroxyl hydrogen and O(5') of the carbonyl oxygen via H(3). The existence of the hydrogen bonds is inferred since the respective O-O distances are shorter than twice the van der Waals radius of oxygen atoms (1.4 Å).<sup>18</sup> In fact the hydrogen atom positions for H(1) and H(3) were calculated with this observation in mind. Since the angle O(1)-O(6')-C(24') is calculated to be 110.3°, it appears that the first hydrogen bond lies along one of the sp<sup>3</sup>-lone pairs on the sp<sup>3</sup> hybridized O(6'). The second hydrogen bond seems to have an unusual orientation; the angle between the plane of O(4')-O(5')-C(14')-C(15') and the plane of C(11)-O(3)-H(3)-O(5') is nearly 80° (Table 8). Thus the orbital description of this hydrogen bond is made difficult. This hydrogen bond is longer and hence weaker than the previous one.

Structure of C<sub>34</sub>H<sub>16</sub>Cl<sub>4</sub>I<sub>4</sub>O<sub>5</sub> (2) The final atomic positional and anisotropic thermal parameters are listed in Tables 9 and 10 respectively while the refined bond distances and bond angles are listed in Tables 11 and 12 respectively. Table 13 furnishes some details about a few least squares planes. Figure 3 shows the ORTEP<sup>15</sup> drawing of the main molecule (omitting the hydrogen atoms and the benzylic substituents for clarity) whereas Figure 4 shows the unit cell drawing (the hydrogen atoms and the benzylic substituents are again omitted for clarity).

Analysis of the crystal structure of compound 2 was not quite routine; refinement had to be discontinued at a stage when several of the lighter atoms (oxygen and carbon) started showing non-positive definite temperature factors upon anisotropic refinement; the crystallo-

Table 9. Positional parameters<sup>a</sup> ( $\times 10^4$ ) for C<sub>34</sub>H<sub>16</sub>CL<sub>4</sub>I<sub>4</sub>O<sub>5</sub> (2)

Atom	x	y	z	U <sub>iso</sub> <sup>b</sup>
I(1)	9671(4)	2953(4)	9622(6)	89(3)
I(2)	14098(4)	5155(4)	13184(6)	93(3)
I(3)	16866(4)	4443(4)	11900(6)	109(3)
I(4)	16498(4)	1275(4)	6351(7)	118(3)
CL(1)	12639(17)	3221(13)	5272(23)	102(11)
CL(2)	10931(16)	1871(14)	2439(22)	97(11)
CL(3)	10180(14)	-0330(13)	2133(24)	104(11)
CL(4)	10983(16)	-1107(13)	4746(23)	106(11)
O(1)	11601(28)	4404(25)	12181(43)	75(12)
O(2)	14512(28)	3824(26)	10462(45)	55(13)
O(3)	17317(37)	2820(33)	9559(57)	102(18)
O(4)	13146(34)	-0056(31)	7248(53)	97(16)
O(5)	12189(38)	0536(33)	8639(59)	103(17)
C(1)	13461(41)	3636(38)	10255(64)	61(18)
C(2)	13016(36)	4138(33)	11344(56)	35(15)
C(3)	12051(45)	3959(41)	11091(71)	68(20)
C(4)	11277(51)	3331(46)	9719(79)	80(22)
C(5)	11651(40)	2747(37)	8713(63)	51(17)
C(6)	12753(53)	2820(49)	8740(82)	86(25)
C(7)	13323(49)	2419(45)	7812(77)	68(22)
C(8)	14337(38)	2474(35)	7970(59)	37(16)
C(9)	14855(47)	1959(42)	7148(71)	54(21)
C(10)	15786(43)	2089(40)	7694(67)	53(19)
C(11)	16439(52)	2773(48)	9037(80)	96(23)
C(12)	15947(45)	3336(41)	9954(69)	72(20)
C(13)	14910(43)	3229(40)	9509(67)	45(19)
C(14)	12545(44)	0359(40)	7301(67)	59(19)
C(15)	12199(42)	0772(39)	6301(66)	52(18)
C(16)	11445(40)	0117(36)	4757(62)	36(16)
C(17)	11107(42)	0481(37)	3690(64)	51(18)
C(18)	11409(53)	1431(48)	3774(84)	69(24)
C(19)	12142(44)	2049(39)	5337(67)	54(18)
C(20)	12537(40)	1686(37)	6287(63)	39(17)

<sup>a</sup>The estimated standard deviations in the parentheses are for the least significant digits. Parameters for hydrogen atoms are multiplied by  $10^3$ .

<sup>b</sup>For anisotropically refined atoms,  $U_{iso} \equiv 10^3/3 \sum U_{ij} a_i^* a_j^* \vec{a}_i \cdot \vec{a}_j$ , where the temperature factors are defined as  $\exp(-2\pi^2 \sum h_j a_j^* a_i^* U_{ij})$ .

Table 9. (continued)

---

Atom	x	y	z	U <sub>iso</sub>
C(21)	12502(57)	0069(52)	9874(90)	127
C(22)	13475(62)	0899(56)	10973(96)	127
C(23)	14323(55)	0547(49)	11220(85)	127
C(24)	15274(64)	1315(58)	12067(97)	127
C(25)	15240(60)	2100(55)	13075(92)	127
C(26)	14413(67)	2474(60)	12901(97)	127
C(27)	13409(67)	1744(76)	11843(99)	127
C(28)	11446(65)	5279(58)	11963(98)	127
C(29)	11109(69)	5939(62)	13995(97)	127
C(30)	10209(67)	5615(58)	13283(95)	127
C(31)	9537(62)	5920(56)	14004(96)	127
C(32)	10172(60)	6380(55)	15406(93)	127
C(33)	11389(50)	6769(46)	15697(77)	127
C(34)	11983(53)	6215(48)	14628(83)	127

---



Table 10. Anisotropic thermal parameters<sup>a</sup> ( $\times 10^3$ ) for  
 $C_{34}H_{16}CL_4I_4O_5$  (2)

Atom	U <sub>11</sub>	U <sub>22</sub>	U <sub>33</sub>	U <sub>23</sub>	U <sub>13</sub>	U <sub>12</sub>
I(1)	64(3)	98(4)	78(4)	-01(3)	06(3)	07(3)
I(2)	80(4)	87(4)	59(4)	-25(3)	-07(3)	-05(3)
I(3)	74(4)	116(5)	78(4)	-15(4)	-12(3)	-09(3)
I(4)	89(4)	119(5)	119(5)	-11(4)	36(4)	23(4)
CL(1)	133(18)	78(14)	71(16)	19(12)	12(13)	06(13)
CL(2)	117(16)	93(15)	65(15)	09(12)	01(12)	26(13)
CL(3)	78(14)	78(16)	106(17)	-19(14)	08(12)	-09(13)
CL(4)	113(17)	65(14)	101(17)	16(12)	05(13)	-16(13)

<sup>a</sup>The estimated standard deviations in the parentheses are for the least significant digits. The anisotropic temperature factors are defined as  $\exp(-2\pi^2 \sum h_i h_j a_i^* a_j^* U_{ij})$ .

Table 11. Refined bond distances<sup>a</sup> (Å) for C<sub>34</sub>H<sub>16</sub>CL<sub>4</sub>I<sub>4</sub>O<sub>5</sub> (2)

Atoms	Distance	Atoms	Distance
I(1) - C(4)	2.07(5)	C(8) - C(13)	1.54(6)
I(2) - C(2)	2.06(4)	C(9) - C(10)	1.25(7)
I(3) - C(12)	2.10(5)	C(10) - C(11)	1.41(7)
I(4) - C(10)	2.08(4)	C(11) - C(12)	1.43(7)
CL(1) - C(19)	1.72(5)	C(12) - C(13)	1.37(6)
CL(2) - C(18)	1.66(6)	C(14) - C(15)	1.33(6)
CL(3) - C(17)	1.73(5)	C(15) - C(16)	1.56(6)
CL(4) - C(16)	1.78(4)	C(15) - C(20)	1.33(6)
O(1) - C(3)	1.38(6)	C(16) - C(17)	1.32(6)
O(1) - C(28)	1.47(7)	C(17) - C(18)	1.36(7)
O(2) - C(1)	1.35(5)	C(18) - C(19)	1.55(7)
O(2) - C(13)	1.39(5)	C(19) - C(20)	1.27(6)
O(3) - C(11)	1.21(6)	C(21) - C(22)	1.57(9)
O(4) - C(14)	1.18(6)	C(22) - C(23)	1.43(9)
O(5) - C(14)	1.36(6)	C(22) - C(27)	1.39(10)
O(5) - C(21)	1.53(7)	C(23) - C(24)	1.44(9)
C(1) - C(2)	1.42(6)	C(24) - C(25)	1.36(9)
C(1) - C(6)	1.60(7)	C(25) - C(26)	1.42(9)
C(2) - C(3)	1.24(6)	C(26) - C(27)	1.52(10)
C(3) - C(4)	1.46(7)	C(28) - C(29)	2.07(10)
C(4) - C(5)	1.39(7)	C(29) - C(30)	1.21(10)
C(5) - C(6)	1.47(7)	C(29) - C(34)	1.16(9)
C(6) - C(7)	1.38(8)	C(30) - C(31)	1.32(9)
C(7) - C(8)	1.35(6)	C(31) - C(32)	1.35(9)
C(7) - C(20)	1.60(7)	C(32) - C(33)	1.55(8)
C(8) - C(9)	1.37(6)	C(33) - C(34)	1.60(8)

<sup>a</sup>The estimated standard deviations in the parentheses are for the least significant digits.

Table 12. Refined bond angles<sup>a</sup> (°) for C<sub>34</sub>H<sub>16</sub>CL<sub>4</sub>I<sub>4</sub>O<sub>5</sub> (2)

Atoms	Angle	Atoms	Angle
C(3) - O(1) - C(28)	116(4)	O(4) - C(14) - C(15)	131(5)
C(1) - O(2) - C(13)	120(3)	O(5) - C(14) - C(15)	111(4)
C(14) - O(5) - C(21)	116(4)	C(14) - C(15) - C(16)	118(4)
O(2) - C(1) - C(2)	121(4)	C(14) - C(15) - C(20)	129(4)
O(2) - C(1) - C(6)	118(4)	C(16) - C(15) - C(20)	112(4)
C(2) - C(1) - C(6)	122(4)	CL(4) - C(16) - C(15)	113(3)
I(2) - C(2) - C(1)	114(3)	CL(4) - C(16) - C(17)	125(3)
I(2) - C(2) - C(3)	126(3)	C(15) - C(16) - C(17)	121(4)
C(1) - C(2) - C(3)	119(4)	CL(3) - C(17) - C(16)	116(3)
O(1) - C(3) - C(2)	119(4)	CL(3) - C(17) - C(18)	120(4)
O(1) - C(3) - C(4)	112(4)	C(16) - C(17) - C(18)	125(4)
C(2) - C(3) - C(4)	128(5)	CL(2) - C(18) - C(17)	123(4)
I(1) - C(4) - C(3)	123(4)	CL(2) - C(18) - C(19)	124(4)
I(1) - C(4) - C(5)	119(4)	C(17) - C(18) - C(19)	112(4)
C(3) - C(4) - C(5)	114(4)	CL(1) - C(19) - C(18)	110(3)
C(4) - C(5) - C(6)	127(4)	CL(1) - C(19) - C(20)	125(4)
C(1) - C(6) - C(5)	108(4)	C(18) - C(19) - C(20)	122(4)
C(1) - C(6) - C(7)	114(4)	C(7) - C(20) - C(15)	116(4)
C(5) - C(6) - C(7)	138(5)	C(7) - C(20) - C(19)	116(4)
C(6) - C(7) - C(8)	134(5)	C(15) - C(20) - C(19)	126(4)
C(6) - C(7) - C(20)	109(4)	O(5) - C(21) - C(22)	102(4)
C(8) - C(7) - C(20)	117(4)	C(21) - C(22) - C(23)	109(5)
C(7) - C(8) - C(9)	133(4)	C(21) - C(22) - C(27)	123(6)
C(7) - C(8) - C(13)	106(4)	C(23) - C(22) - C(27)	126(6)
C(9) - C(8) - C(13)	121(4)	C(22) - C(23) - C(24)	111(5)
C(8) - C(9) - C(10)	119(4)	C(23) - C(24) - C(25)	121(6)
I(4) - C(10) - C(9)	116(4)	C(24) - C(25) - C(26)	124(6)
I(4) - C(10) - C(11)	116(3)	C(25) - C(26) - C(27)	113(6)
C(9) - C(10) - C(11)	128(5)	C(22) - C(27) - C(26)	117(7)
O(3) - C(11) - C(10)	124(5)	C(30) - C(29) - C(33)	118(6)
O(3) - C(11) - C(12)	119(5)	C(30) - C(29) - C(34)	176(8)
C(10) - C(11) - C(12)	116(5)	C(33) - C(29) - C(34)	64(5)
I(3) - C(12) - C(11)	119(3)	C(29) - C(30) - C(31)	115(7)
I(3) - C(12) - C(13)	119(3)	C(30) - C(31) - C(32)	99(6)
C(11) - C(12) - C(13)	121(4)	C(31) - C(32) - C(33)	125(5)
O(2) - C(13) - C(8)	128(4)	C(29) - C(33) - C(32)	81(5)
O(2) - C(13) - C(12)	117(4)	C(29) - C(33) - C(34)	41(4)
C(8) - C(13) - C(12)	115(4)	C(32) - C(33) - C(34)	119(4)
O(4) - C(14) - O(5)	118(4)	C(29) - C(34) - C(33)	73(5)

<sup>a</sup>The estimated standard deviations in the parentheses are for the least significant digits.

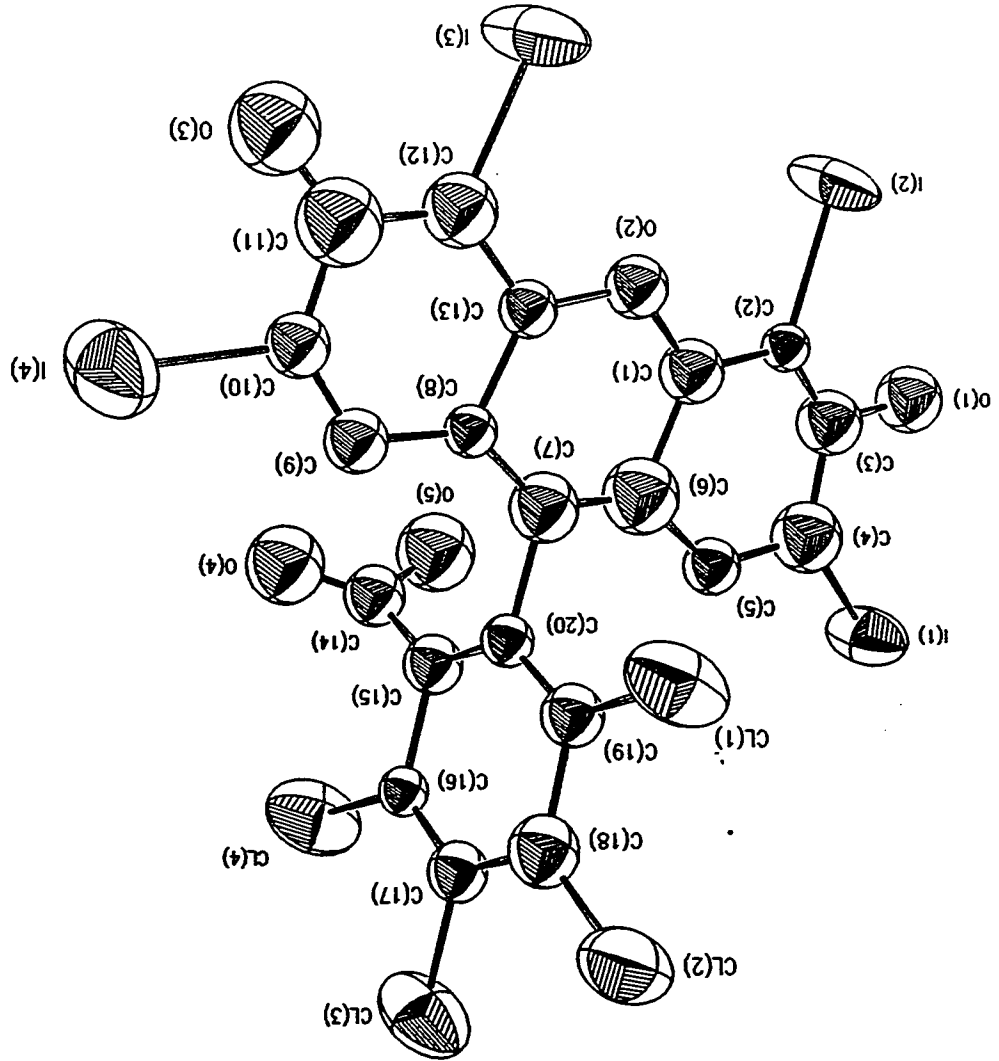
Table 13. Equations of least squares planes (in the triclinic coordinate system) and interplanar angles for 2

Atom	Distance from Plane(Å)	Atom	Distance from Plane(Å)
Plane I fitting I(1)-I(2)-O(1)-C(1)-C(2)-C(3)-C(4)-C(5)-C(6)			
$-1.1479*X + 12.8942*Y - 6.3023*Z + 3.2909 = 0.0$			
I(1)	-0.0760	C(3)	0.0220
I(2)	0.0110	C(4)	0.1664
O(1)	-0.0387	C(5)	0.0050
C(1)	-0.0286	C(6)	-0.0447
C(2)	-0.0163		
Plane II fitting I(3)-I(4)-O(3)-C(8)-C(9)-C(10)-C(11)-C(12)-C(13)			
$1.8089*X + 11.5995*Y - 6.6560*Z - 0.1660 = 0.0$			
I(3)	0.1180	C(10)	-0.0089
I(4)	0.0701	C(11)	0.0087
O(3)	-0.1254	C(12)	-0.0378
C(8)	-0.0070	C(13)	-0.0537
C(9)	0.0360		
Plane III fitting O(2)-C(1)-C(6)-C(7)-C(8)-C(13)			
$-0.1579*X + 12.4849*Y - 6.4901*Z + 2.3118 = 0.0$			
O(2)	0.0677	C(7)	0.0517
C(1)	-0.0165	C(8)	0.0025
C(6)	-0.0408	C(13)	-0.0646
Plane IV fitting CL(1) through CL(4)-C(7)-C(14) through C(20)			
$12.0938*X - 3.7179*Y - 4.9812*Z - 11.3683 = 0.0$			
CL(1)	0.0939	C(15)	-0.0414
CL(2)	-0.0595	C(16)	0.0599
CL(3)	0.0037	C(17)	0.0472
CL(4)	-0.0378	C(18)	0.0175
C(7)	-0.0465	C(19)	-0.1048
C(14)	0.0331	C(20)	0.0348
Plane V fitting O(4)-O(5)-C(14)-C(15)			
$6.8642*X + 8.8832*Y + 0.9192*Z - 9.6292 = 0.0$			
O(4)	0.0112	C(14)	-0.0285
O(5)	0.0078	C(15)	0.0094

Table 13. (continued)

Atom	Distance from Plane(Å)	Atom	Distance from Plane(Å)
Plane VI fitting C(21) through C(27)			
$3.5398*X + 7.6632*Y - 8.1748*Z + 3.5815 = 0.0$			
C(21)	0.0117	C(25)	0.1033
C(22)	-0.0697	C(26)	-0.0326
C(23)	0.1008	C(27)	0.0168
C(24)	-0.1303		
Plane VII fitting C(28) through C(34)			
$1.0013*X - 13.8383*Y + 5.2715*Z - 0.2125 = 0.0$			
C(28)	0.0656	C(32)	-0.0990
C(29)	-0.0583	C(33)	0.1644
C(30)	-0.0415	C(34)	-0.0984
C(31)	0.0672		
Plane VIII fitting C(3)-O(1)-C(28)			
$9.8885*X + 2.5067*Y + 3.0597*Z - 16.3025 = 0.0$			
Interplanar Angles(°)			
<u>Plane</u>		<u>Plane</u>	<u>Angle</u>
I		II	167.46
I		VI	28.29
I		VII	8.93
I		VIII	89.26
II		VI	19.84
II		VII	15.78
II		VIII	81.28
III		IV	75.09
III		VI	24.86
III		VII	10.38
III		VIII	93.20
IV		V	107.33
V		VI	108.80
VI		VIII	91.48
VII		VIII	82.77

Figure 3. ORTEP drawing of  $C_{34}H_{16}Cl_4I_4O_5$  (2) excluding the hydrogen atoms and the benzylic groups



graphic residual factor at such a stage was 12.3%. Upon examining the intensity data we find that there are not many observed reflections beyond a  $2\theta$  of  $25^\circ$ . Obviously this explains a higher crystallographic residual and the ensuing large estimated standard deviations (e.s.d's) (Tables 9 - 12). In particular the e.s.d's in the positional and anisotropic thermal parameters and hence the e.s.d's of the derived results for the benzylic atoms show abnormally high values. This is due to the observation that during refinement these atoms showed no tendency to "settle down". Thus any discussion of the geometrical features of these groups is not going to be fruitful (however see later). Nevertheless it appears fairly certain that compound 2 has two benzyl groups, one of which is involved in an ether linkage with the phenolic oxygen O(1) while the other is involved in an ester linkage with carboxylic oxygen O(5).

We need then to focus our attention on the xanthene dye component with which we are really concerned. The molecular conformation (Figure 3) shows that the tetrachlorobenzene ring and the xanthene heterocycle moiety are at an angle of  $75^\circ$  to each other. On the other hand these same planes, in the case of fluorescein perchlorate<sup>4</sup> or erythrosin<sup>5</sup>, are only about  $7^\circ$  away from being perpendicular to each other. An explanation for this difference comes from packing considerations (see later).

The tetrachlorobenzene part appears to be executing two kinds of thermal motion. One is a rotational oscillation about the C(7)-C(20) bond. The other is the "nodding" vibration about C(7) and it is in the plane of the group. These are visible from the directions of maximum amplitude of vibration for the chlorine atoms. These thermal motions are



partly responsible for the large temperature factors observed for benzylic carbon atoms C(21)-C(27) and for their unwillingness to "settle down" during refinement.

The shorter bond distance of 1.21(7) Å for O(3)-C(11) bond can be taken to indicate that O(3) is indeed the quinoidal oxygen. This conclusion is supported by the longer bond distance of 1.38(6) Å observed for O(1)-C(3), a distance which is normal for a phenolic ether linkage. The quinoid and the phenolic rings are about 13° from being coplanar. This is perhaps the result of ring B being in a deformed boat conformation as is the case with compound 1 (Table 13).

The carboxyl group is tipped 107° with respect to the tetrachlorobenzene group, whereas in the case of fluorescein perchlorate<sup>4</sup> and erythrosin<sup>5</sup> (with free carboxylate group and free carboxylic acid group respectively) these groups are coplanar. In the latter cases, this orientation makes sense as it would be expected to favor the stabilizing effect of the overlap of the  $\pi$ -electrons of the carboxyl group with the aromatic  $\pi$ -electron cloud. In our case this overlap is clearly not possible; the O(5)-benzyl group folds towards the xanthene heterocycle (during nucleation of the crystals) rotating the carboxylic group about the C(14)-C(15) bond in such a way that the plane of the O(5)-benzyl group aligns almost parallel (Table 13) to the xanthene plane thereby enhancing the packing efficiency. The abnormally low C(14)-C(15) distance of 1.33(6) Å and other unusual distances throughout the molecule are likely only a consequence of the incomplete refinement.

Unlike compound 1, no solvent of crystallization was seen in the final electron density map. The benzylic planes VI and VII and the planes of rings A, B and C are not far from being parallel to each other

Figure 4. Unit cell drawing of  $C_{34}H_{16}Cl_4I_4O_5$  (2) excluding the hydrogen atoms and the benzylic groups

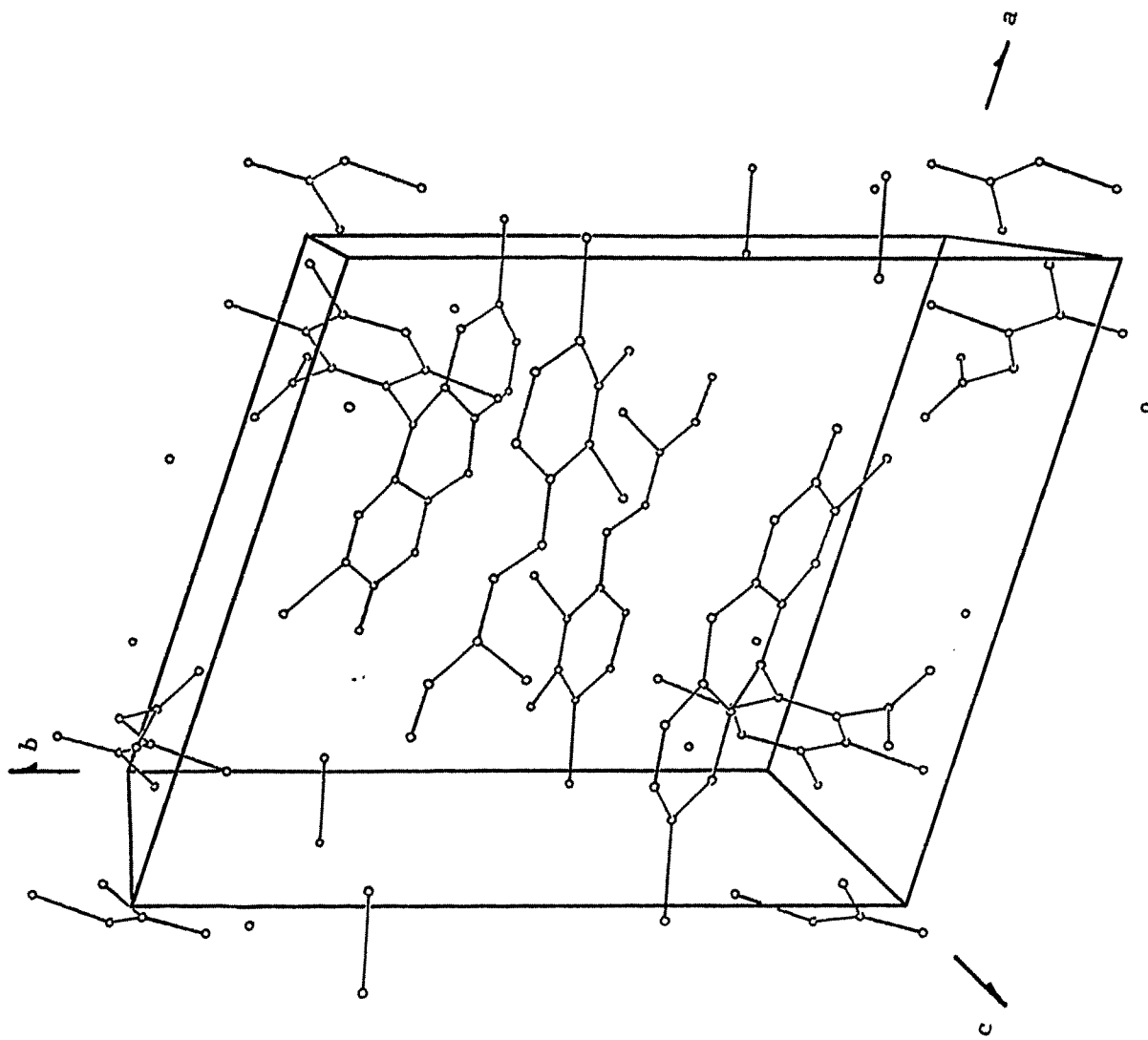


(Table 13) and thus they seem to stack up in the crystal (Figure 4). Both these benzyl groups are hanging into large voids caused during the nucleation of the crystals as a result of the awkward shape of the main molecule. And it is likely that the lack of significant interaction directly contributes to the large thermal motion/disorder that is observed.

Structure of C<sub>32</sub>H<sub>34</sub>Cl<sub>4</sub>I<sub>4</sub>N<sub>2</sub>O<sub>5</sub> (3) The final atomic positional and anisotropic thermal parameters are listed respectively in Tables 14 and 15 while the refined bond distances and bond angles are listed in Tables 16 and 17 respectively. Table 18 furnishes some details about a few least squares planes. Figure 5 and 6 show the ORTEP<sup>15</sup> drawings of the two independent molecules (omitting the hydrogen atoms and the triethylammonium counter-ions for clarity) whereas Figure 7 shows the unit cell drawing (the hydrogen atoms H(5), H(9), H(37) and H(41) and the ethyl groups of the counter-ions are omitted, again for the sake of clarity).

x-ray crystal structure analysis of 3 reveals that the asymmetric unit is made up of two independent molecules of the bistriethylammonium salt of rose bengal. The presence of two independent molecules (94 non-hydrogen atoms) presented a lot of problems during the initial stages of structure determination and refinement. It was mentioned in the previous section that the carbon atoms of the rings A, B, C and E and the atoms of the cations were all refinable only isotropically and that the final crystallographic residual was 6.9%. This incomplete, but justifiably sufficient, refinement explains the relatively large e.s.d's of the positional parameters, thermal parameters and the derived results.

Table 14. Positional parameters<sup>a</sup> ( $\times 10^4$ ) for  $C_{32}H_{34}CL_4I_4N_2O_5$  (3)

Atom	x	y	z	$U_{iso}^b$
I(1)	2757(2)	7889(2)	-1880(2)	74(1)
I(2)	0438(1)	7665(2)	1103(2)	67(1)
I(3)	1036(2)	7665(2)	4396(2)	92(2)
I(4)	4149(2)	7895(2)	5992(2)	80(2)
CL(1)	3287(5)	9307(5)	1718(6)	63(5)
CL(2)	4838(6)	9348(6)	0779(7)	80(6)
CL(3)	6522(6)	7765(7)	0457(8)	98(7)
CL(4)	6670(6)	6163(6)	1157(8)	101(6)
O(1)	1259(12)	7660(13)	-0919(13)	67(12)
O(2)	1962(11)	7610(11)	2457(12)	46(10)
O(3)	2400(14)	7783(16)	5869(15)	88(15)
O(4)	5334(15)	6021(15)	2790(17)	93(16)
O(5)	4763(20)	5873(15)	1369(21)	127(20)
N(1)	1408(17)	6473(16)	-2357(20)	76
N(2)	4206(17)	4878(16)	2107(20)	76
C(1)	2142(18)	7654(17)	1506(20)	47(8)
C(2)	1590(18)	7657(17)	0781(21)	51(9)
C(3)	1753(17)	7680(16)	-0233(19)	40(8)
C(4)	2525(19)	7739(18)	-0398(22)	55(9)
C(5)	3097(17)	7734(16)	0258(20)	42(8)
C(6)	2904(17)	7710(16)	1302(20)	43(8)
C(7)	3474(17)	7666(16)	2051(19)	39(8)
C(8)	3237(16)	7679(16)	3035(19)	37(8)
C(9)	3754(17)	7707(16)	3851(19)	40(8)
C(10)	3452(17)	7770(16)	4752(19)	40(8)
C(11)	2675(17)	7736(16)	5014(20)	43(8)
C(12)	2216(19)	7677(17)	4171(21)	52(9)
C(13)	2461(16)	7642(15)	3203(18)	35(8)
C(14)	4253(17)	7713(16)	1790(19)	37(8)
C(15)	5002(17)	6975(16)	1672(19)	38(8)
C(16)	5691(18)	7069(17)	1313(21)	50(9)
C(17)	5665(18)	7730(17)	1007(21)	49(9)
C(18)	4922(19)	8479(18)	1143(22)	59(9)
C(19)	4214(18)	8424(17)	1543(21)	49(9)
C(20)	5064(20)	6180(19)	1993(23)	65(10)

<sup>a</sup>The estimated standard deviations in the parentheses are for the least significant digits. Parameters for hydrogen atoms are multiplied by  $10^3$ .

<sup>b</sup>For anisotropically refined atoms,  $U_{iso} \equiv 10^3/3 \sum_{i,j} a_i^* a_j^* \vec{a}_i \cdot \vec{a}_j$ , where the temperature factors are defined as  $\exp(-2\pi^2 \sum_{h,j} h_j a_j^* U_{ij})$ .

Table 14. (continued)

Atom	x	y	z	U <sub>iso</sub>
C(21)	0620(22)	6889(21)	-2948(25)	95(9)
C(22)	-0116(22)	7193(21)	-2278(25)	119(13)
C(23)	2111(22)	6196(21)	-3131(25)	115(14)
C(24)	2953(22)	5814(20)	-2639(25)	148(17)
C(25)	1414(22)	5837(21)	-1785(25)	103(13)
C(26)	1295(22)	5224(21)	-2432(25)	138(17)
C(27)	4430(21)	4735(21)	3171(25)	137(15)
C(28)	4058(22)	5394(21)	4002(25)	181(19)
C(29)	4703(22)	4125(21)	1463(25)	112(13)
C(30)	4490(22)	3442(21)	1533(25)	152(16)
C(31)	3283(22)	5281(21)	2048(25)	207(20)
C(32)	3158(22)	5462(20)	0993(25)	171(18)
I(5)	2538(2)	0214(1)	-0920(2)	75(1)
I(6)	0726(2)	3880(1)	-0307(2)	78(1)
I(7)	1026(2)	5352(2)	2440(2)	102(2)
I(8)	3537(2)	3785(1)	5576(2)	76(1)
CL(5)	4684(5)	1453(5)	2029(6)	70(5)
CL(6)	5858(6)	-0110(6)	2968(7)	84(5)
CL(7)	5071(6)	-0945(5)	4192(7)	83(5)
CL(8)	3116(6)	-0195(5)	4483(6)	69(5)
O(6)	1367(13)	2055(13)	-1260(14)	70(13)
O(7)	1700(11)	3514(11)	1673(13)	53(11)
O(8)	2024(17)	5113(14)	4461(19)	112(16)
O(9)	1823(13)	0859(12)	2737(14)	60(12)
O(10)	1641(12)	1765(12)	4052(13)	62(11)
N(3)	0664(17)	0289(16)	2518(20)	76
N(4)	1647(17)	2507(16)	5870(20)	76
C(33)	1872(18)	2765(17)	1103(20)	47(8)
C(34)	1490(17)	2785(16)	0244(19)	39(8)
C(35)	1668(18)	2075(17)	-0431(21)	50(9)
C(36)	2240(17)	1292(16)	-0018(19)	37(8)
C(37)	2594(19)	1313(18)	0902(21)	53(9)
C(38)	2406(17)	2051(16)	1497(19)	39(8)
C(39)	2831(18)	2068(18)	2381(22)	54(9)
C(40)	2659(19)	2821(18)	2915(22)	55(9)
C(41)	3071(17)	2926(16)	3828(19)	40(8)
C(42)	2900(19)	3669(18)	4303(22)	55(9)
C(43)	2268(20)	4413(19)	3982(23)	61(9)
C(44)	1872(20)	4328(19)	3070(23)	60(9)
C(45)	2063(18)	3591(17)	2581(21)	52(9)
C(46)	3376(18)	1314(17)	2822(21)	47(8)
C(47)	3025(18)	0946(17)	3357(21)	48(8)
C(48)	3558(21)	0264(20)	3831(24)	67(10)
C(49)	4415(19)	-0069(18)	3696(22)	58(9)
C(50)	4773(19)	0290(19)	3150(22)	60(9)

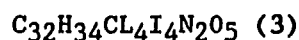
Table 14. (continued)

Atom	x	y	z	U <sub>iso</sub>
C(51)	4247(16)	1007(16)	2720(19)	36(7)
C(52)	2066(18)	1207(17)	3392(20)	46(8)
C(53)	-0264(22)	0800(21)	2776(25)	78(10)
C(54)	-0764(22)	0308(21)	2783(26)	79(10)
C(55)	1147(22)	-0375(21)	3158(25)	79(11)
C(56)	0991(22)	-0012(20)	4265(25)	79(11)
C(57)	0873(22)	-0109(20)	1432(25)	86(11)
C(58)	0574(22)	0520(21)	0737(25)	117(14)
C(59)	1092(22)	2318(21)	6510(25)	77(10)
C(60)	1350(22)	1439(20)	6454(25)	82(11)
C(61)	1284(22)	3424(21)	5850(25)	87(12)
C(62)	0642(22)	3720(20)	5090(25)	116(13)
C(63)	2575(22)	2138(21)	6126(25)	84(11)
C(64)	2726(21)	2414(20)	7168(25)	83(12)
H(5)	378	774	12	76
H(9)	434	773	370	76
H(211)	60	652	-352	76
H(212)	70	739	-316	76
H(221)	-49	784	-220	76
H(222)	6	707	-148	76
H(223)	-50	691	-245	76
H(231)	212	674	-332	76
H(232)	215	581	-369	76
H(241)	329	616	-264	76
H(242)	289	572	-191	76
H(243)	334	523	-305	76
H(251)	98	609	-122	76
H(252)	203	548	-154	76
H(261)	177	474	-266	76
H(262)	88	506	-193	76
H(263)	84	552	-297	76
H(271)	506	436	318	76
H(272)	409	441	336	76
H(281)	467	562	400	76
H(282)	420	521	468	76
H(283)	361	590	389	76
H(291)	535	394	146	76
H(292)	454	427	64	76
H(301)	390	365	150	76
H(302)	479	325	218	76
H(303)	485	299	92	76
H(311)	305	584	263	76
H(312)	301	494	231	76

Table 14. (continued)

Atom	x	y	z	U <sub>iso</sub>
H(321)	362	498	54	76
H(322)	321	600	93	76
H(323)	256	553	78	76
H(37)	305	77	116	76
H(41)	348	237	411	76
H(531)	-57	125	230	76
H(532)	-33	108	352	76
H(541)	-141	74	276	76
H(542)	-63	3	339	76
H(543)	-59	-7	212	76
H(551)	176	-61	309	76
H(552)	89	-78	315	76
H(561)	133	-35	481	76
H(562)	30	24	455	76
H(563)	103	59	442	76
H(571)	71	-58	125	76
H(572)	161	-46	135	76
H(581)	98	78	71	76
H(582)	-2	91	93	76
H(583)	60	21	-1	76
H(591)	47	261	625	76
H(592)	110	255	725	76
H(601)	203	106	643	76
H(602)	112	125	705	76
H(603)	115	119	578	76
H(611)	170	361	563	76
H(612)	97	372	651	76
H(621)	41	434	516	76
H(622)	13	360	535	76
H(623)	87	341	444	76
H(631)	285	237	563	76
H(632)	279	155	605	76
H(641)	275	298	714	76
H(642)	211	261	758	76
H(643)	318	200	742	76
H(1)	135	693	-180	76
H(2)	441	525	183	76
H(3)	110	50	260	76
H(4)	165	222	517	76



Table 15. Anisotropic thermal parameters<sup>a</sup> ( $\times 10^3$ ) for

Atom	U <sub>11</sub>	U <sub>22</sub>	U <sub>33</sub>	U <sub>23</sub>	U <sub>13</sub>	U <sub>12</sub>
I(1)	96(2)	92(2)	36(1)	16(1)	-07(1)	-45(2)
I(2)	65(2)	100(2)	54(1)	21(1)	-16(1)	-52(2)
I(3)	94(2)	154(3)	59(2)	26(2)	-08(2)	-83(2)
I(4)	95(2)	124(2)	41(1)	25(1)	-25(1)	-66(2)
CL(1)	74(7)	49(5)	60(6)	14(4)	-07(5)	-23(5)
CL(2)	108(8)	81(7)	80(7)	28(5)	-01(6)	-65(7)
CL(3)	78(7)	143(10)	102(8)	37(7)	-10(6)	-71(7)
CL(4)	53(6)	103(8)	121(9)	17(7)	-08(6)	-15(6)
O(1)	41(14)	110(18)	39(13)	-01(12)	-20(11)	-28(13)
O(2)	41(13)	62(14)	35(11)	08(10)	-12(10)	-25(11)
O(3)	80(18)	151(23)	41(14)	21(14)	00(13)	-58(17)
O(4)	110(21)	113(21)	77(17)	51(15)	-39(16)	-64(18)
O(5)	192(30)	91(20)	139(25)	54(18)	-82(23)	-95(22)
I(5)	92(2)	73(2)	55(2)	04(1)	-14(1)	-36(2)
I(6)	81(2)	68(2)	76(2)	34(1)	-32(1)	-24(1)
I(7)	109(2)	56(2)	109(2)	15(2)	-37(2)	-12(2)
I(8)	91(2)	77(2)	57(2)	04(1)	-21(1)	-40(2)
CL(5)	66(6)	84(7)	73(6)	35(5)	-13(5)	-41(6)
CL(6)	56(6)	87(7)	107(8)	35(6)	-22(6)	-29(6)
CL(7)	79(7)	69(6)	94(7)	50(6)	-29(6)	-22(6)
CL(8)	80(7)	70(6)	75(6)	40(5)	-15(5)	-44(6)
O(6)	80(17)	99(18)	41(13)	23(12)	-35(12)	-49(15)
O(7)	51(14)	55(13)	54(13)	32(11)	-21(11)	-23(12)
O(8)	138(24)	62(17)	108(21)	-07(15)	-38(18)	-30(17)
O(9)	77(16)	74(16)	50(13)	18(12)	-17(12)	-53(14)
O(10)	60(15)	68(15)	35(12)	-03(11)	-09(11)	-14(12)

<sup>a</sup>The estimated standard deviations in the parentheses are for the least significant digits. The anisotropic temperature factors are defined as  $\exp(-2\pi^2 \sum h_i h_j a_i^* a_j^* U_{ij})$ .

Table 16. Refined bond distances<sup>a</sup> (Å) for C<sub>32</sub>H<sub>34</sub>CL<sub>4</sub>I<sub>4</sub>N<sub>2</sub>O<sub>5</sub> (3)

Atoms	Distance	Atoms	Distance
I(1) - C(4)	2.13(4)	I(5) - C(36)	2.10(3)
I(2) - C(2)	2.15(4)	I(6) - C(34)	2.07(3)
I(3) - C(12)	2.20(4)	I(7) - C(44)	2.07(4)
I(4) - C(10)	2.15(3)	I(8) - C(42)	2.11(4)
CL(1) - C(19)	1.71(4)	CL(5) - C(51)	1.75(3)
CL(2) - C(18)	1.70(4)	CL(6) - C(50)	1.76(4)
CL(3) - C(17)	1.78(4)	CL(7) - C(49)	1.71(4)
CL(4) - C(16)	1.78(4)	CL(8) - C(48)	1.74(4)
O(1) - C(3)	1.30(4)	O(6) - C(35)	1.25(4)
O(2) - C(1)	1.35(4)	O(7) - C(33)	1.43(4)
O(2) - C(13)	1.36(4)	O(7) - C(45)	1.42(4)
O(3) - C(11)	1.25(4)	O(8) - C(43)	1.28(5)
O(4) - C(20)	1.18(5)	O(9) - C(52)	1.25(4)
O(5) - C(20)	1.24(5)	O(10) - C(52)	1.25(4)
N(1) - C(21)	1.53(5)	N(3) - C(53)	1.52(5)
N(1) - C(23)	1.52(5)	N(3) - C(55)	1.49(5)
N(1) - C(25)	1.49(5)	N(3) - C(57)	1.55(5)
N(2) - C(27)	1.51(5)	N(4) - C(59)	1.53(5)
N(2) - C(29)	1.47(5)	N(4) - C(61)	1.53(5)
N(2) - C(31)	1.49(5)	N(4) - C(63)	1.54(5)
C(1) - C(2)	1.39(5)	C(33) - C(34)	1.34(5)
C(1) - C(6)	1.48(5)	C(33) - C(38)	1.39(5)
C(2) - C(3)	1.42(5)	C(34) - C(35)	1.44(5)
C(3) - C(4)	1.49(5)	C(35) - C(36)	1.50(5)
C(4) - C(5)	1.36(5)	C(36) - C(37)	1.40(5)
C(5) - C(6)	1.47(5)	C(37) - C(38)	1.43(5)
C(6) - C(7)	1.42(5)	C(38) - C(39)	1.42(5)
C(7) - C(8)	1.40(5)	C(39) - C(40)	1.42(5)
C(7) - C(14)	1.52(5)	C(39) - C(46)	1.47(5)
C(8) - C(9)	1.45(5)	C(40) - C(41)	1.48(5)
C(8) - C(13)	1.48(4)	C(40) - C(45)	1.45(5)
C(9) - C(10)	1.32(5)	C(41) - C(42)	1.37(5)
C(10) - C(11)	1.50(5)	C(42) - C(43)	1.43(5)
C(11) - C(12)	1.43(5)	C(43) - C(44)	1.45(5)
C(12) - C(13)	1.38(5)	C(44) - C(45)	1.36(5)
C(14) - C(15)	1.41(5)	C(46) - C(47)	1.40(5)
C(14) - C(19)	1.39(5)	C(46) - C(51)	1.41(5)
C(15) - C(16)	1.45(5)	C(47) - C(48)	1.40(5)

<sup>a</sup>The estimated standard deviations in the parentheses are for the least significant digits.

Table 16. (continued)

Atoms	Distance	Atoms	Distance
C(15) - C(20)	1.56(5)	C(47) - C(52)	1.58(5)
C(16) - C(17)	1.33(5)	C(48) - C(49)	1.39(5)
C(17) - C(18)	1.41(5)	C(49) - C(50)	1.41(5)
C(18) - C(19)	1.46(5)	C(50) - C(51)	1.41(5)
C(21) - C(22)	1.47(6)	C(53) - C(54)	1.59(6)
C(23) - C(24)	1.53(6)	C(55) - C(56)	1.55(6)
C(25) - C(26)	1.48(6)	C(57) - C(58)	1.48(6)
C(27) - C(28)	1.49(6)	C(59) - C(60)	1.49(6)
C(29) - C(30)	1.53(6)	C(61) - C(62)	1.48(6)
C(31) - C(32)	1.49(6)	C(63) - C(64)	1.52(6)
N(1) - O(1) <sup>b</sup>	2.73(4)	N(3) - O(9)	2.80(4)
N(2) - O(5)	2.80(5)	N(4) - O(10)	2.71(4)

<sup>b</sup>The N - O distances are non-bonding distances and these are the lengths of the hydrogen-bonds.

Table 17. Refined bond Angles<sup>a</sup> (°) for C<sub>32</sub>H<sub>34</sub>CL<sub>4</sub>I<sub>4</sub>N<sub>2</sub>O<sub>5</sub> (3)

Atoms	Angle	Atoms	Angle
C(1) - O(2) - C(13)	120(3)	C(33)- O(7) - C(45)	126(3)
C(21)- N(1) - C(23)	104(3)	C(53)- N(3) - C(55)	116(3)
C(21)- N(1) - C(25)	113(3)	C(53)- N(3) - C(57)	114(3)
C(23)- N(1) - C(25)	117(3)	C(55)- N(3) - C(57)	106(3)
C(27)- N(2) - C(29)	109(3)	C(59)- N(4) - C(61)	111(3)
C(27)- N(2) - C(31)	109(3)	C(59)- N(4) - C(63)	117(3)
C(29)- N(2) - C(31)	118(3)	C(61)- N(4) - C(63)	109(3)
O(2) - C(1) - C(2)	118(3)	O(7) - C(33)- C(34)	119(3)
O(2) - C(1) - C(6)	118(3)	O(7) - C(33)- C(38)	118(3)
C(2) - C(1) - C(6)	124(3)	C(34)- C(33)- C(38)	123(3)
I(2) - C(2) - C(1)	123(3)	I(6) - C(34)- C(33)	120(2)
I(2) - C(2) - C(3)	116(2)	I(6) - C(34)- C(35)	115(2)
C(1) - C(2) - C(3)	121(3)	C(33)- C(34)- C(35)	124(3)
O(1) - C(3) - C(2)	121(3)	O(6) - C(35)- C(34)	127(3)
O(1) - C(3) - C(4)	125(3)	O(6) - C(35)- C(36)	119(3)
C(2) - C(3) - C(4)	113(3)	C(34)- C(35)- C(36)	113(3)
I(1) - C(4) - C(3)	116(2)	I(5) - C(36)- C(35)	117(2)
I(1) - C(4) - C(5)	114(3)	I(5) - C(36)- C(37)	123(2)
C(3) - C(4) - C(5)	130(3)	C(35)- C(36)- C(37)	119(3)
C(4) - C(5) - C(6)	115(3)	C(36)- C(37)- C(38)	123(3)
C(1) - C(6) - C(5)	117(3)	C(33)- C(38)- C(37)	117(3)
C(1) - C(6) - C(7)	123(3)	C(33)- C(38)- C(39)	120(3)
C(5) - C(6) - C(7)	120(3)	C(37)- C(38)- C(39)	122(3)
C(6) - C(7) - C(8)	118(3)	C(38)- C(39)- C(40)	120(3)
C(6) - C(7) - C(14)	120(3)	C(38)- C(39)- C(46)	121(3)
C(8) - C(7) - C(14)	122(3)	C(40)- C(39)- C(46)	119(3)
C(7) - C(8) - C(9)	121(3)	C(39)- C(40)- C(41)	126(3)
C(7) - C(8) - C(13)	117(3)	C(39)- C(40)- C(45)	122(3)
C(9) - C(8) - C(13)	122(3)	C(41)- C(40)- C(45)	112(3)
C(8) - C(9) - C(10)	116(3)	C(40)- C(41)- C(42)	124(3)
I(4) - C(10)- C(9)	118(3)	I(8) - C(42)- C(41)	122(3)
I(4) - C(10)- C(11)	116(2)	I(8) - C(42)- C(43)	116(3)
C(9) - C(10)- C(11)	127(3)	C(41)- C(42)- C(43)	122(3)
O(3) - C(11)- C(10)	126(3)	O(8) - C(43)- C(42)	124(3)
O(3) - C(11)- C(12)	120(3)	O(8) - C(43)- C(44)	120(3)
C(10)- C(11)- C(12)	114(3)	C(42)- C(43)- C(44)	115(3)
I(3) - C(12)- C(11)	120(2)	I(7) - C(44)- C(43)	120(3)
I(3) - C(12)- C(13)	117(2)	I(7) - C(44)- C(45)	118(3)
C(11)- C(12)- C(13)	124(3)	C(43)- C(44)- C(45)	122(3)
O(2) - C(13)- C(8)	124(3)	O(7) - C(45)- C(40)	114(3)
O(2) - C(13)- C(12)	119(3)	O(7) - C(45)- C(44)	122(3)

<sup>a</sup>The estimated standard deviations in the parentheses are for the least significant digits.

Table 17. (continued)

Atoms	Angle	Atoms	Angle
C(8) - C(13)- C(12)	118(3)	C(40)- C(45)- C(44)	124(3)
C(7) - C(14)- C(15)	116(3)	C(39)- C(46)- C(47)	120(3)
C(7) - C(14)- C(19)	122(3)	C(39)- C(46)- C(51)	118(3)
C(15)- C(14)- C(19)	121(3)	C(47)- C(46)- C(51)	122(3)
C(14)- C(15)- C(16)	112(3)	C(46)- C(47)- C(48)	119(3)
C(14)- C(15)- C(20)	121(3)	C(46)- C(47)- C(52)	124(3)
C(16)- C(15)- C(20)	126(3)	C(48)- C(47)- C(52)	117(3)
CL(4)- C(16)- C(15)	115(2)	CL(8)- C(48)- C(47)	118(3)
CL(4)- C(16)- C(17)	116(3)	CL(8)- C(48)- C(49)	122(3)
C(15)- C(16)- C(17)	128(3)	C(47)- C(48)- C(49)	120(4)
CL(3)- C(17)- C(16)	125(3)	CL(7)- C(49)- C(48)	120(3)
CL(3)- C(17)- C(18)	115(3)	CL(7)- C(49)- C(50)	118(3)
C(16)- C(17)- C(18)	120(3)	C(48)- C(49)- C(50)	122(3)
CL(2)- C(18)- C(17)	123(3)	CL(6)- C(50)- C(49)	123(3)
CL(2)- C(18)- C(19)	123(3)	CL(6)- C(50)- C(51)	117(3)
C(17)- C(18)- C(19)	114(3)	C(49)- C(50)- C(51)	119(3)
CL(1)- C(19)- C(14)	119(3)	CL(5)- C(51)- C(46)	122(2)
CL(1)- C(19)- C(18)	117(3)	CL(5)- C(51)- C(50)	120(3)
C(14)- C(19)- C(18)	124(3)	C(46)- C(51)- C(50)	118(3)
O(4) - C(20)- O(5)	133(4)	O(9) - C(52)- O(10)	128(3)
O(4) - C(20)- C(15)	115(3)	O(9) - C(52)- C(47)	117(3)
O(5) - C(20)- C(15)	112(3)	O(10)- C(52)- C(47)	115(3)
N(1) - C(21)- C(22)	109(3)	N(3) - C(53)- C(54)	115(3)
N(1) - C(23)- C(24)	110(3)	N(3) - C(55)- C(56)	109(3)
N(1) - C(25)- C(26)	112(3)	N(3) - C(57)- C(58)	110(3)
N(2) - C(27)- C(28)	122(3)	N(4) - C(59)- C(60)	114(3)
N(2) - C(29)- C(30)	116(3)	N(4) - C(61)- C(62)	110(3)
N(2) - C(31)- C(32)	102(3)	N(4) - C(63)- C(64)	114(3)
C(3) - O(1) - N(1)	131(3)	C(52)- O(9) - N(3)	138(3)
C(20)- O(5) - N(2)	113(3)	C(52)- O(10)- N(4)	146(3)
O(1) - N(1) - C(21)	109	O(9) - N(3) - C(53)	105
O(1) - N(1) - C(23)	108	O(9) - N(3) - C(55)	107
O(1) - N(1) - C(25)	106	O(9) - N(3) - C(57)	107
O(5) - N(2) - C(27)	108	O(10)- N(4) - C(59)	106
O(5) - N(2) - C(29)	105	O(10)- N(4) - C(61)	107
O(5) - N(2) - C(31)	106	O(10)- N(4) - C(63)	106

Table 18. Equations of least squares planes (in the triclinic coordinate system) and interplanar angles for 3

Atom	Distance from Plane(Å)	Atom	Distance from Plane(Å) <sup>a</sup>
Plane I fitting I(1)-I(2)-O(1)-C(1)-C(2)-C(3)-C(4)-C(5)-C(6)			
$-0.6822*X + 16.0456*Y + 0.6458*Z - 12.2417 = 0.0$			
I(1)	0.1079	C(3)	-0.0537
I(2)	0.0988	C(4)	-0.0225
O(1)	-0.0961	C(5)	-0.0265
C(1)	-0.0098	C(6)	0.0153
C(2)	-0.0133	N(1)	-2.0952*
		H(1)	-1.3262*
Plane II fitting I(3)-I(4)-O(3)-C(8)-C(9)-C(10)-C(11)-C(12)-C(13)			
$-0.6730*X + 16.2324*Y - 0.9445*Z - 11.9320 = 0.0$			
I(3)	0.0252	C(10)	-0.0002
I(4)	0.0377	C(11)	-0.0287
O(3)	-0.0149	C(12)	-0.0141
C(8)	0.0286	C(13)	0.0047
C(9)	-0.0385		
Plane III fitting O(2)-C(1)-C(6)-C(7)-C(8)-C(13)			
$-0.6362*X + 16.1257*Y + 0.3197*Z - 12.2532 = 0.0$			
O(2)	-0.0273	C(7)	-0.0469
C(1)	0.0007	C(8)	0.0211
C(6)	0.0364	C(13)	0.0160
Plane IV fitting CL(1) through CL(4)-C(7)-C(14) through C(20)			
$6.5004*X + 4.9558*Y + 12.2689*Z - 8.7615 = 0.0$			
CL(1)	0.0951	C(15)	-0.0023
CL(2)	-0.0282	C(16)	0.0520
CL(3)	-0.1135	C(17)	-0.0125
CL(4)	0.0479	C(18)	0.0427
C(7)	-0.1878	C(19)	0.0458
C(14)	0.0222	C(20)	0.0385

<sup>a</sup>The distances marked with a \* are for those atoms not included in the calculation of the planes.

Table 18. (continued)

Atom	Distance from Plane(Å)	Atom	Distance from Plane(Å)
Plane V fitting O(4)-O(5)-C(15)-C(20)			
$13.6949*X - 1.4746*Y - 5.3501*Z - 4.9334 = 0.0$			
O(4)	-0.0096	C(15)	-0.0057
O(5)	-0.0090	C(20)	0.0243
N(2)	-1.0131*	H(2)	-0.6363*
Plane VI fitting I(5)-I(6)-O(6)-C(33)-C(34)-C(35)-C(36)-C(37)-C(38)			
$16.4355*X + 9.1568*Y - 6.1481*Z - 4.9063 = 0.0$			
I(5)	0.0261	C(35)	0.0003
I(6)	0.0294	C(36)	-0.0299
O(6)	-0.0035	C(37)	0.0050
C(33)	0.0243	C(38)	0.0060
C(34)	-0.0577		
Plane VII fitting I(7)-I(8)-O(8)-C(40)-C(41)-C(42)-C(43)-C(44)-C(45)			
$15.2023*X + 8.9250*Y - 7.7131*Z - 4.3466 = 0.0$			
I(7)	0.1087	C(42)	0.0182
I(8)	0.1080	C(43)	-0.0319
O(8)	-0.1465	C(44)	-0.0055
C(40)	-0.0351	C(45)	0.0038
C(41)	-0.0197		
Plane VIII fitting O(7)-C(33)-C(38)-C(39)-C(40)-C(45)			
$15.6830*X + 8.6521*Y - 7.1665*Z - 4.5097 = 0.0$			
O(7)	-0.0023	C(39)	0.0137
C(33)	0.0282	C(40)	0.0119
C(38)	-0.0345	C(45)	-0.0170
Plane IX fitting CL(5) through CL(8)-C(39)-C(46) through C(52)			
$5.0588*X + 10.3909*Y + 10.5015*Z - 6.0231 = 0.0$			
CL(5)	-0.0122	C(47)	0.0158
CL(6)	-0.0570	C(48)	0.0743
CL(7)	-0.0378	C(49)	0.0203
CL(8)	0.0589	C(50)	0.0009
C(39)	0.0577	C(51)	0.0283
C(46)	0.0131	C(52)	-0.1625

Table 18. (continued)

Atom	Distance from Plane(Å)	Atom	Distance from Plane(Å)
Plane X fitting O(9)-O(10)-C(47)-C(52)			
$3.8031*X + 14.4654*Y - 9.4397*Z + 0.6538 = 0.0$			
O(9)	0.0061	C(47)	0.0042
O(10)	0.0060	C(52)	-0.0163
N(3)	1.0511*	H(3)	0.6549*
N(4)	0.6332*	H(4)	0.3854*
Interplanar Angles(°)			
<u>Plane</u>		<u>Plane</u>	<u>Angle</u>
I		II	173.26
III		IV	102.11
IV		V	101.07
VI		VII	172.24
VIII		IX	99.54
IX		X	84.36



Figure 5. ORTEP drawing of  $C_{32}H_{34}Cl_4I_4N_2O_5$  (3) excluding the hydrogen atoms and the triethylammonium counterions (first independent molecule)

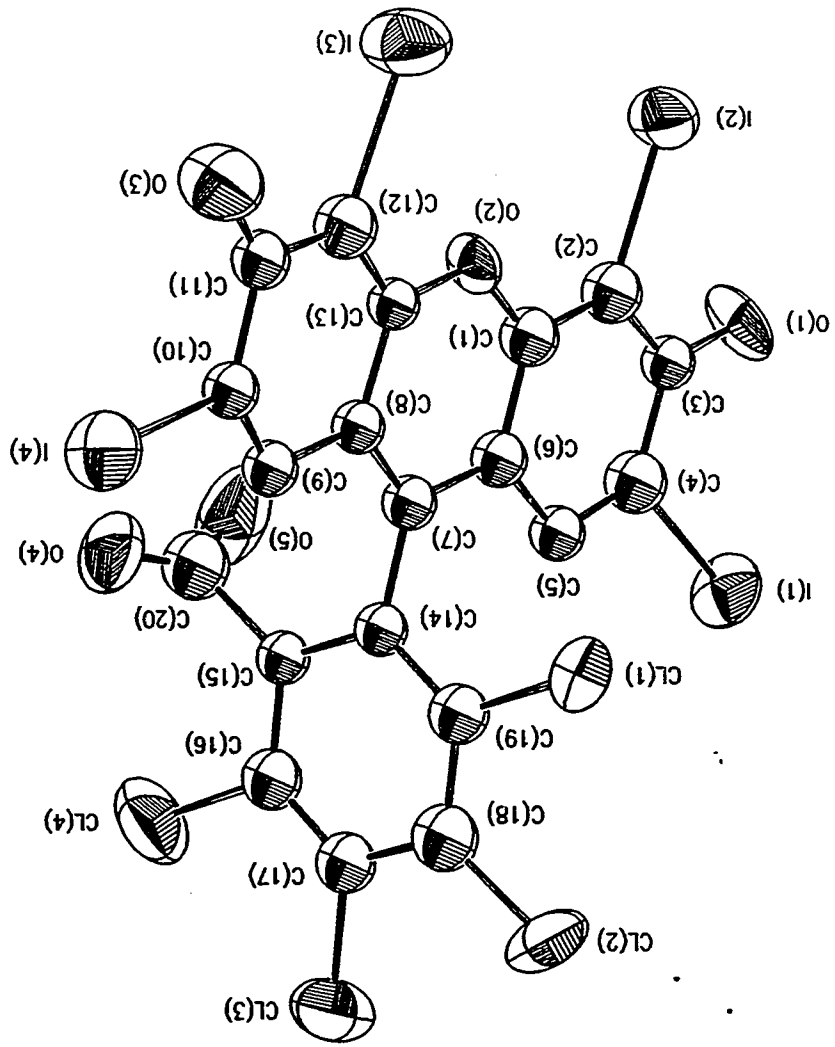
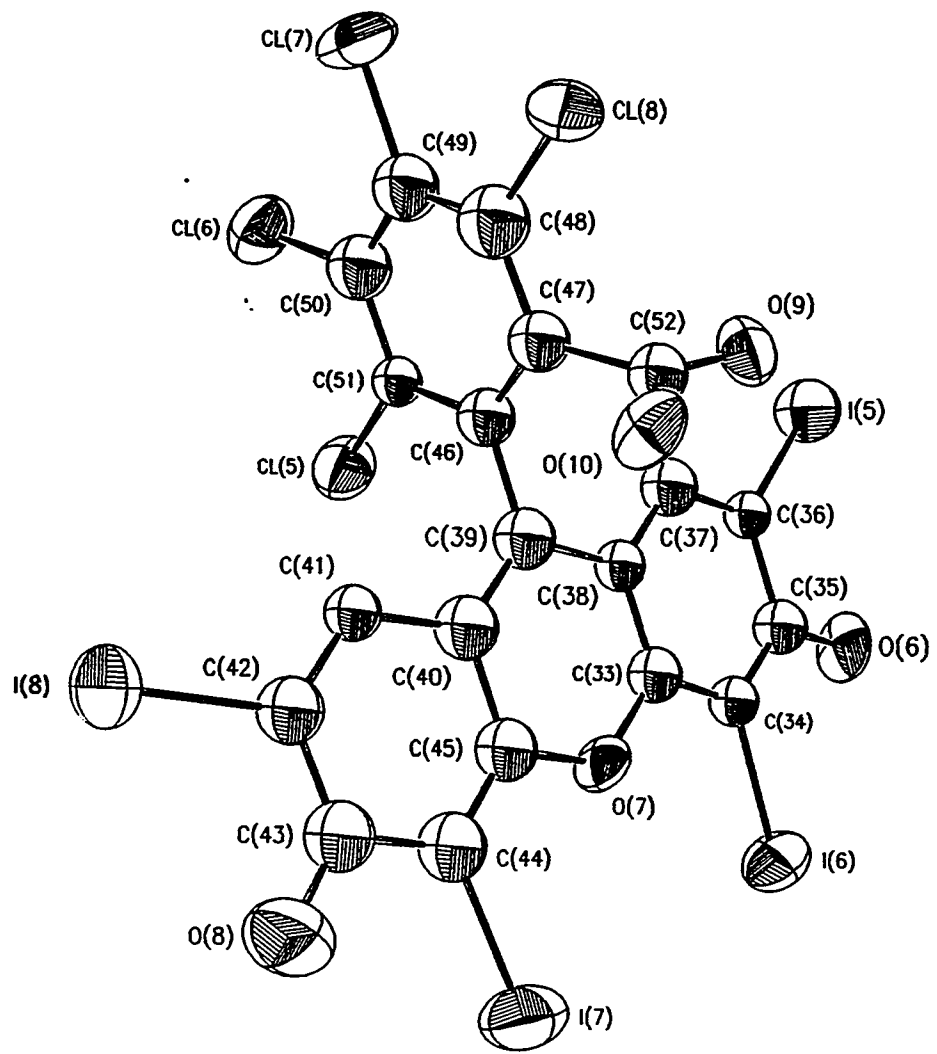


Figure 6. ORTEP drawing of  $C_{32}H_{34}Cl_4I_4N_2O_5$  (3) excluding the hydrogen atoms and the triethylammonium counterions (second independent molecule)

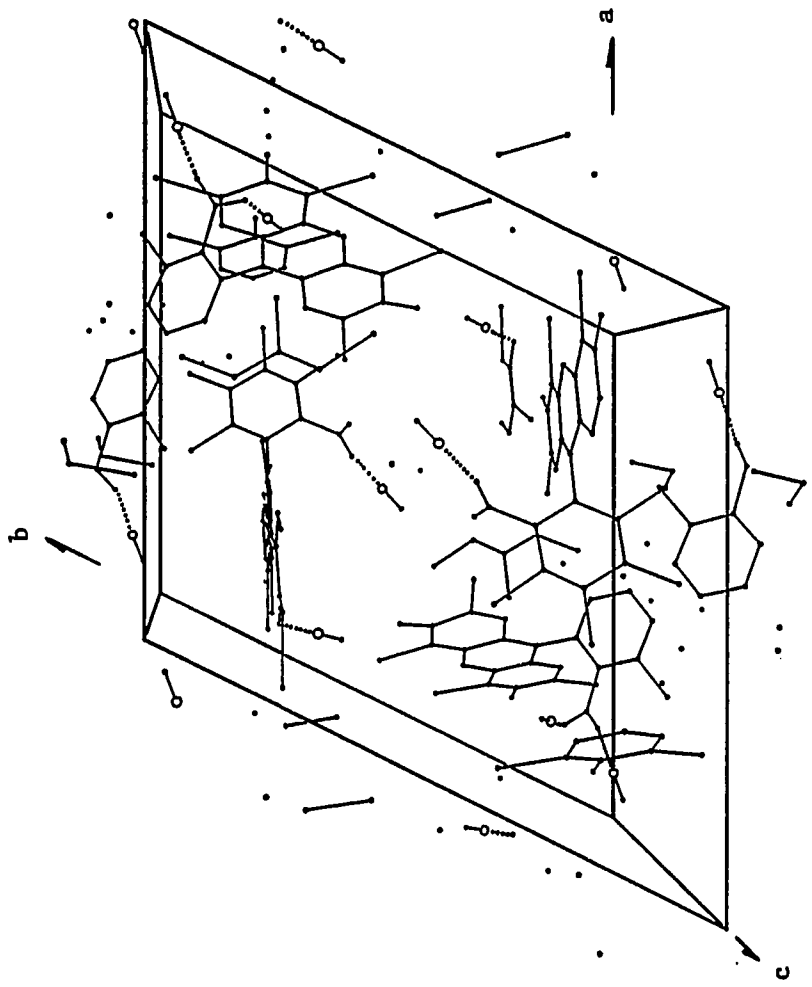


Both the independent molecules show very similar geometrical features. The relative orientations of the tetrachlorobenzene groups and the corresponding xanthene groups are within  $10^\circ$  from being normal to each other as are the carboxylate groups with respect to the tetrachlorobenzene groups. The latter groups, it must be noted, appear to be mainly undergoing the "nodding" vibrations about C(7) and C(39) atoms. These seemingly forced vibrations could be explained as due to the packing forces and the existence of the hydrogen bonds (see later).

The B rings are nearly planar and could not be clearly described as in a deformed boat conformation as was done in the case of compound 1. This makes sense as we expect rings A, B and C to be coplanar: The negative charge(s) on the phenoxide oxygen atom(s) has(have) nearly equal probability to be at either end of the xanthene group(s) by virtue of the fact that there is a series of alternate double bonds from one end to the other. This is reflected in the O(1)-C(3) and O(8)-C(43) distances (1.30(4) and 1.28(5) Å) being shorter than the usual C-O  $sp^2$ - $sp^3$  bond distance of 1.36 Å and in the O(3)-C(11) and O(6)-C(35) distances (1.25(5) and 1.25(4) Å) being larger than the usual C-O  $sp^2$ - $sp^2$  bond distance of 1.15 Å in extensively conjugated systems. However it seems likely that O(1) and O(8) are less quinoidic than O(3) and O(6).

Earlier it was mentioned that the carboxylate groups are within  $10^\circ$  of being normal to the respective tetrachlorobenzene groups. Unlike compound 2, we may expect these groups to be coplanar due to the easier possibility of the stabilizing overlap between the aromatic  $\pi$ -electrons and the  $\pi$ -system of the carboxylate group. However we are dealing with dianions and the two negative charges would tend to be as far apart as possible. Such is the situation when the carboxylate group is normal to

Figure 7. Unit cell drawing of  $C_{32}H_{34}Cl_4I_4N_2O_5$  (3) excluding the hydrogen atoms H(5), H(9), H(37) and H(41) and the ethyl groups of the triethylammonium counterions. Big circles are the hydrogen atoms. Hydrogen bonds are indicated by dotted lines



the tetrachlorobenzene part, which in turn must be normal to the xanthene heterocycle for a free dianion. The geometry in the two asymmetric units observed is close to the ideal one just described and the deviations from the ideal geometry are energetically compensated for in the crystal lattice by packing forces which include the existing hydrogen bonding.

The non-hydrogen atoms of the cations show large thermal motion as noted during refinement. This is clearly due to these groups occupying large cavities in the crystal. These cations take part in hydrogen bonding thereby adding to the lattice stability. The four symmetry independent cations exhibit hydrogen bonding in three different environments (Figure 7): N(2), which is close to the inversion center (1/2,1/2,1/2), hydrogen bonds to O(5) through H(2). As a result oxygen atom O(4), which is again close to (1/2,1/2,1/2), cannot be involved in any hydrogen bonding. This feature around one of the carboxylate anions means that O(4)-C(20) bond must be shorter than O(5)-C(20) and this is what is observed (Table 16). The other carboxylate group is such that both O(9) and O(10) are involved in hydrogen bonding with N(3) and N(4) through H(3) and H(4), respectively. Thus the distances O(9)-C(52) and O(10)-C(52) are not only longer than a regular C-O  $sp^2-sp^2$  bond but also nearly equal. The fourth hydrogen bond is between N(1) and O(1) through H(1). The evidence for all these four hydrogen bonds comes from the observation that the lengths of these hydrogen bonds are shorter than the sum of the van der Waals radii of the two atoms (N: 1.50 Å; O: 1.40 Å)<sup>18</sup> and the observation that the various O-N-C angles are not far from the tetrahedral angle of 109.5°. It is interesting to note that whereas O(1), one of the phenoxy oxygen atoms, can participate in hydrogen bonding, neither O(3) nor O(6) nor O(8) can do so due to packing



considerations. The various oxygen atoms involved in hydrogen bonding can be assumed to be in some  $sp^x$  hybridization ( $2 < x < 1$ ) state with one of the lone pair lobes pointing along the hydrogen bond charge.

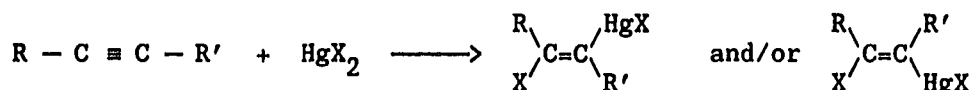
### Conclusion

The x-ray crystal structure analyses of the rose bengal derivatives establish unequivocally the independent existence of the colorless lactone form and the deeply red colored quinoid form in the solid state. The quinoid form 1 upon standing in atmosphere gradually changes its color to initially pale yellow and then to pale red. Perhaps the solvent of crystallization, 1,4-dioxane, gradually diffuses out of the crystal and the lactone bond cleaves resulting in the yellow colored zwitterion. The latter, on contact with moisture, gets transformed to the red colored quinoid form. However these chemical changes were minimized during our data collection by wedging the crystal in a sealed capillary. On a microscopic slide exposed to the atmosphere, these chemical changes result in the formation of an amorphous red colored layer on the surfaces of the crystals. The crystals of 2 and 3 on the other hand showed no observable changes, as one would expect, even after a long time. Finally it seems that the zwitterion form of rose bengal itself could be crystallized under suitably dry conditions using appropriate solution conditions; a single crystal study then would shed light on the conformations of these molecular forms in solution as well.

CRYSTAL STRUCTURE OF [N-(E-3-CHLOROMERCURIOPUT-2-ENYL)-  
N,N-DIMETHYLAMMONIUM]TRICHLOROMERCURATE(II) (4)

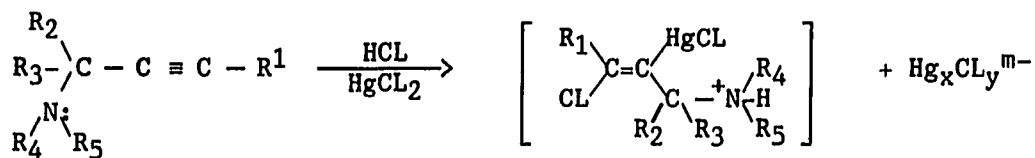
Introduction

Vinyl mercurials have proven to be versatile intermediates in organic synthesis.<sup>19</sup> While a number of methods are currently available for the synthesis of vinyl mercurials, the most elegant procedure involves the direct addition of mercury(II) salts to acetylenes:



These vinyl mercurials undergo a number of transformations useful in the regio- and stereospecific organic synthesis.<sup>19</sup>

Analogous to propargylic alcohols,<sup>20,21</sup> propargylic amines react with 1-2M mercuric chloride in 2-6M hydrochloric acid (to avoid polymerization via intermolecular aminomercuriation and to protect the amino group from oxidation) to precipitate the corresponding ammonium chloromercurate:<sup>22</sup>



The structure determination of these salts involves characterizing the organomercury cation as well as that of the chloromercurate anion. Elemental analyses of the salts can result in either the

$[R_3N(CLRHgCL)]HgCL_2$  or  $[R_3N(CLRHgCL)]HgCL_3$  composition. The  $^1H$  NMR spectra of the organomercury cations from terminal propargylic amines can unequivocally establish the addition product as the trans product, as is indicated in the above equation.<sup>23</sup> But establishing the nature of the anion in the case of chloromercurates based solely on elemental analysis is rather questionable because the halomercurates in general can be present in the monomeric, dimeric or polymeric forms. In particular especially when  $^1H$  NMR presents difficulty with regard to the regio- and stereochemistry of the mercuric chloride addition, the exact nature of the salt in its entirety can only be established by resorting to the x-ray single crystal study.<sup>22,23</sup>

This research involved x-ray structure determination of the title compound 4, which gave an elemental analysis corresponding to the second of the compositions given above. The  $^1H$  NMR spectra of compound 4, the mercuration product of 1-N,N-dimethylaminobut-2-yne (with internal acetylenic bond), was complicated by the apparent instability of the salt while in solution; thus no meaningful conclusion could be reached with regard to the regio- and stereochemistry of the mercuric chloride addition. Thus a single crystal of 4, prepared in Dr. Larock's research group (Department of Chemistry, Iowa State University), was subjected to analysis by x-ray crystallography.

### Experimental

Data collection      A nearly spherical single crystal of title compound with about 0.2mm diameter was wedged into a Lindeman glass capillary which was sealed with wax and mounted on a goniometer head.

The crystal is then optically centered on a four-circle diffractometer. Four  $\omega$ -oscillation photographs were taken from which the settings for sixteen reflections were obtained and input into an automatic indexing algorithm.<sup>7</sup> The resulting reduced cell and cell scalars revealed primitive monoclinic crystal symmetry. Crystal data are summarized in Table 19. Data were collected for the octants  $h,k,l$  and  $h,k,-l$  (see later). The intensities of eight standard near axial reflections were measured every 75 reflections during data collection to monitor any crystal decay. The decay for this compound was so severe that  $h,k,l$  data were collected on one crystal and  $h,k,-l$  data on another. Nearly 25% intensity decay was observed for both the crystals. The final unit cell parameters and their standard deviations were calculated from the tuned angles for twenty-nine reflections ( $15^\circ \leq 2\theta \leq 36^\circ$ ).

Reduction of x-ray intensity data      Decay corrections were applied to the data from both the crystals; they were based upon the observed decrease in standard reflection intensities with respect to reflection number. Empirical absorption corrections<sup>9</sup> were made based on observed variations in the intensity distribution(s) as a function of the orientation of the crystal(s) for reflection(s) near  $\chi = 90^\circ$ . Data were corrected for Lorentz and polarization effects. The two reduced data sets thus obtained for the two different crystals were then scaled using 120 reflections common to both the data sets; the scaled data sets were then merged and averaged (however, see later). The estimated variance in each intensity was calculated by

$$\sigma_I^2 = C_T + K_T^2 C_B + (0.03C_T)^2 + (0.03C_B)^2 + (0.03C_N)^2$$

Table 19. Crystal data for  $[\text{CLC}_6\text{H}_{12}\text{NHgCL}]\text{HgCL}_3$  (4)

---

F.W.	: 676.61
Space Group	: Pc
a, Å	: 10.532(6) <sup>a</sup>
b, Å	: 9.866(2)
c, Å	: 14.093(7)
$\beta$ , °	: 99.23(6)
V, Å <sup>3</sup>	: 1445.4(1.1)
$\rho_{\text{calc}}$ , g/cm <sup>3</sup>	: 3.11
Z	: 4 (two independent units)
Temperature, °K	: 298
Radiation, Å	: Mo K $\alpha$
$\lambda$ , Å	: 0.70966 (graphite monochromator)
$\mu$ , cm <sup>-1</sup>	: 221.62 (correction applied)
$2\theta_{\text{max}}$ , °	: 50.0
Number of reflections collected	: 3058
Number of reflections observed	: 1572
Min of I/ $\sigma$ (I)	: 3.0
Number of variables	: 181
Observations/Variables	: 8.7
R, % <sup>b</sup>	: 4.7
$R_{\omega}$ , %	: 5.1
Intensity(I) vs. Refln. No.(X)	:
1. h,k,l Data for crystal 1	: 11376 - 1.8237*X = I(X)
2. h,k,-l Data for crystal 2	: 18204 - 2.6101*X = I(X)

---

<sup>a</sup>Estimated standard deviations shown in parentheses are for the least significant digits.

$${}^bR = \frac{\sum ||F_o| - |F_c||}{\sum |F_o|}$$

$$R_{\omega} = [\frac{\sum \omega (|F_o| - |F_c|)^2}{\sum \omega |F_o|^2}]^{1/2}, \text{ where } \omega = 1/\sigma^2(F).$$

where  $C_T, C_B, C_N$  and  $K_T$  represent respectively the total count, background count, net count and counting time factor while the factor 0.03 represents an estimate of non-statistical errors. The estimated deviations in the structure factors were calculated by the finite difference method.<sup>10</sup>

### Structure Determination and Refinement

The structure determination was initiated with the determination of the space group: Systematic absences of  $h0l$  ( $l = 2n + 1$ ) narrowed the space group choices to  $P2/c$  and  $Pc$ . A three dimensional sharpened Patterson map was then computed and analyzed using assuming  $P2/c$  as the space group. No meaningful set of co-ordinates could be obtained for an initial model from Patterson map. ALCAMPS<sup>24</sup> (which was quite successful with two other chloromercurates) analyses of superposition maps also failed to yield a good starting model.

A statistical test<sup>8</sup> at this point indicated acentric distribution with respect to two-fold symmetry and thus the space group  $Pc$  was considered next. Analysis of the Patterson map was again difficult, and after several unsuccessful superpositions, co-ordinates of three mercury atoms of compound 4 were obtained from a superposition map generated using a vector which appeared to be a Hg-CL vector and three other vectors which were considered to be single Hg-Hg vectors. The remaining Hg atom and five of the ten chlorine atoms were then located from a subsequent difference electron density map. The positional and isotropic

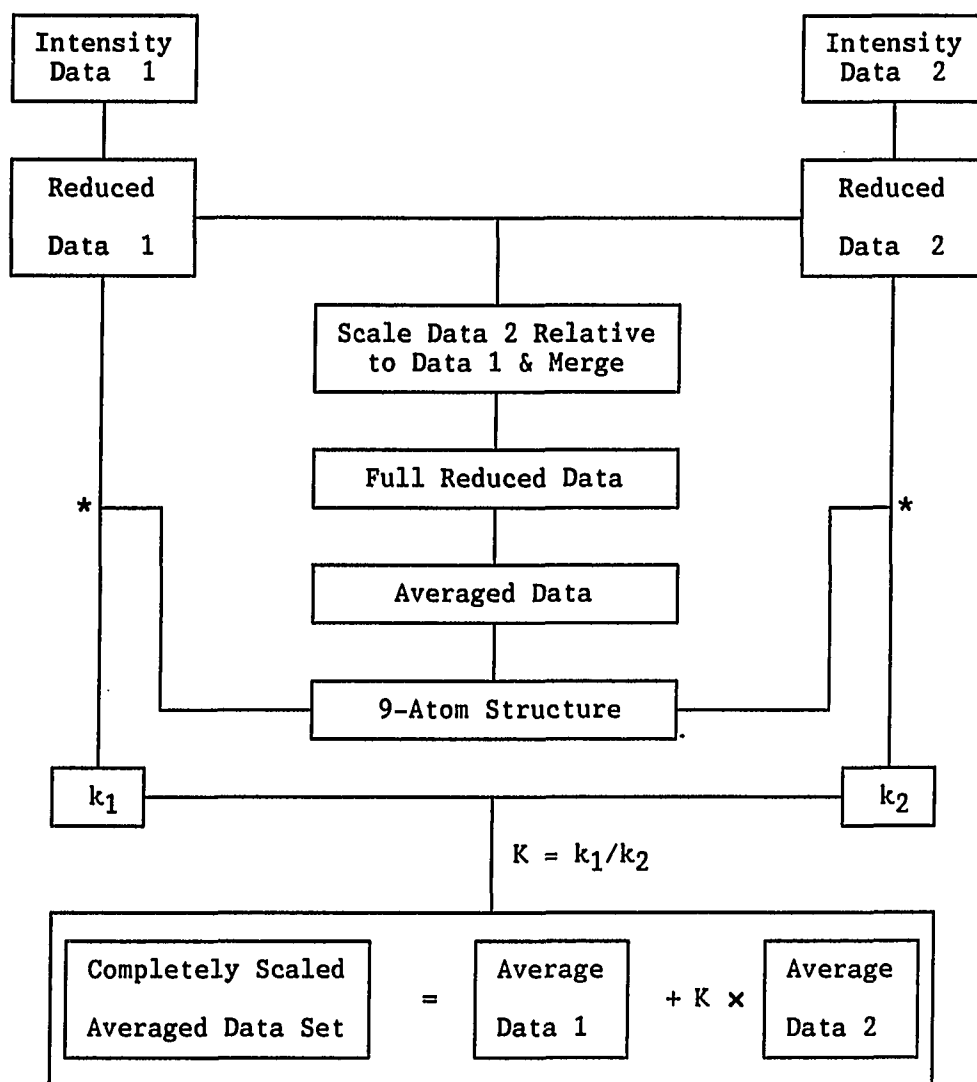
thermal parameters were refined using a block-diagonal matrix least squares procedure.<sup>12</sup> The R-factor at this stage was 17%.

A difference electron density map calculated at this stage did not show any recognizable organic fragments. Thus it was conjectured that the relative scaling of the observed structure factors corresponding to the two data sets (based on 120 common reflections for the two crystals) may have been inadequate. The method shown in Scheme 2 was then used in the hopes of obtaining a better estimate of relative scaling. A subsequent calculation of a difference Fourier map revealed using the rescaled combined averaged data revealed that the new scaling was in deed a better one. In the difference map was seen not only the remaining chlorine atoms but also the entire organic fragments. In a final full-matrix least squares refinement the heavier atoms (Hg and Cl) were refined anisotropically while the rest of the non-hydrogen atoms were refined isotropically; all the hydrogen atom positions were calculated but not refined. The final R-factor was 4.7%. Refinement of all non hydrogen atoms anisotropically, while resulting in no significant improvement of the residual, resulted in the increase of shift to error ratios of almost every variables.

A careful examination of the co-ordinates in Table 20 together with their symmetry related counter parts unambiguously ruled out the possibility of the centrosymmetric space group  $P2/c$ .

The atomic scattering factors were those from reference 13; those of mercury and chlorine atoms were modified for anomalous dispersion effects.<sup>14</sup>

Scheme 2. Scaling of x-ray data from two crystals of compound 4



\*Only the scale factors  $k$ 's are varied at this point, the subscripts corresponding to crystal 1 and 2. They turn out to be  $k_1 = 0.340$  and  $k_2 = 0.415$ ; The scaling constant  $K$  is applied to both  $F_0$  and  $\sigma(F_0)$ .



## Discussion of the Structure

The final atomic positional and thermal parameters are listed in Tables 20 and 21 respectively while the refined bond distances and bond angles are listed in Tables 22 and 23 respectively. Table 24 furnishes some details about a few least squares planes. Figure 8 shows an ORTEP<sup>15</sup> drawing of 4. In Figure 9 is shown the 'chain' of asymmetric units along the b direction. Figure 10 depicts a unit cell drawing. In all these figures the hydrogen atoms attached to the carbon atoms are left out for the sake of clarity.

There is a great variety of mercury complexes which exist in solution or in the solid state. According to the convention of Grdenic,<sup>25</sup> mercury atoms have a 'characteristic' coordination number of two. On the other hand, 'effective' coordination number, which is defined as the number of nearest neighbours with a distance that is smaller than the sum of van der Waals radii<sup>18</sup> of the interacting atoms (3.20 to 3.40 Å in the case of Hg<sup>2+</sup> and Cl<sup>-</sup>), range from two to six. This is perhaps due to relatively small energy differences among the filled d orbitals and the empty s and p orbitals (5d<sup>10</sup>, 6s<sup>0</sup>, 6p<sup>0</sup> for Hg(II)) which permit extensive hybridization of these orbitals resulting in the 'effective' coordination numbers of two to six. Thus the structural chemistry of mercuric halides is diverse.<sup>25-48</sup>

The structure reported here is interesting in that in mercuration of 1-N,N-dimethylaminobut-2-yne, HgCl<sub>3</sub><sup>-</sup> anions are observed perhaps for the first time in the solid state without forming polymeric [HgCl<sub>3</sub><sup>-</sup>]<sub>n</sub> chains.

Table 20. Positional parameters<sup>a</sup> ( $\times 10^4$ ) for  $[\text{CLC}_6\text{H}_{12}\text{NHgCL}]\text{HgCL}_3$  (4)

Atom	x	y	z	$U_{\text{iso}}^b$
HG(1) <sup>c</sup>	1087	7731(2)	3478	53.0(5)
HG(1')	2601(1)	13341(2)	5982(1)	52.7(5)
HG(2)	3086(2)	10887(2)	3444(2)	69.4(7)
HG(2')	0686(2)	16534(2)	6899(2)	65.9(7)
CL(1)	3278(8)	7606(10)	3289(8)	55(4)
CL(1')	0525(8)	13242(11)	6242(8)	55(4)
CL(2)	-3159(9)	7086(12)	3764(9)	67(4)
CL(2')	7032(9)	12945(13)	6007(10)	76(5)
CL(3)	2103(8)	10491(12)	4891(8)	61(4)
CL(4)	1251(10)	10583(12)	2194(8)	66(4)
CL(5)	5334(9)	11055(13)	3565(10)	74(5)
CL(3')	1859(9)	16433(12)	5463(8)	62(4)
CL(4')	2361(13)	16117(13)	8235(10)	85(5)
CL(5')	-1506(8)	16695(12)	6498(9)	67(4)
N(1)	-088(3)	1033(3)	417(2)	48(8)
N(1')	468(3)	1613(3)	630(2)	45(8)
C(1)	-105(4)	552(4)	382(3)	53(10)
C(2)	-148(4)	688(4)	373(3)	50(10)
C(3)	-082(3)	793(3)	354(2)	33(8)
C(4)	-130(3)	938(3)	336(2)	33(8)
C(5)	-121(4)	1178(4)	384(3)	52(10)
C(6)	-124(4)	995(5)	512(3)	61(11)
C(1')	514(4)	1124(4)	633(3)	58(11)
C(2')	537(3)	1269(4)	604(3)	46(9)
C(3')	451(4)	1365(4)	582(3)	50(10)
C(4')	491(4)	1511(5)	554(3)	57(11)
C(5')	542(4)	1569(5)	724(3)	65(12)
C(6')	504(4)	1748(4)	596(3)	66(12)
H(1)	12	1038	441	63
H(1')	369	1621	600	63
H(11)	-5	547	383	63
H(12)	-125	510	448	63

<sup>a</sup>The estimated standard deviations in the parentheses are for the least significant digits. Parameters for N, C and H atoms are multiplied by  $10^3$ .

<sup>b</sup>For anisotropically refined atoms,  $U_{\text{iso}} \equiv 10^3/3 \sum U_{ij} a_i^* a_j^* \vec{a}_i \cdot \vec{a}_j$ , where the temperature factors are defined as  $\exp(-2\pi^2 \sum h_j a_j^* U_{ij})$ .

<sup>c</sup>The x and z coordinates of this atom were fixed due to the polar nature of the space group  $Pc$ .

Table 20. (continued)

---

Atom	x	y	z	U <sub>iso</sub>
H(13)	-151	493	325	63
H(41)	-231	939	322	63
H(42)	-95	977	275	63
H(51)	-37	1236	383	63
H(52)	-177	1226	430	63
H(53)	-175	1179	314	63
H(61)	-222	1017	513	63
H(62)	-67	1049	568	63
H(63)	-109	890	525	63
H(11')	414	1106	635	63
H(12')	563	1104	704	63
H(13')	545	1053	586	63
H(41')	436	1540	485	63
H(42')	589	1512	544	63
H(51')	642	1587	725	63
H(52')	513	1625	781	63
H(53')	528	1465	736	63
H(61')	424	1817	595	63
H(62')	583	1788	642	63
H(63')	524	1743	526	63

---

Table 21. Anisotropic thermal parameters<sup>a</sup> ( $\times 10^3$ ) for  
 $[\text{CLC}_6\text{H}_{12}\text{NHgCL}]\text{HgCL}_3$  (4)

Atom	U <sub>11</sub>	U <sub>22</sub>	U <sub>33</sub>	U <sub>23</sub>	U <sub>13</sub>	U <sub>12</sub>
HG(1)	34.3(6)	67(1)	60(1)	-01(1)	12.5(6)	00.0(8)
HG(1')	33.0(6)	60(1)	65(1)	00(1)	10.3(6)	-02.4(8)
HG(2)	38.0(7)	85(1)	87(1)	05(1)	14.0(8)	-06.8(9)
HG(2')	37.6(7)	88(1)	73(1)	-01(1)	10.5(7)	08.3(9)
CL(1)	37(4)	60(7)	68(7)	-03(6)	11(5)	02(5)
CL(1')	39(4)	61(7)	66(7)	01(6)	11(5)	-05(5)
CL(2)	35(5)	89(8)	77(8)	-15(7)	06(5)	-04(5)
CL(2')	36(5)	74(8)	118(11)	-17(8)	14(6)	05(5)
CL(3)	38(5)	91(8)	51(7)	-02(6)	01(5)	-07(5)
CL(4)	66(6)	71(8)	58(7)	-08(6)	01(5)	-14(6)
CL(5)	36(5)	81(8)	107(10)	11(8)	21(6)	04(5)
CL(3')	49(5)	78(8)	59(7)	18(6)	11(5)	12(5)
CL(4')	86(8)	63(8)	93(10)	11(7)	-29(7)	08(7)
CL(5')	31(4)	93(8)	78(8)	08(7)	08(5)	-04(5)

<sup>a</sup>The estimated standard deviations in the parentheses are for the least significant digits. The anisotropic temperature factors are defined as  $\exp(-2\pi^2 \sum h_i h_j a_i^* a_j^* U_{ij})$ .

Table 22. Refined bond distances<sup>a</sup> (Å) for [CLC<sub>6</sub>H<sub>12</sub>NHgCL]HgCL<sub>3</sub> (4)

Atoms	Distance	Atoms	Distance
HG(1) - CL(1)	2.37(1)	HG(1') - CL(1')	2.28(1)
HG(2) - CL(3)	2.46(1)	HG(2') - CL(3')	2.54(1)
HG(2) - CL(4)	2.42(1)	HG(2') - CL(4')	2.40(1)
HG(2) - CL(5)	2.35(1)	HG(2') - CL(5')	2.29(1)
CL(2) - C(2)	1.79(3)	CL(2') - C(2')	1.78(4)
N(1) - C(4)	1.48(4)	N(1') - C(4')	1.51(5)
N(1) - C(5)	1.54(5)	N(1') - C(5')	1.49(5)
N(1) - C(6)	1.49(5)	N(1') - C(6')	1.49(5)
C(1) - C(2)	1.42(5)	C(1') - C(2')	1.51(5)
C(2) - C(3)	1.30(5)	C(2') - C(3')	1.31(5)
C(3) - HG(1)	2.03(3)	C(3') - HG(1')	2.09(4)
C(3) - C(4)	1.53(4)	C(3') - C(4')	1.57(5)
Contact distances:			
HG(1) - HG(2)	3.76	HG(1') - HG(2')	4.06 <sup>b</sup>
HG(1) - HG(2')	5.05	HG(1') - HG(2)	4.42
HG(1) - CL(3)	3.44	HG(1') - CL(3')	3.21
HG(1) - CL(4)	3.37	HG(1') - CL(4')	4.23
HG(1) - CL(3')	3.07	HG(1') - CL(3)	3.21
HG(2) - CL(1)	3.25	HG(2') - CL(1')	3.38
Hydrogen bonds:			
N(1) - CL(3)	3.14	N(1') - CL(3')	3.03

<sup>a</sup>The estimated standard deviations in the parentheses are for the least significant digits.

<sup>b</sup>Here the primed atoms have the symmetry code (x,y-1,z).

Table 23. Refined bond angles<sup>a</sup> (°) for [CLC<sub>6</sub>H<sub>12</sub>NHgCL]HgCL<sub>3</sub> (4)

Atoms	Angle	Atoms	Angle
CL(1) - HG(1) - C(3)	175.3( 9)	CL(1')- HG(1')- C(3')	173.6(10)
CL(3) - HG(2) - CL(4)	101.0( 4)	CL(3')- HG(2')- CL(4')	103.2( 4)
CL(3) - HG(2) - CL(5)	120.2( 4)	CL(3')- HG(2')- CL(5')	114.0( 4)
CL(4) - HG(2) - CL(5)	137.7( 4)	CL(4')- HG(2')- CL(5')	142.1( 4)
C(4) - N(1) - C(5)	109(3)	C(4') - N(1') - C(5')	108(3)
C(4) - N(1) - C(6)	116(3)	C(4') - N(1') - C(6')	107(3)
C(5) - N(1) - C(6)	115(3)	C(5') - N(1') - C(6')	115(3)
C(4) - N(1) - CL(3)	116(3)	C(4') - N(1') - CL(3')	92(2)
C(5) - N(1) - CL(3)	103(3)	C(5') - N(1') - CL(3')	136(3)
C(6) - N(1) - CL(3)	97(3)	C(6') - N(1') - CL(3')	95(3)
CL(2) - C(2) - C(1)	114(3)	CL(2')- C(2') - C(1')	110(3)
CL(2) - C(2) - C(3)	119(3)	CL(2')- C(2') - C(3')	122(3)
C(1) - C(2) - C(3)	127(3)	C(1') - C(2') - C(3')	128(3)
HG(1) - C(3) - C(2)	120(3)	HG(1')- C(3') - C(2')	121(3)
HG(1) - C(3) - C(4)	113(2)	HG(1')- C(3') - C(4')	117(3)
C(2) - C(3) - C(4)	127(3)	C(2') - C(3') - C(4')	122(3)
N(1) - C(4) - C(3)	114(3)	N(1') - C(4') - C(3')	111(3)

Other angles of interest:<sup>b</sup>

CL(1) - HG(2) - CL(3)	86	CL(1')- HG(2')- CL(3')	76
CL(1) - HG(2) - CL(4)	83	CL(1')- HG(2')- CL(4')	93
CL(1) - HG(2) - CL(5)	90	CL(1')- HG(2')- CL(5')	90
CL(1) - HG(1) - CL(3)	84	CL(1')- HG(1')- CL(3')	83
CL(1) - HG(1) - CL(4)	81	CL(1')- HG(1')- CL(4')	75
CL(1) - HG(1) - CL(3 <sup>''</sup> )	88	CL(1')- HG(1')- CL(3)	87
CL(1) - HG(1) - CL(4 <sup>''</sup> )	93	CL(1')- HG(1')- CL(4)	92
HG(1) - CL(1) - HG(2)	83	HG(1')- CL(1')- HG(2')	90
HG(1) - CL(3) - HG(2)	77	HG(1')- CL(3')- HG(2')	89
HG(1) - CL(4) - HG(2)	79	HG(1')- CL(4')- HG(2')	69
HG(1) - CL(3 <sup>''</sup> )- HG(2)	128	HG(1')- CL(3) - HG(2)	102
CL(3) - HG(1')- CL(3')	80	CL(4) - HG(1) - CL(3 <sup>''</sup> )	144
C(3) - HG(1) - CL(3)	97	C(3') - HG(1')- CL(3')	92
C(3) - HG(1) - CL(4)	95	C(3') - HG(1')- CL(4')	100
C(3) - HG(1) - CL(3 <sup>''</sup> )	97	C(3') - HG(1')- CL(3)	93
C(3) - HG(1) - CL(4 <sup>''</sup> )	91	C(3') - HG(1')- CL(4)	94
CL(3) - N(1) - C(4)	116	CL(3')- N(1') - C(4')	93
CL(3) - N(1) - C(5)	103	CL(3')- N(1') - C(5')	136
CL(3) - N(1) - C(6)	97	CL(3')- N(1') - C(6')	94
N(1) - CL(3) - HG(2)	106	N(1') - CL(3')- HG(2')	106

<sup>a</sup>The estimated standard deviations in the parentheses are for the least significant digits.

<sup>b</sup>The doubly primed atoms are related to the corresponding primed atoms by the symmetry code (x,y-1,z).

Table 24. Equations of least squares planes (in the monoclinic coordinate system) and interplanar angles for 4

Atom	Distance from Plane(Å)	Atom	Distance from Plane(Å)
Plane I fitting C(1)-C(2)-C(3)-C(4)-HG(1)-CL(1)-CL(2)			
$0.8369*X + 1.6607*Y + 13.4876*Z - 6.0094 = 0.0$			
C(1)	-0.023	HG(1)	0.057
C(2)	0.034	CL(1)	-0.036
C(3)	0.012	CL(2)	-0.020
C(4)	-0.024		
Plane II fitting C(1')-C(2')-C(3')-C(4')-HG(1')-CL(1')-CL(2')			
$0.6376*X + 2.8443*Y + 13.1562*Z - 11.9080 = 0.0$			
C(1')	-0.051	HG(1')	-0.077
C(2')	-0.006	CL(1')	0.104
C(3')	-0.087	CL(2')	0.125
C(4')	-0.007		
Plane III fitting HG(2)-CL(3)-CL(4)-CL(5)			
$-1.4177*X + 9.7696*Y + 0.8105*Z - 10.3746 = 0.0$			
HG(2)	0.103	CL(4)	-0.035
CL(3)	-0.027	CL(5)	-0.041
Plane IV fitting HG(2)-CL(3)-CL(4)-CL(5)-N(1)-H(1)			
$-1.1688*X + 9.8015*Y + 0.6248*Z - 10.4311 = 0.0$			
HG(2)	0.094	CL(4)	-0.068
CL(3)	-0.088	CL(5)	0.004
N(1)	0.052	H(1)	0.005
Plane V fitting HG(2')-CL(3')-CL(4')-CL(5')			
$1.0753*X + 9.7826*Y + 0.8831*Z - 16.7769 = 0.0$			
HG(2')	0.081	CL(4')	-0.029
CL(3')	-0.019	CL(5')	-0.033

Table 24. (continued)

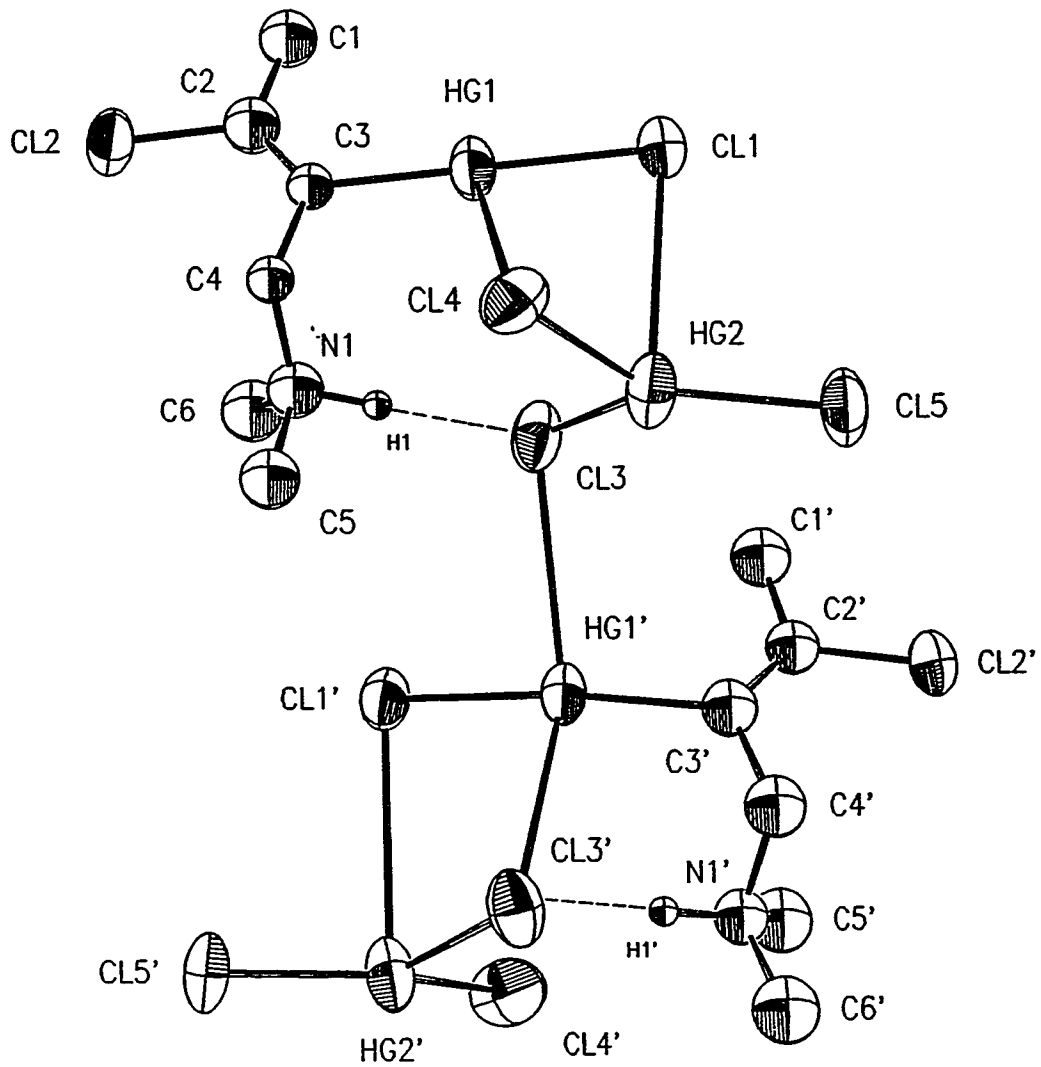
Atom	Distance from Plane(Å)	Atom	Distance from Plane(Å)
Plane VI fitting HG(2')-CL(3')-CL(4')-CL(5')-N(1')-H(1')			
$1.0040*X + 9.7886*Y + 0.9098*Z - 16.8015 = 0.0$			
HG(2')	0.080	CL(4')	-0.039
CL(3')	-0.032	CL(5')	-0.019
N(1')	0.030	H(1')	-0.019
Interplanar Angles(°)			
<u>Plane</u>		<u>Plane</u>	<u>Angle</u>
I		II	7
I		III	79
I		IV	79
I		V	75
I		VI	75
II		III	72
II		IV	72
II		V	68
II		VI	68
III		V	14
III		VI	13
IV		V	13
IV		VI	12



The whole structure is built up of  $\text{HgCl}_3^-$  anions and  $[\text{CLC}_6\text{H}_{12}\text{NHgCL}]^+$  cations (two independent units in the asymmetric unit). As can be seen from Figure 8 and Table 22, in the anion the 'characteristic' coordination of mercury is trigonal and not digonal. As noted in references 48 (which reported the first case of a 'characteristic' trigonal coordination for a chloromercurate) and 28, three chlorine atoms [CL(n) or CL(n'); n = 3,4,5] are at the vertices of an oblique triangle (Table 23). The metal atoms HG(2) and HG(2') together with the respective chlorine atoms lie in planes that are almost parallel to each other (Planes III,V; Table 24). HG(2) and HG(2') are respectively 0.14 Å and 0.11 Å from the planes of the respective chlorine atoms. Thus the environment about HG(2) and HG(2') can best be considered as planar but distorted from that expected for  $sp^2$  (or  $sd^2$  or a combination of  $sp^2$  and  $sd^2$ ) hybridized mercury, on the basis of bond distances and angles about these metal atoms. The HG(2)-CL(n) and HG(2')-CL(n') (n = 3,4,5) bond lengths (2.29 - 2.54 Å) are intermediate between digonal (2.27 Å)<sup>49</sup> and tetrahedral (2.58 and 2.62 Å)<sup>50</sup> bonds, and they are certainly in the range reported for the polymeric  $[\text{HgCl}_3^-]_n$  ion (ranging from 2.37 to 2.54 Å).<sup>28,41,42,48</sup>

The distances HG(2)-CL(1) (3.25 Å) and HG(2')-CL(1') (3.37 Å) however, which still are in the van der Waals distance range given earlier, are significantly longer than the previously reported mercury to apical chlorine distances of 2.90 to 3.11 Å in the polymeric  $[\text{HgCl}_3^-]_n$  ion. Furthermore, unlike the polymeric  $[\text{HgCl}_3^-]_n$  species in which the apical chlorine atoms belong to the adjacent trigonal  $\text{HgCl}_3$  groups, CL(1) and CL(1') are part of the organomercury cations. While under these circumstances the  $\text{HgCl}_3^-$  species observed in our study can be considered

Figure 8. ORTEP drawing of  $[\text{ClC}_6\text{H}_{12}\text{NHgCl}]\text{HgCl}_3$  (4) excluding the hydrogen atoms attached to the carbon atoms; dashed lines indicate hydrogen bonds



as discrete anionic species, one could still be tempted to assign an 'effective' coordination number of four for these metal atoms, Hg(2) and Hg(2'), based on the angles CL(1)-Hg(2)-CL(n), CL(1')-Hg(2')-CL(n') [n = 3,4,5] being closer to 90° (Table 23).

Three coordinate mercury has been found in many mercury(II) compounds. In most of these, the different nature of the atoms bonded to Hg seems to be responsible for the significant deviation from ideal trigonal geometry.<sup>51-53</sup> Even in those cases where Hg is surrounded by three atoms of the same kind, severe distortion in bond angles can be found, as in Hg<sub>3</sub>O<sub>2</sub>CL<sub>2</sub><sup>28,54</sup> or significant displacement (0.3 Å) of metal atom from the triangle plane as in [NMe<sub>4</sub>][HgBr<sub>3</sub>].<sup>46</sup> Only in [Me<sub>3</sub>S]HgX<sub>3</sub> (X = I<sup>47</sup>, CL<sup>48</sup>) has a nearly perfect trigonal bipyramidal geometry been realised. In our case, the severe distortion in bond angles with respect to the ideal trigonal geometry could be due to the non-spherical nature of the cation and the hydrogen bonding that exists between the N atom of the cations and the CL atom of the trichloromercurate anion (see later).

The crystal structural analysis clearly reveals that the mercuric chloride addition to the internal acetylene was also trans in nature with the mercury atom going towards the amino group (Figure 8), as has been documented by Larock *et al.*<sup>23</sup> The 'effective' coordination appears to be four for both HG(1) and HG(1') atoms: The d(HG(1)-CL(3')) of 3.07 Å is well within the range of 'effective' coordination, while the distances d(HG(1)-CL(4)) = 3.37 Å, d(HG(1')-CL(3')) and d(HG(1')-CL(3)), each equal to 3.21 Å, are longer; the latter might not be considered significantly beyond the range of 'effective' coordination. Nonetheless the geometrical environment about these metal atoms can be considered as only digonal and only slightly distorted from that expected for sd hybridized

Figure 9. 'Chain' of units of  $[\text{CLC}_6\text{H}_{12}\text{NHgCL}]\text{HgCL}_3$  (4) along the b axis. Mercury atoms are indicated with a \* in the middle. Solid circles (●) represent hydrogen atoms. Dashed lines indicate hydrogen bonds. Hydrogen atoms attached to the carbon atoms are left out for the sake of clarity

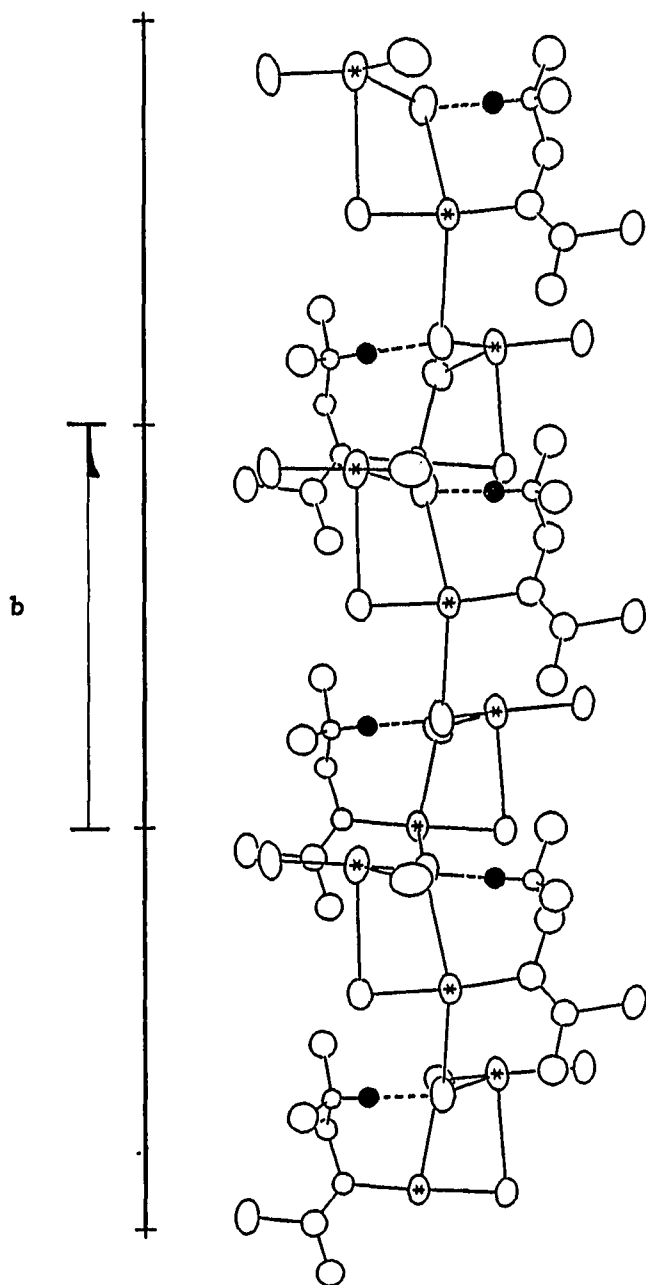
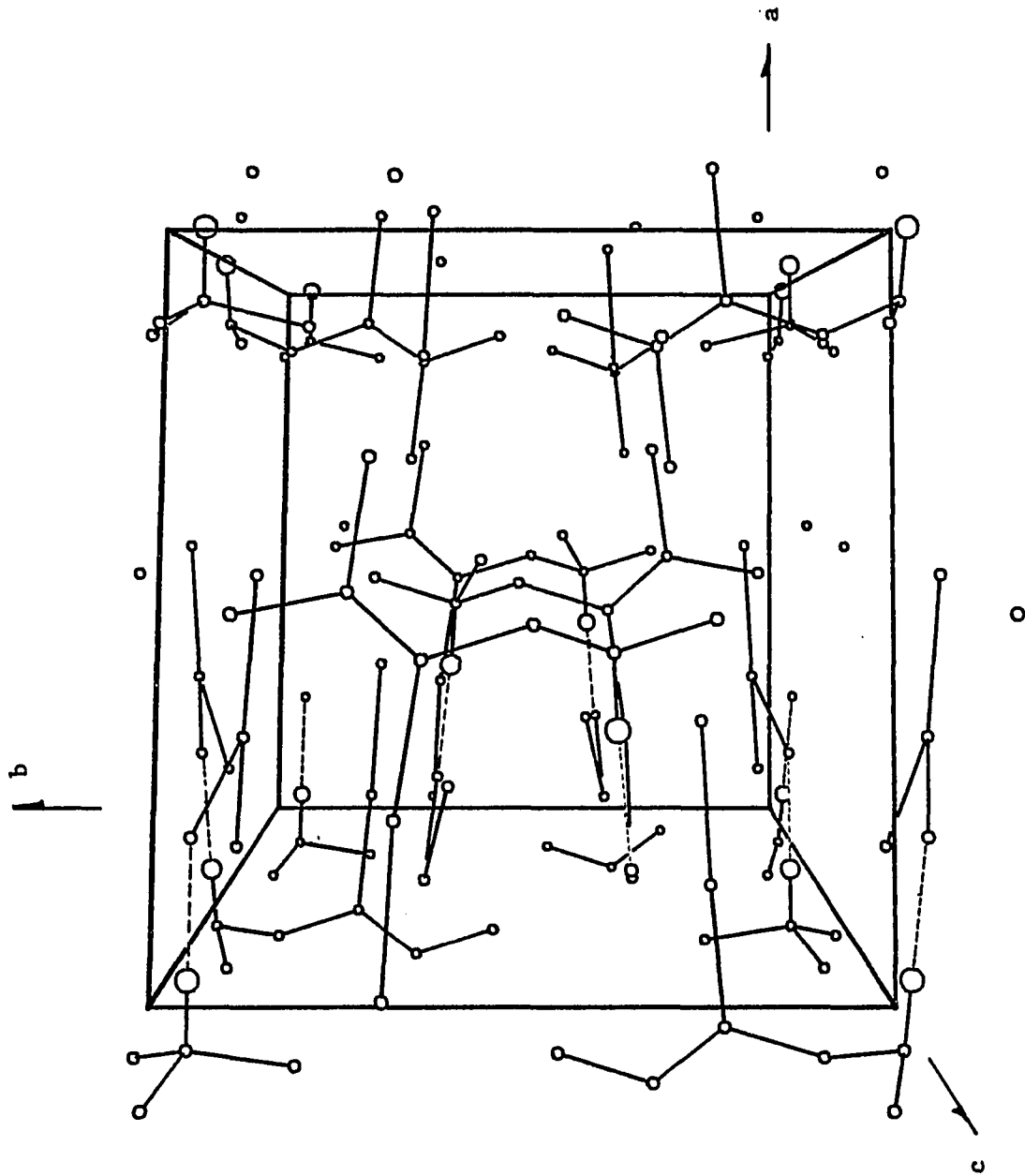


Figure 10. Unit cell drawing of  $[\text{ClC}_6\text{H}_{12}\text{NHgCl}]\text{HgCl}_3$  (4)  
excluding the hydrogen atoms attached to  
the carbon atoms; dashed lines indicate  
hydrogen bonds





mercury on the basis of the C(3)-HG(1)-CL(1) and C(3')-HG(1')-CL(1') angles being  $175.3(9)^\circ$  and  $173.6(10)^\circ$  respectively; these angles are in good agreement with those previously reported in the literature.<sup>34,35</sup> The slight deviation from linearity is to be expected considering the increased 'coordination' and the proximity of HG(2) and HG(2') to CL(1) and CL(1') respectively.

Figure 10 shows the packing arrangement in the unit cell. The distances  $d(N(1)-CL(3))$  and  $d(N(1')-CL(3'))$  [respectively 3.14 and 3.03 Å] are significantly shorter than the sum of the van der Waals radii<sup>18</sup> for N (1.50 Å) and CL (1.80 Å) and imply the existence of hydrogen bonds via H(1) and H(1'). These hydrogen bonds run nearly perpendicular to the  $\vec{b}$  direction. It is interesting to note these bonds lie almost on the nearby HgCL<sub>3</sub> planes (Planes IV and VI; Table 24). Also the organomercury planes (Plane I and II, Table 24) go almost parallel to each other along the  $b$  direction. This is illustrated in Figure 9 which also shows how the HgCL<sub>3</sub> planes line up almost parallel to each other and the  $b$  axis is nearly perpendicular to these planes. The packing arrangement shown here (and more easily seen than in Figure 10) perhaps explains why the relatively less heavy atoms of the organomercury complex do not show much thermal motion even though it seems that there is plenty of space for these groups to move about.

### Conclusion

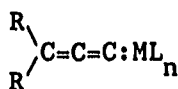
Crystal packing shows that several interatomic vectors are almost parallel to each other. This explains why there was so much difficulty encountered in unravelling the Patterson map. Many of the

trihalomercurates reported in the literature exhibit the property of ferroelectricity. It would be interesting to determine whether compound 4, which has (unlike any other trihalomercurates reported earlier) discrete trichlomercurate anions, show any ferroelectricity. Finally the following must be noted: The fact that a halomercurate has a composition of  $LHgX_3$  does not necessarily mean that the coordination around Hg can be predicted. The compounds with this composition have been found to contain either discrete  $HgX_3^-$  (our case), polymeric  $[HgX_3^-]_n$  or discrete  $Hg_2X_6^{2-}$  ions. In the case of polymeric  $[HgX_3^-]_n$  Hg can show either trigonal bipyramidal coordination ( $X = Cl, Br, I$ ) or tetrahedral coordination ( $X = Br, I$ ). And in the case of discrete  $Hg_2X_6^{2-}$  ions both edge-shared bitetrahedron<sup>28</sup> and edge-shared squared pyramidal coordination geometries have been noted.

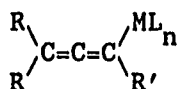
CRYSTAL STRUCTURE OF BIS(TRIPHENYLPHOSPHINE)CHLORO( $\eta^2$ -1,2,3-  
CYCLONONATRIENE)RHODIUM(I) (5)

Introduction

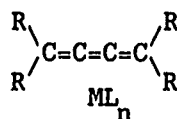
There are three simple modes of attaching a cumulene ligand to a metal; namely the carbene mode (a),  $\eta^1$ -allenyl (cumulenyl) mode (b), and  $\eta^2$ -olefin mode (c); these are illustrated below below:



(a)



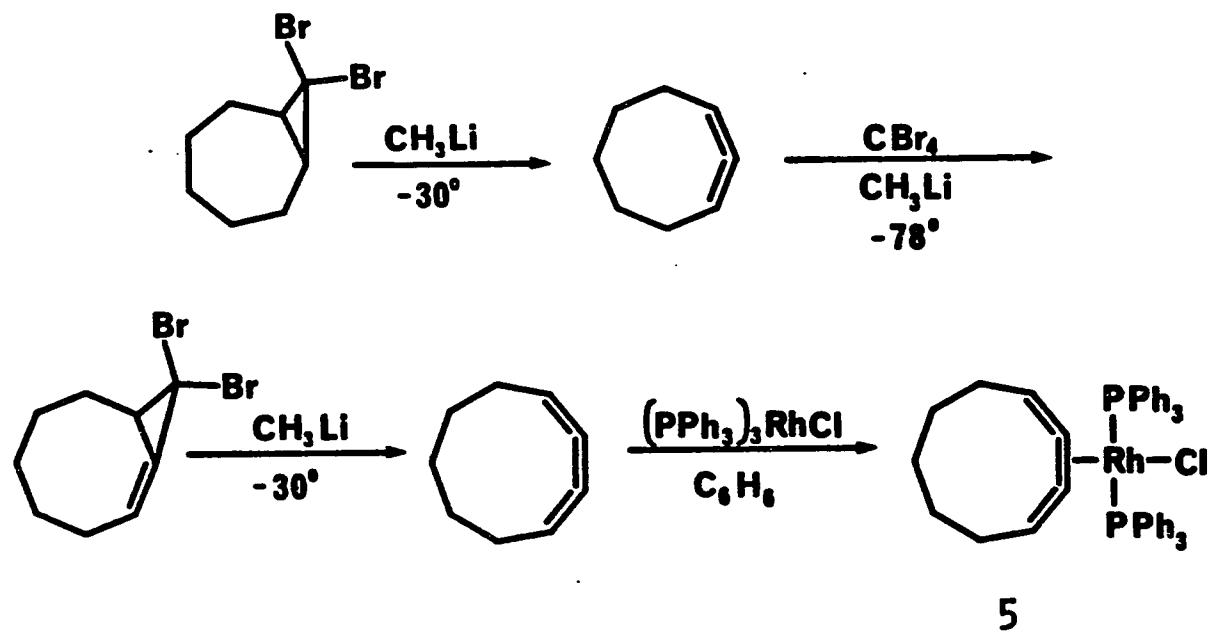
(b)



(c)

Of these three modes, mode (c) is quite common in the case of allenes.<sup>55</sup> There are several reports of acyclic butatrienes  $\pi$  bound to metals, but only a few involve mononuclear  $\pi$  complexes of butatrienes with  $\eta^2$ -olefin mode (c).<sup>56</sup>

In contrast, very little is known about the structure and chemistry of cyclic butatrienes and coordination chemistry.<sup>57</sup> While the generation of ten-,<sup>58</sup> nine-,<sup>57</sup> and seven-<sup>59</sup> membered cyclic butatrienes have been reported, attempts to generate the six-membered compound have been unsuccessful.<sup>60,61</sup> Of those reported, 1,2,3-cyclononatriene (hereafter ligand) may be the smallest isolable cyclic butatriene. Molecular orbital calculations<sup>57</sup> led to the prediction that the normally linear butatriene moiety should be bent ca. 15 - 18° in the free ligand. Although cold dilute solutions of the ligand are stable for several days, concentration, prolonged standing, or exposure to oxygen, like in the



Scheme 3. Preparation of bis(triphenylphosphine)chloro( $\eta$ -1,2,3-cyclononatriene)rhodium(I) (5)

case of many acyclic butatrienes and 1,2,3-cyclodecatriene, results in polymerization.

In order to fully characterize this novel ligand, the crystal structure analysis of the title compound (5) was undertaken. Scheme 3 shows the preparation of the ligand as well as the title compound, both of which were prepared in Dr. Johnson's research group (Department of Chemistry, Iowa State University, 1986).

### Experimental

Data collection A yellow single crystal of compound 5 with approximate dimensions of 0.08 × 0.2 × 0.4 mm was obtained from a solution of 5 in pentanes containing iso-amylacetate and was then mounted at the tip of a glass fiber and subsequently placed on a goniometer head. Twelve reflections from a rotation photograph ( $9.5^\circ < 2\theta < 20^\circ$ ) were centered on a Syntex P2<sub>1</sub> automated four circle diffractometer and indexed by the indexing program BLIND.<sup>7</sup> The resulting reduced cell and cell scalars revealed primitive orthorhombic crystal symmetry, confirmation of which came from the mirror symmetry observed in the three axial photographs. The intensity of one strong reflection was measured every 100 reflections during data collection to monitor any crystal decay. Two octants (h,k,l; h,k,-l) of data were collected within a 2θ sphere of 50°. Crystal data are summarized in Table 25.

Reduction of x-ray intensity data There was no noticeable change in intensity of the standard reflection throughout the data collection and thus the data were corrected only for absorption and Lorentz and

Table 25. Crystal data for  $\text{RhCl}[\text{P}(\text{C}_6\text{H}_6)_3]_2\text{C}_9\text{H}_{12}$  (5)

---

F.W.	: 783.14
Space Group	: Pbcu
a, Å	: 23.629(6) <sup>a</sup>
b, Å	: 23.91(3)
c, Å	: 13.173(8)
V, Å <sup>3</sup>	: 7442.8(10.7)
$\rho_{\text{calc}}$ , g/cm <sup>3</sup>	: 1.397
Z	: 8
Temperature, °K	: 298
Radiation, Å	: Mo K $\alpha$
$\lambda$ , Å	: 0.71069 (graphite monochromator)
$\mu$ , cm <sup>-1</sup>	: 13.99 (correction applied)
$2\theta_{\text{max}}$ , °	: 50.0
Number of reflections collected	: 13912 (two octants)
Number of reflections observed	: 3247
Min of I/ $\sigma$ (I)	: 3.0
Number of variables	: 440
Observations/Variables	: 7.38
R, % <sup>b</sup>	: 4.8
$R_{\omega}$ , %	: 6.5

---

<sup>a</sup>Estimated standard deviations shown in parentheses are for the least significant digits.

$${}^b R = \frac{\sum ||F_o| - |F_c||}{\sum |F_o|}$$

$$R_{\omega} = [\sum \omega (|F_o| - |F_c|)^2 / \sum \omega |F_o|^2]^{1/2}, \text{ where } \omega = 1/\sigma^2(F).$$

polarization effects. Empirical absorption corrections<sup>9</sup> were made based on observed variations in the intensity distribution as function of the orientation of the crystal for a reflection near  $\chi = 90^\circ$ . The estimated variance in each intensity was calculated by

$$\sigma_I^2 = C_T + K_T^2 C_B + (0.03C_T)^2 + (0.03C_B)^2 + (0.03C_N)^2$$

where  $C_T, C_B, C_N$  and  $K_T$  represent respectively the total count, background count, net count and counting time factors while the factor 0.03 represents an estimate of non-statistical errors. The estimated deviations in the structure factors were calculated by the finite difference method.<sup>10</sup>

#### Structure Determination and Refinement

The structure determination was begun with the determination of the space group: Systematic absences of  $h0l$  ( $l = 2n + 1$ ),  $0kl$  ( $k = 2n + 1$ ) and  $hk0$  ( $h = 2n + 1$ ) uniquely defined the space group as the centrosymmetric group  $Pbca$ . The position of the rhodium, chlorine and the two phosphorus atoms were obtained from an ALCAMPS analysis<sup>24</sup> of a superposition map. These same coordinates were also obtained by the direct method program MULTAN\_80;<sup>62</sup> the latter could not provide any further information about the rest of the asymmetric unit. All the remaining non-hydrogen atoms were found from successive structure factor and Fourier and difference Fourier map calculations. A final difference electron density map also revealed a "flapping" disorder for a carbon

atom of the ligand (see later). The positional and anisotropic thermal parameters for the non-hydrogen atoms were refined by a combination of block-matrix/full-matrix least-squares calculations.<sup>12</sup> The positional parameters of the aromatic hydrogen atoms and the two cumulenic hydrogen atoms [H(39) and H(42)] were calculated and they were not varied during the refinement; they were all assigned an isotropic temperature factor of 5.0 Å<sup>2</sup>. The methylenic hydrogen atoms on C(37), C(38), C(43), C(44) and C(45)[C(45')] were not included in the refinement. The final conventional residual (R) was 4.8%.

The atomic scattering factors used were those from reference 13; those of rhodium and chlorine and phosphorus were modified for anomalous dispersion effects.<sup>14</sup>

#### Discussion of the Structure

Angus and Johnson<sup>57</sup> observed that the <sup>1</sup>H NMR spectrum of the free ligand was essentially identical to that for its immediate higher homologue, viz., 1,2,3-cyclodecatriene.<sup>58</sup> This, together with the product of hydrogenation (cyclononane) provided evidence for the generation and isolation of the ligand. MO calculations, mentioned earlier, predicted (i) C<sub>s</sub> and not C<sub>2</sub> as the preferred conformation and (ii) a cis bending of 15 - 18° for the cumulene bond of the free ligand. Thus in the hope of assigning the structure as well as the geometry for the ligand, we determined the x-ray crystal structure of the derivative 5, the structure of which could not be unambiguously established by other physical methods.<sup>63</sup>



The results of the x-ray diffraction study on the complex 5 are summarized in Tables 26-30. The final atomic positional and thermal parameters are listed in Tables 26 and 27 respectively while the refined bond distances and bond angles are listed in Tables 28 and 29 respectively. Table 30 furnishes some details about a few least-squares planes and a few torsional angles. Figure 11 shows the ORTEP<sup>15</sup> drawing of 5, the hydrogen atoms being excluded from the drawing for clarity. In Figure 12 is shown the ligand as viewed down the Rh(1)-CL(1) bond (the CL(1) atom is eclipsed by Rh(1); the phenyl groups off the phosphorus atoms and the hydrogen atoms are omitted again for the sake of clarity). Figure 13 shows the arrangement of the RhP<sub>2</sub>CL unit in the unit cell; other atoms are left out again for the sake of clarity.

The crystal structure analysis clearly reveals  $\eta^2$ -olefin bonding, as observed in other M-[acyclic butatriene] complexes (M = Fe, Rh).<sup>56,64,65</sup> Coordination about the rhodium is best described as square planar (consistent with the  $dsp^2$  hybridization for Rh(I) with a  $4d^8, 5s^0, 5p^0$  configuration) with the least-squares plane of the cumulene moiety being nearly perpendicular to the P<sub>2</sub>RhCL plane (Figures 11 and 12; Table 30). Although triphenylphosphine ligands occupy trans positions, they are not exactly linearly opposed, the angle P(1)-Rh(1)-P(2) being 174.8°. Coordination of Rh to the central  $\pi$  bond is symmetrical ( $d[\text{Rh}(1)-\text{C}(40)] = 2.046(9)$  Å and  $d[\text{Rh}(1)-\text{C}(41)] = 2.059(9)$  Å) within experimental error. The average Rh-C bond length (2.053 Å) is only slightly longer than the distance reported by Stang and White in the [1,1,2,2-tetramethyl-3-(3-methyl-1,2-butadienylidene)cyclopropane]rhodium complex A (2.025 Å)<sup>56</sup> and that reported by Hagelee et al. in the(diquino-ethylene)rhodium complex B (2.000 Å).<sup>64</sup>

Table 26. Positional parameters<sup>a</sup> ( $\times 10^4$ ) for RhCL[P(C<sub>6</sub>H<sub>6</sub>)<sub>3</sub>]<sub>2</sub>C<sub>9</sub>H<sub>12</sub> (5)

Atom	x	y	z	U <sub>iso</sub> <sup>b</sup>
Rh(1)	3235(1)	1420(1)	4180(1)	35(0)
CL(1)	3268(1)	0412(1)	4342(1)	28(1)
P(1)	2262(1)	1368(1)	4467(2)	36(1)
P(2)	4198(1)	1398(1)	3798(2)	38(1)
C(1)	2008(3)	1095(3)	5672(7)	36(3)
C(2)	2357(4)	0747(4)	6241(7)	46(3)
C(3)	2166(4)	0550(4)	7171(7)	56(4)
C(4)	1642(4)	0693(4)	7527(8)	56(4)
C(5)	1302(4)	1027(4)	6970(8)	65(4)
C(6)	1482(4)	1231(4)	6037(7)	54(4)
C(7)	1846(4)	2012(3)	4354(7)	44(3)
C(8)	1870(4)	2405(4)	5123(8)	59(4)
C(9)	1559(5)	2888(4)	5032(10)	76(5)
C(10)	1220(5)	2986(4)	4195(10)	93(6)
C(11)	1195(5)	2613(5)	3464(10)	86(5)
C(12)	1496(5)	2118(4)	3517(9)	63(4)
C(13)	1953(4)	0907(4)	3525(6)	38(3)
C(14)	1542(5)	0509(4)	3724(8)	61(4)
C(15)	1312(5)	0192(5)	2977(9)	76(5)
C(16)	1487(4)	0252(5)	2006(9)	68(4)
C(17)	1902(5)	0629(5)	1770(8)	71(5)
C(18)	2134(4)	0951(4)	2528(8)	58(4)
C(19)	4610(4)	1035(3)	4747(7)	40(3)
C(20)	5144(4)	0814(4)	4548(8)	53(4)
C(21)	5445(4)	0547(4)	5315(8)	59(4)
C(22)	5228(5)	0505(4)	6256(8)	67(4)
C(23)	4703(4)	0739(4)	6491(8)	63(4)
C(24)	4395(4)	0993(4)	5713(7)	52(4)
C(25)	4562(4)	2066(4)	3688(7)	49(3)
C(26)	4869(5)	2283(4)	4486(8)	66(4)
C(27)	5091(5)	2816(4)	4479(10)	86(5)
C(28)	5027(5)	3130(4)	3612(11)	88(5)
C(29)	4728(5)	2913(5)	2785(10)	78(5)
C(30)	4497(4)	2383(4)	2847(8)	57(4)
C(31)	4371(4)	1060(4)	2583(7)	50(3)
C(32)	4900(5)	1158(5)	2126(8)	78(5)
C(33)	4993(6)	0891(6)	1165(9)	94(6)
C(34)	4592(6)	0552(5)	0749(10)	109(6)

<sup>a</sup>The estimated standard deviations in the parentheses are for the least significant digits. Parameters for hydrogen atoms are multiplied by  $10^3$ .

<sup>b</sup>For anisotropically refined atoms,  $U_{iso} \equiv 10^3/3 \sum U_{ij} a_i^* a_j^* \vec{a}_i \cdot \vec{a}_j$ , where the temperature factors are defined as  $\exp(-2\pi^2 \sum h_j a_j^* U_{ij})$ .

Table 26. (continued)

Atom	x	y	z	U <sub>iso</sub>
C(35)	4093(6)	0463(5)	1216(9)	97(6)
C(36)	3971(5)	0712(4)	2136(7)	60(4)
C(37)	3240(6)	3465(5)	3122(11)	102(6)
C(38)	2806(6)	3076(4)	2659(11)	98(6)
C(39)	2919(5)	2452(4)	2827(9)	67(4)
C(40)	3125(4)	2215(4)	3640(8)	48(4)
C(41)	3310(4)	2244(4)	4616(7)	49(3)
C(42)	3500(5)	2513(4)	5410(8)	66(4)
C(43)	3572(6)	3140(5)	5504(11)	103(6)
C(44)	3136(7)	3471(5)	5028(11)	111(7)
C(45)*	2802(13)	3430(13)	4241(22)	114
C(45')	3627(13)	3432(13)	3986(23)	114
H(39)	290(4)	217(4)	210(8)	63
H(42)	357(4)	233(4)	604(8)	63
H(2)	278(4)	058(4)	588(7)	63
H(3)	244(4)	028(4)	752(8)	63
H(4)	150(4)	054(4)	813(8)	63
H(5)	092(4)	118(4)	738(8)	63
H(6)	123(4)	151(4)	556(7)	63
H(8)	206(4)	232(4)	575(7)	63
H(9)	158(4)	305(4)	560(7)	63
H(10)	100(4)	331(4)	407(7)	63
H(11)	094(4)	269(4)	289(7)	63
H(12)	143(4)	183(4)	293(8)	63
H(14)	139(4)	052(4)	441(8)	63
H(15)	107(4)	-010(4)	318(8)	63
H(16)	139(4)	-004(4)	128(8)	63
H(17)	200(4)	065(4)	106(8)	63
H(18)	243(4)	122(4)	229(8)	63
H(20)	538(4)	086(4)	422(8)	63
H(21)	592(4)	035(4)	514(7)	63
H(22)	552(4)	034(4)	677(8)	63
H(23)	433(4)	063(4)	649(8)	63
H(24)	388(4)	103(4)	585(8)	63
H(26)	513(4)	210(4)	525(8)	63
H(27)	534(4)	304(4)	516(8)	63
H(28)	525(4)	351(4)	370(8)	63
H(29)	467(4)	316(4)	196(7)	63
H(30)	425(4)	227(4)	230(7)	63
H(32)	520(4)	145(4)	272(8)	63
H(33)	548(4)	102(4)	093(8)	63
H(34)	470(4)	045(4)	012(8)	63
H(35)	382(4)	023(4)	120(7)	63
H(36)	354(4)	065(4)	249(8)	63

\*The multipliers for C(45) and C(45') are 47% and 53% respectively.

Table 27. Anisotropic thermal parameters<sup>a</sup> ( $\times 10^3$ )for RhCL[P(C<sub>6</sub>H<sub>12</sub>)]<sub>2</sub>C<sub>9</sub>H<sub>12</sub> (5)

Atom	U <sub>11</sub>	U <sub>22</sub>	U <sub>33</sub>	U <sub>23</sub>	U <sub>13</sub>	U <sub>12</sub>
Rh(1)	34(0)	29(0)	41(0)	-01(0)	-02(0)	03(0)
CL(1)	33(1)	19(0)	33(1)	-03(0)	01(1)	07(0)
P(1)	34(1)	32(1)	42(1)	01(1)	-03(1)	03(1)
P(2)	35(1)	35(1)	44(1)	00(1)	00(1)	02(1)
C(1)	40(5)	24(4)	45(6)	02(4)	-01(4)	-04(4)
C(2)	50(6)	46(6)	43(6)	05(5)	06(5)	14(5)
C(3)	68(7)	44(6)	55(7)	08(5)	-01(6)	15(5)
C(4)	57(7)	56(6)	56(6)	12(6)	13(5)	01(5)
C(5)	56(7)	67(8)	73(8)	23(6)	14(6)	12(6)
C(6)	48(6)	62(7)	51(7)	15(5)	07(5)	05(5)
C(7)	39(6)	35(5)	59(7)	12(5)	05(5)	03(4)
C(8)	59(7)	48(6)	71(7)	-03(6)	10(6)	10(5)
C(9)	84(9)	44(6)	101(10)	-04(6)	27(7)	13(6)
C(10)	89(9)	48(6)	141(12)	39(8)	30(9)	37(6)
C(11)	92(9)	66(9)	101(10)	23(8)	-08(8)	32(7)
C(12)	57(7)	60(7)	73(8)	11(6)	-15(6)	21(6)
C(13)	39(5)	37(5)	39(5)	08(4)	-08(4)	03(4)
C(14)	67(7)	61(7)	54(6)	-13(5)	04(6)	-17(6)
C(15)	71(8)	88(9)	68(8)	-22(7)	00(7)	-30(7)
C(16)	53(7)	64(7)	89(9)	-27(7)	-26(6)	09(6)
C(17)	89(9)	78(8)	45(6)	-17(6)	-12(6)	10(7)
C(18)	60(7)	59(6)	56(6)	04(6)	00(5)	-11(6)
C(19)	45(6)	25(5)	49(6)	-01(4)	-07(5)	02(4)
C(20)	45(6)	37(5)	78(8)	-03(5)	-14(5)	07(5)
C(21)	54(7)	54(6)	70(8)	-02(6)	-22(6)	04(5)
C(22)	79(8)	37(6)	86(8)	05(5)	-58(7)	-11(5)
C(23)	64(7)	48(6)	76(8)	00(6)	-22(6)	-19(6)
C(24)	55(6)	54(6)	48(6)	10(5)	-08(5)	-01(5)
C(25)	43(6)	46(6)	60(6)	08(5)	05(5)	01(5)
C(26)	65(7)	55(6)	77(9)	11(6)	-20(6)	-09(5)
C(27)	98(10)	54(7)	107(11)	14(7)	-30(8)	-31(7)
C(28)	59(8)	48(7)	157(13)	15(8)	07(8)	-12(6)
C(29)	66(8)	68(7)	101(11)	33(7)	02(8)	07(6)
C(30)	53(6)	48(6)	71(7)	22(5)	01(6)	-05(5)
C(31)	57(7)	46(6)	46(6)	12(5)	09(5)	22(5)
C(32)	78(8)	92(9)	64(8)	22(7)	09(7)	43(7)

<sup>a</sup>The estimated standard deviations in the parentheses are for the least significant digits. The anisotropic temperature factors are defined as  $\exp(-2\pi^2 \sum_i h_i a_i^* U_{ij})$ .

Table 27. (continued)

---

Atom	U <sub>11</sub>	U <sub>22</sub>	U <sub>33</sub>	U <sub>23</sub>	U <sub>13</sub>	U <sub>12</sub>
C(33)	107(10)	120(11)	56(8)	17(7)	38(7)	67(9)
C(34)	175(14)	77(8)	75(9)	-11(8)	06(9)	51(9)
C(35)	156(14)	63(8)	72(8)	16(6)	09(9)	07(8)
C(36)	97(8)	37(6)	45(6)	-07(5)	-07(6)	06(6)
C(37)	118(12)	66(8)	124(12)	-07(8)	-19(10)	04(8)
C(38)	108(10)	36(6)	151(12)	30(8)	-32(9)	02(6)
C(39)	80(8)	47(6)	75(8)	19(6)	03(7)	01(6)
C(40)	39(6)	40(5)	65(7)	05(5)	01(5)	-02(5)
C(41)	39(6)	49(6)	59(6)	04(5)	06(5)	02(5)
C(42)	76(7)	59(7)	63(7)	-20(6)	-04(6)	-17(6)
C(43)	123(12)	44(7)	142(13)	-32(8)	-49(10)	26(7)
C(44)	147(15)	78(9)	109(11)	00(8)	-39(10)	-03(9)

---

Table 28. Refined bond distances<sup>a</sup> (Å) for RhCL[P(C<sub>6</sub>H<sub>6</sub>)<sub>3</sub>]<sub>2</sub>C<sub>9</sub>H<sub>12</sub> (5)

Atoms	Distance	Atoms	Distance
Rh(1) - CL(1)	2.421( 2)	C(40) - C(41)	1.360(13)
Rh(1) - P(1)	2.333( 2)	C(41) - C(42)	1.308(14)
Rh(1) - P(2)	2.331( 2)	C(42) - C(43)	1.512(17)
Rh(1) - C(40)	2.046( 9)	C(43) - C(44)	1.443(20)
Rh(1) - C(41)	2.059( 9)	C(44) - C(45)	1.31(3)
C(37) - C(38)	1.514(19)	C(44) - C(45')	1.80(3)
C(38) - C(39)	1.534(17)	C(45) - C(37)	1.80(3)
C(39) - C(40)	1.305(14)	C(45') - C(37)	1.46(3)
P(1) - C(1)	1.817( 8)	P(2) - C(19)	1.808( 9)
P(1) - C(7)	1.833( 9)	P(2) - C(25)	1.821(10)
P(1) - C(13)	1.814( 9)	P(2) - C(31)	1.840( 9)
C(1) - C(2)	1.389(12)	C(19) - C(20)	1.392(13)
C(2) - C(3)	1.388(13)	C(20) - C(21)	1.391(14)
C(3) - C(4)	1.366(14)	C(21) - C(22)	1.345(15)
C(4) - C(5)	1.350(14)	C(22) - C(23)	1.398(15)
C(5) - C(6)	1.388(14)	C(23) - C(24)	1.395(14)
C(6) - C(1)	1.373(13)	C(24) - C(19)	1.374(13)
C(7) - C(8)	1.382(13)	C(25) - C(26)	1.379(14)
C(8) - C(9)	1.375(15)	C(26) - C(27)	1.378(16)
C(9) - C(10)	1.383(17)	C(27) - C(28)	1.376(17)
C(10) - C(11)	1.313(17)	C(28) - C(29)	1.398(17)
C(11) - C(12)	1.382(16)	C(29) - C(30)	1.383(15)
C(12) - C(7)	1.401(14)	C(30) - C(25)	1.351(13)
C(13) - C(14)	1.383(13)	C(31) - C(32)	1.407(15)
C(14) - C(15)	1.356(15)	C(32) - C(33)	1.435(17)
C(15) - C(16)	1.351(16)	C(33) - C(34)	1.363(19)
C(16) - C(17)	1.368(16)	C(34) - C(35)	1.345(19)
C(17) - C(18)	1.375(15)	C(35) - C(36)	1.381(16)
C(18) - C(13)	1.385(13)	C(36) - C(31)	1.390(14)

<sup>a</sup>The estimated standard deviations in the parentheses are for the least significant digits.

Table 29. Refined bond angles<sup>a</sup> (°) for RhCl[P(C<sub>6</sub>H<sub>6</sub>)<sub>3</sub>]<sub>2</sub>C<sub>9</sub>H<sub>12</sub> (5)

Atoms	Angle	Atoms	Angle
CL(1) - Rh(1) - P(1)	88.0( 1)	CL(1) - Rh(1) - P(2)	88.0( 1)
P(1) - Rh(1) - C(40)	89.0( 3)	P(2) - Rh(1) - C(40)	93.9( 3)
P(1) - Rh(1) - C(41)	95.3( 3)	P(2) - Rh(1) - C(41)	89.8( 3)
CL(1) - Rh(1) - C(40)	163.7( 3)	CL(1) - Rh(1) - C(41)	157.7( 3)
P(1) - Rh(1) - P(2)	174.8( 1)	C(40) - Rh(1) - C(41)	38.7( 4)
C(38) - C(37) - C(45)	84.9(12)	Rh(1) - C(41) - C(42)	136.4( 8)
C(38) - C(37) - C(45')	134.8(16)	C(40) - C(41) - C(42)	153.1(10)
C(45) - C(37) - C(45')	73.8(16)	C(41) - C(42) - C(43)	126.3(10)
C(37) - C(38) - C(39)	114.9(10)	C(42) - C(43) - C(44)	115.3(11)
C(38) - C(39) - C(40)	127.2(10)	C(43) - C(44) - C(45)	137.4(18)
Rh(1) - C(40) - C(39)	137.3( 8)	C(43) - C(44) - C(45')	80.9(13)
Rh(1) - C(40) - C(41)	71.2( 6)	C(45) - C(44) - C(45')	77.4(18)
C(39) - C(40) - C(41)	150.9(10)	C(37) - C(45) - C(44)	107.4(20)
Rh(1) - C(41) - C(40)	70.1( 6)	C(37) - C(45') - C(44)	100.8(18)
Rh(1) - P(1) - C(1)	119.0( 3)	Rh(1) - P(2) - C(19)	112.8( 3)
Rh(1) - P(1) - C(7)	118.0( 3)	Rh(1) - P(2) - C(25)	117.3( 3)
Rh(1) - P(1) - C(13)	108.5( 3)	Rh(1) - P(2) - C(31)	114.6( 3)
C(1) - P(1) - C(7)	101.3( 4)	C(19) - P(2) - C(25)	102.8( 4)
C(1) - P(1) - C(13)	104.3( 4)	C(19) - P(2) - C(31)	105.6( 4)
C(7) - P(1) - C(13)	103.8( 4)	C(25) - P(2) - C(31)	102.2( 4)
P(1) - C(1) - C(2)	119.4( 6)	P(2) - C(19) - C(20)	122.8( 7)
P(1) - C(1) - C(6)	121.3( 7)	P(2) - C(19) - C(24)	118.5( 7)
P(1) - C(7) - C(8)	119.2( 7)	P(2) - C(25) - C(26)	121.2( 7)
P(1) - C(7) - C(12)	122.2( 7)	P(2) - C(25) - C(30)	120.2( 7)
P(1) - C(13) - C(14)	124.8( 7)	P(2) - C(31) - C(32)	119.8( 7)
P(1) - C(13) - C(18)	118.6( 7)	P(2) - C(31) - C(36)	118.7( 7)
C(2) - C(1) - C(6)	119.3( 8)	C(20) - C(19) - C(24)	118.7( 8)
C(1) - C(2) - C(3)	119.2( 8)	C(19) - C(20) - C(21)	120.1( 9)
C(2) - C(3) - C(4)	120.8( 9)	C(20) - C(21) - C(22)	120.6(10)
C(3) - C(4) - C(5)	120.0( 9)	C(21) - C(22) - C(23)	120.9(10)
C(4) - C(5) - C(6)	120.5(10)	C(22) - C(23) - C(24)	118.3( 9)
C(5) - C(6) - C(1)	120.3( 9)	C(23) - C(24) - C(19)	121.4( 9)
C(8) - C(7) - C(12)	118.6( 9)	C(26) - C(25) - C(30)	118.4( 9)
C(7) - C(8) - C(9)	119.0( 9)	C(25) - C(26) - C(27)	122.8(10)
C(8) - C(9) - C(10)	121.4(11)	C(26) - C(27) - C(28)	117.9(11)

<sup>a</sup>The estimated standard deviations in the parentheses are for the least significant digits.

Table 29. (continued)

Atoms	Angle	Atoms	Angle
C(9) - C(10) - C(11)	119.7(11)	C(27) - C(28) - C(29)	120.1(11)
C(10) - C(11) - C(12)	121.4(11)	C(28) - C(29) - C(30)	119.5(11)
C(11) - C(12) - C(7)	119.9(10)	C(29) - C(30) - C(25)	121.1( 9)
C(14) - C(13) - C(18)	116.7( 8)	C(32) - C(31) - C(36)	121.6( 9)
C(13) - C(14) - C(15)	121.9(10)	C(31) - C(32) - C(33)	116.0(10)
C(14) - C(15) - C(16)	120.3(11)	C(32) - C(33) - C(34)	121.0(12)
C(15) - C(16) - C(17)	120.2(10)	C(33) - C(34) - C(35)	121.2(13)
C(16) - C(17) - C(18)	119.3(10)	C(34) - C(35) - C(36)	121.2(12)
C(17) - C(18) - C(13)	121.5( 9)	C(35) - C(36) - C(31)	119.1(10)



Table 30. Equations of least squares planes (in the orthorhombic coordinate system) and the interplanar angles for 5

Atom	Distance from Plane(Å)	Atom	Distance from Plane(Å) <sup>a</sup>
Plane I fitting Rh(1)-CL(1)-P(1)-P(2) 4.4059*X + 2.6760*Y + 12.8577*Z - 7.1315 = 0.0			
Rh(1)	0.0485	CL(1)	0.0017
P(1)	-0.0251	P(2)	-0.0251
C(45)	0.4741*	C(45')	0.5109*
Plane II fitting Rh(1)-CL(1)-C(40)-C(41) 22.3744*X + 0.1235*Y - 4.2348*Z - 5.4801 = 0.0			
Rh(1)	0.0044	CL(1)	-0.0020
C(40)	-0.0014	C(41)	-0.0010
C(37)	0.4899*	C(44)	-0.5507*
C(38)	-0.2909*	C(43)	0.2206*
C(39)	-0.1162*	C(42)	0.0919*
C(45)	-0.9652*	C(45')	0.9901*
Plane III fitting C(37)-C(44)-C(45)-C(45') -0.0031*X + 23.9119*Y - 0.0446*Z - 8.2293 = 0.0			
C(37)	0.0419	C(44)	0.0463
C(45)	-0.0472	C(45')	-0.0409
Interplanar Angles(°)			
<u>Plane</u>		<u>Plane</u>	<u>Angle</u>
I		II	82.15
I		III	83.77
II		III	81.96
Torsional Angles (°)			
C(38)-C(37)-C(45)-C(44)			147.47
C(38)-C(37)-C(45')-C(44)			-70.65
C(37)-C(45)-C(44)-C(43)			-67.33
C(37)-C(45')-C(44)-C(43)			150.49

<sup>a</sup>The distances marked with a \* are those of the atoms not included in the calculation of the planes.

**Figure 11. ORTEP drawing for complex 5. Hydrogen atoms are omitted for clarity**

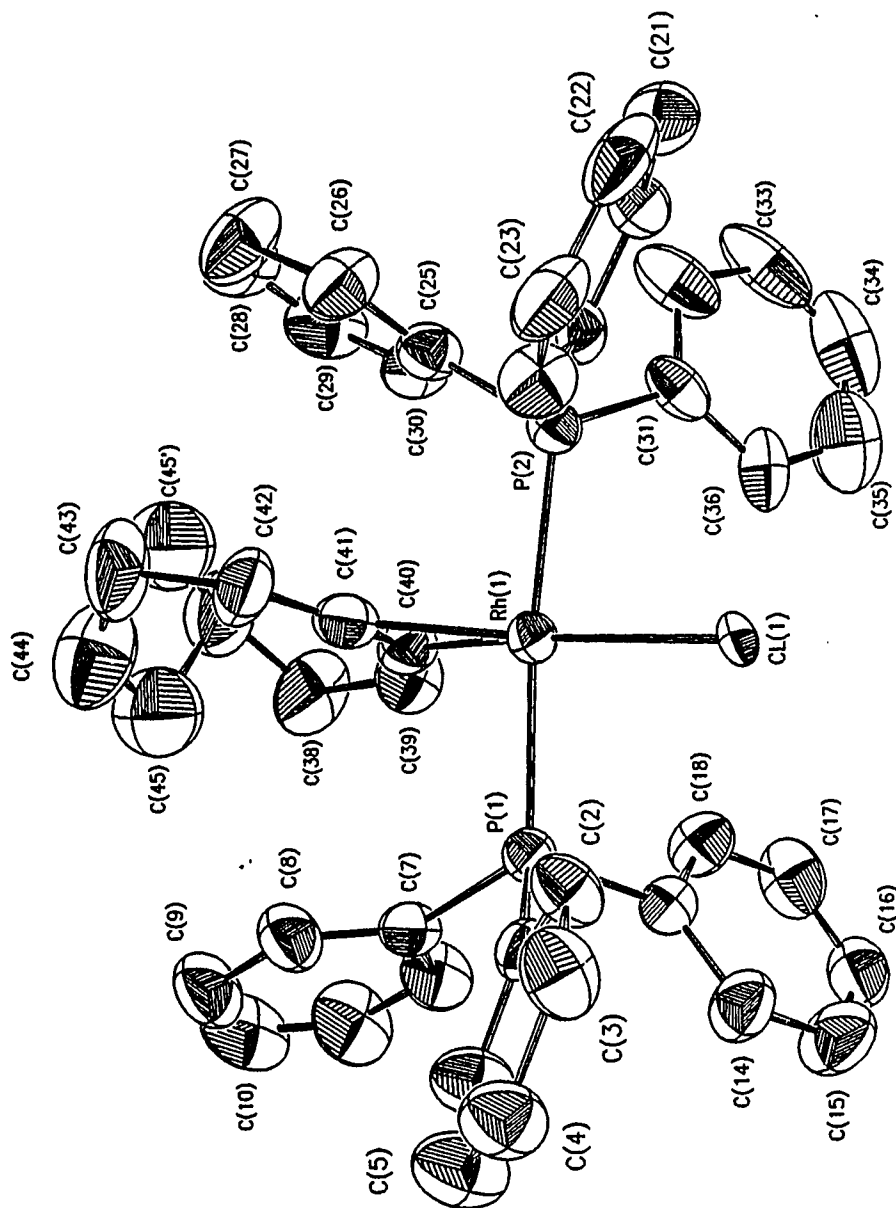
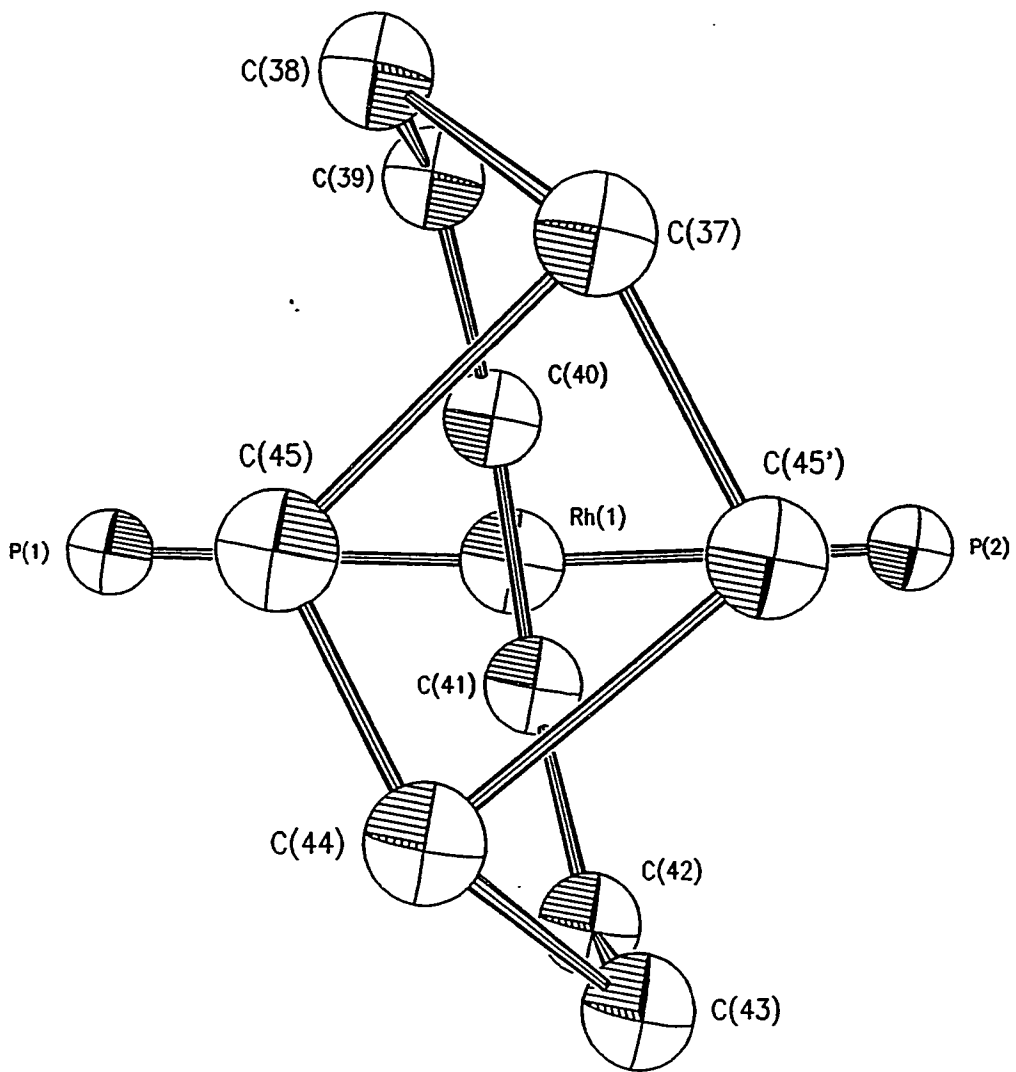


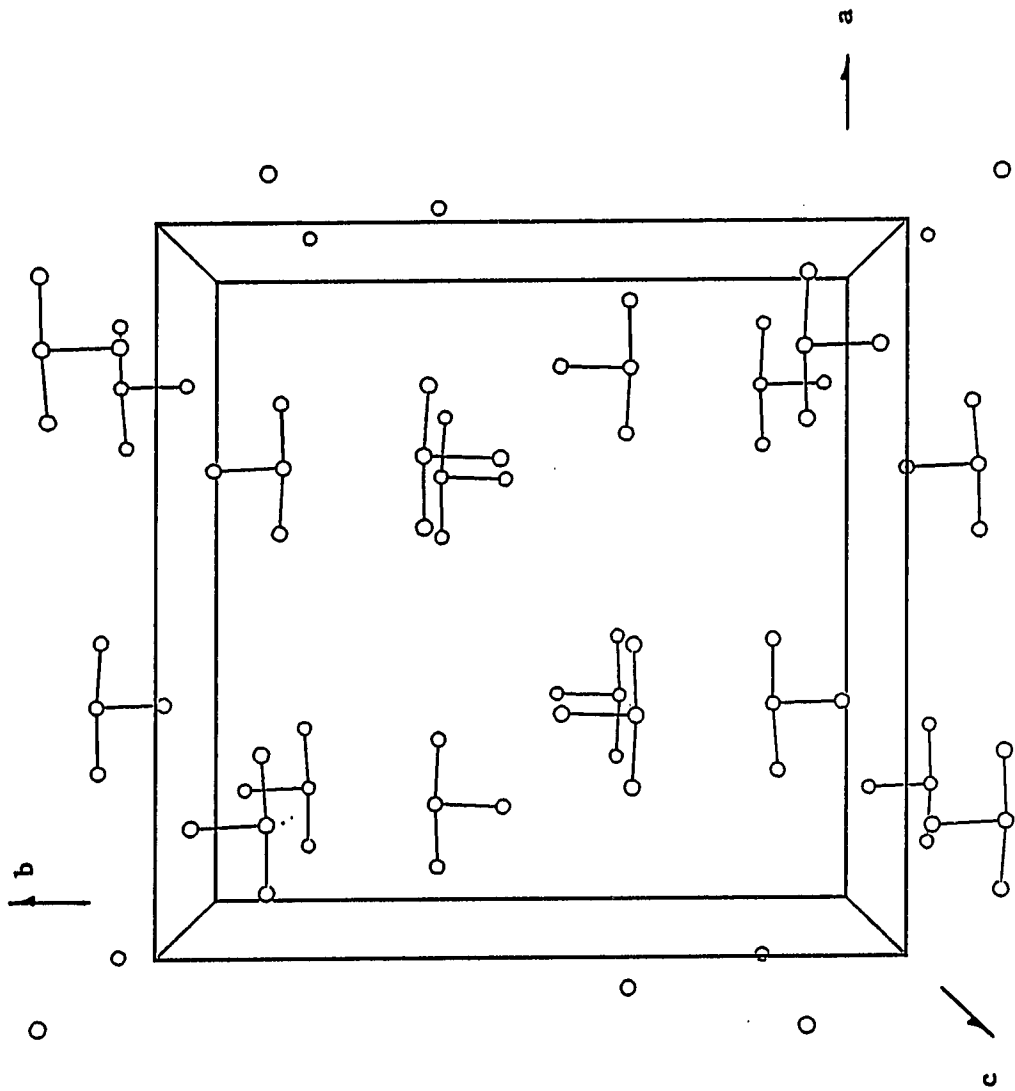
Figure 12 shows that in the complex the butatriene ligand is held in a nearly  $C_2$  conformation. This is in contrast to the  $C_s$  conformation predicted for the free ligand (see earlier). As expected, the central  $\pi$  bond is lengthened [ $d(C(40)-C(41)) = 1.36 \text{ \AA}$ ] relative to the free ligand [predicted<sup>57</sup> to be  $1.269 \text{ \AA}$ ]; however it is only slightly longer than that in complexes A and B ( $1.34 \text{ \AA}$  each) and in the (tetraphenylbutatriene)iron complex C ( $1.35 \text{ \AA}$ ).<sup>65</sup> Although these bond lengths are comparable to simple olefins ( $1.34 \text{ \AA}$ ), they are significantly longer than the central double bond in simple butatrienes ( $1.26 \text{ \AA}$ ).<sup>66</sup>

There is considerable cis bending of the uncomplexed portion of the ligand in 5,  $C(39)-C(40)-C(41)$  and  $C(40)-C(41)-C(42)$  angles being  $150.9$  and  $153.1^\circ$  respectively. A similar cis bending by about  $30^\circ$  at each originally  $sp$  carbon has been noted in all the  $\eta^2$ -butatriene complexes:  $147.8$  and  $154.0^\circ$  in A;<sup>56</sup>  $149.7$  and  $153.8^\circ$  in B;<sup>64</sup>  $151^\circ$  each in C.<sup>65</sup> The cis bending observed in the complex 5 is ca.  $10^\circ$  greater than that predicted for the free ligand (ca.  $16^\circ$ ). Comparing with the acyclic cases A, B and C, one may conclude that maximum relief of ring strain (introduced by the cumulenic bond) is realized by the ligand as soon as the cis bending in the complex 5 is in the vicinity of ca.  $30^\circ$ . A novel feature of the crystal structure is the disorder exhibited by the methylene carbon farthest from the rhodium atom. The difference electron density map revealed two positions for this carbon, which are labelled as C(45) and C(45'). When these two atoms were input into the least-squares refinement, each with an occupancy of 50%, little change from these values was noted (last footnote in Table 26); this suggests nearly equal probability for the two locations. This is also reflected in the increasing size of the thermal ellipsoids as one moves around the

Figure 12. The cyclononatriene ligand viewed along Rh-CL bond. CL(1) is eclipsed by Rh(1). Phenyl groups and the hydrogen atoms in the ligand are omitted for clarity



**Figure 13. Packing arrangement of the RhP2CL unit of the asymmetric unit. Phenyl groups and the ligand are left out for clarity**





ring from the rhodium side and in the relative constancy in the direction of the maximum amplitude of motion. This "flapping disorder" may be accounted for by the "maximum relief of strain" (discussed above) which can be expected to introduce ambient temperature conformational mobility to the complexed ligand; in addition the ligand (seen in Figure 11 as being 'sandwiched' between two phenyl rings) has enough room to undergo this conformational mobility. Another plausible reason for the "flapping disorder" is the existence of two equally probable conformations throughout the crystal.

Figure 13 illustrates the packing of the RhP2CL unit in the unit cell. It shows that planes of this unit align nearly parallel to the ab-plane. Rh-CL and Rh-P bonds are nearly parallel and perpendicular to the b axis respectively.

### Conclusion

Cyclic butatrienes are a fascinating and fundamental class of molecules which have received little attention. Our crystal structure study is first of its kind to provide detailed molecular structure information on a cyclic butatriene, even though in a stabilizing environment. The cis bending observed has been found to be nearly the same for both acyclic and cyclic (present study) butatrienes in their complexed state. Based on this observation we have argued that maximum relief of ring strain may be considered to have been achieved by the ligand upon complexation. If we apply this reasoning to other lower

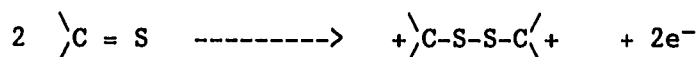
homologues of the ligand, it seems reasonable to predict that of the four lower homologues only cyclooctatriene and cycloheptatriene can be stabilized by such complexation and isolated. The cis bending in these lower homologues, predicted to be 156.3 and 145.0° respectively in their uncomplexed state,<sup>57</sup> are already in the stabilizing cis bending range observed for the complex 5.

CRYSTAL STRUCTURE OF TRI( $\mu$ -CARBONYL- $\mu$ -THIOCARBONYLBIS-  
[CARBONYL- $\eta^5$ -CYCLOPENTADIENYL IRON(II)])SILVER(I) TETRAFLUOROBORATE (6)

Introduction

Although, unlike carbonmonoxide, CS does not exist under ordinary conditions, a number of complexes containing the thiocarbonyl ligand have been made. The first thiocarbonyl complex was reported in 1966;<sup>67</sup> since then more than three hundred thiocarbonyl complexes have been described.<sup>68</sup> In these complexes, CS usually acts as a terminal ligand, but in a number of instances it has been found as a bridging ligand in preference to CO. CS has also been found to act as a semibridging ligand, again in preference to CO, in a couple of cases.<sup>69</sup> In all of these complexes additional ligands are present.

Chemical and electrochemical oxidation of organic compounds containing C=S double bond have been known to produce relatively stable dimeric cations that contain the disulfide linkage:<sup>70</sup>



In a similar way, thiocarbonyl complexes containing bridging CS group can be expected to undergo such oxidative dimerization leading to dithiocarbenium salts. Thus preliminary attempts at oxidatively dimerizing ( $\eta^5$ -C<sub>5</sub>H<sub>5</sub>)<sub>2</sub>Fe<sub>2</sub>(CO)<sub>3</sub>CS with AgBF<sub>4</sub> led Dr. Angelici's research group at Iowa State University to believe that indeed the corresponding dithiocarbenium salt may have been formed, as metallic silver was observed as one of the expected reaction products. However, the structure of the major oxidation product was not determinable solely

based on spectral data; elemental analysis was found to be inconclusive and the mass spectral data shed little light on the nature of the molecular ion. Thus in order to unequivocally establish the presence of the disulfide linkage, an x-ray crystal structure analysis was undertaken. Small single crystals of the major reaction product, here after referred to as 6, were provided by Dr. Angelici's research group. The data were collected and treated and the structure solved by the methods described in earlier chapters. However, because of lack of data with intensities significantly above zero, refinement could not be improved beyond a crystallographic residual of 12.3%. More crystals were prepared and one was used by Dr. Lee M. Daniels of the Iowa State Instrument Services, Iowa State University, on his Nonius diffractometer with its short crystal to film distance. By starting with our coordinates, he was able to refine them somewhat further to a crystallographic residual of 7.6%. Since this residual was slightly lower, these coordinates and other associated data are reported below.

## Experimental

Data collection A dark red crystal of 6 having approximate dimensions 0.15 x 0.20 x 0.20 mm was mounted on a glass fiber in a random orientation and mounted on a goniometer head. The crystal was then optically centered on the diffractometer (see Table 31). Cell constants and an orientation matrix were obtained from least-squares refinement, using the setting angles of 25 reflections in the range  $20^\circ \leq 2\theta \leq 34^\circ$ . Crystal data are summarized in Table 31. The data were collected using

Table 31. Crystal data for  $[\text{Ag}\{(\eta^5\text{-C}_5\text{H}_5)_2\text{Fe}_2(\text{CO})_3\text{CS}\}_3]\text{BF}_4$  (6)

---

F.W.	: 1304.65
Space Group	: $\text{P}\bar{1}$
a, Å	: 13.771(4) <sup>a</sup>
b, Å	: 15.047(7)
c, Å	: 12.544(4)
$\alpha$ , °	: 109.55(3)
$\beta$ , °	: 93.77(3)
$\gamma$ , °	: 90.76(3)
V, Å <sup>3</sup>	: 2442(3)
$\rho_{\text{calc}}$ , g/cm <sup>3</sup>	: 1.774
Z	: 2
Temperature, °K	: 295
Data collection Instrument	: Enraf-Nonius CAD4
Radiation, Å	: Mo $K_{\alpha}$
$\lambda$ , Å	: 0.71073 (graphite monochromator)
$\mu$ , cm <sup>-1</sup>	: 23.1 (correction applied)
$2\theta_{\text{max}}$ , °	: 50.0
Intensity Decay %	: 17.8 (decay correction applied)
Number of reflections collected	: 7949
Number of reflections observed	: 3980
Min of $I/\sigma(I)$	: 2.5
Number of variables	: 542
Observations/Variables	: 7.34
R, % <sup>b</sup>	: 7.58
$R_{\omega}$ , %	: 9.78

---

<sup>a</sup>Estimated standard deviations shown in parentheses are for the least significant digits.

$$R = \frac{\sum (|F_o| - |F_c|)}{\sum |F_o|}$$

$$R_{\omega} = \left[ \frac{\sum \omega (|F_o| - |F_c|)^2}{\sum \omega |F_o|^2} \right]^{1/2}, \text{ where } \omega = 1/\sigma^2(F) \dots$$

the  $\theta$ - $2\theta$  scan technique. For intense reflections an attenuator was automatically inserted in front of the detector; the attenuator factor was 11.9. As a check on crystal and electronic stability, three representative reflections were measured every 60 minutes. The intensity of the standards decreased by a total of 17.8%.

Reduction of x-ray intensity data      A linear decay correction was applied to the data based upon the observed decrease in standard reflection intensities with respect to time. An empirical absorption correction was applied to the data based on observed variations in the intensity distribution as a function of the orientation of the crystal for reflection near  $\chi = 90^\circ$ . Data were corrected for Lorentz and polarization effects. Intensities of equivalent reflections were then averaged.

#### Structure Determination and Refinement

In the beginning, we believed that we were dealing with a dithiocarbenium salt containing the disulfide linkage and hence we calculated that there could be as many as four dications (which means eight iron atoms per asymmetric unit to be found) plus eight tetrafluoroborate anions per unit cell, using  $2.48 \text{ gm/cm}^3$  as the upper estimate of the density for the compound. We initiated the structure determination by computing a sharpened three dimensional Patterson map. Unravelling the structure from Patterson map alone was difficult. A superposition map was then generated using what was assumed to be a

Fe-Fe vector in the Patterson map. Eight heavy peaks were picked out for the starting model and were input into a block-matrix least squares procedure<sup>12</sup> refining only the scale factor, and then the coordinates. The crystallographic residual, the R-factor, turned out to be 52%. Of the eight coordinates chosen, only three pairs of these appeared to be Fe-Fe pairs, based on a inter-coordinate distance of about 2.5 Å. The R-factor, with these six iron atoms in the starting model, was 46%. An electron density map calculated at this stage showed a peak that was heavier than the peaks corresponding to the six iron atoms in the starting model. This peak, given the label Fe7, when included in the model brought the R-factor down to 37%.

While many of the atoms belonging to the asymmetric unit were located by successive structure factor and electron density map calculations,<sup>11</sup> the carbon atoms of the Cp rings and the  $\text{BF}_4^-$  unit were not to be found until after the following was done. The peak that was given the label Fe7 appeared to be bonded to three sulfur atoms and still appeared to be heavier than the iron atom peaks; the Fe7-S distances were about 2.5 Å and the S-Fe7-S angles, which were not far from  $120^\circ$ , added up to nearly  $360^\circ$ . In a separate least squares run we refined only the occupancy factor of Fe7 and an occupancy factor of 1.57 for Fe7 that translates into 41 electrons was observed. Thus we suspected that Fe7 might in fact be a silver atom. Upon relabelling Fe7 as Ag1 and calculating a difference electron density map, the rest of the atoms in the asymmetric unit could be observed. When all the 66 non-hydrogen atoms were refined isotropically, many of the less heavy atoms showed high temperature factors; during anisotropic refinement of all the 66 atoms, many carbon atoms and a few oxygen atoms showed non-positive definite temperature

factors. For this first data set, the 'final' R-factor was 12.3% when the atoms showing such behavior were assigned an isotropic thermal parameter of  $12 \text{ \AA}^2$ ; however many parameters showed no sign of "settling down". Inclusion of calculated hydrogen atoms (60 in number) did not significantly improve the results and thus were not included.

We conclude this section by briefly outlining the structure solution and refinement carried out by Dr. Daniels at the Iowa State Molecular Laboratory. The positions of the Ag and Fe atoms were obtained by a Patterson interpretation method.<sup>71</sup> The rest of the non hydrogen atoms were located by subsequent least-squares and difference Fourier techniques;<sup>72</sup> these coordinates were essentially the same as had been found earlier. Because of the low ratio of number of observations to maximum number of possible parameters, the Cp rings were refined as rigid groups (with a C-C distance of  $1.42 \text{ \AA}$ ), although it was possible to refine the ring atoms anisotropic thermal parameters. Inclusion of calculated hydrogen atoms did not improve the results, and hence were not included. The final conventional R-factor was 7.6%.

The atomic scattering factors used were those from reference 13; those of Ag, Fe and S were modified for anomalous dispersion effects.<sup>14</sup>

#### Discussion of the Structure

The final atomic positional and anisotropic thermal parameters are listed in Tables 32 and 33 respectively while the refined bond distances and bond angles are listed in Tables 34 and 35 respectively. Table 36



Table 32. Postional parameters<sup>a</sup> ( $\times 10^4$ ) for 6

Atom	x	y	z	$U_{iso}^b$
Ag(1)	3047(1)	3092(1)	3213(2)	58(1)
Fe(1)	6267(2)	1745(2)	1015(2)	36(1)
Fe(2)	6002(2)	3393(2)	2283(2)	33(1)
Fe(3)	3267(2)	0953(2)	4757(2)	32(1)
Fe(4)	2910(2)	1907(2)	6736(2)	36(1)
Fe(5)	0904(2)	4801(2)	2381(2)	35(1)
Fe(6)	1937(2)	6013(2)	1973(2)	33(1)
S(1')	4131(4)	1919(4)	1962(5)	54(1)
S(2')	2454(4)	3066(3)	5029(5)	44(1)
S(3')	3244(4)	4650(5)	2936(7)	59(2)
O(1)	5236(13)	1725(11)	-1105(12)	82(6)
O(2)	4955(15)	4075(13)	0636(16)	94(9)
O(3)	5134(11)	1753(10)	4696(13)	61(5)
O(4)	4573(12)	3243(11)	7432(16)	88(6)
O(5)	1148(21)	3170(11)	0372(16)	131(9)
O(6)	2529(14)	4918(11)	-0256(13)	94(6)
O(7)	7657(10)	3164(9)	0914(12)	59(5)
O(8)	4213(10)	0340(9)	6527(12)	54(5)
O(9)	-0080(12)	5836(10)	1087(13)	77(6)
C(1')	5188(13)	2313(13)	1814(15)	29(5)
C(2')	2789(12)	2165(11)	5353(15)	31(5)
C(3')	2234(13)	5046(12)	2522(17)	35(5)
C(1)	5643(15)	1763(14)	-0256(16)	49(6)
C(2)	5354(16)	3808(14)	1292(17)	52(7)
C(3)	4391(12)	1442(11)	4709(15)	34(6)
C(4)	3950(16)	2692(13)	7178(17)	47(6)
C(5)	1017(20)	3830(17)	1157(19)	60(7)
C(6)	2279(18)	5360(12)	0626(17)	58(7)
C(7)	6956(14)	2900(13)	1211(15)	44(6)
C(8)	3718(14)	0836(12)	6191(16)	37(6)
C(9)	0595(14)	5612(12)	1540(15)	50(6)
C(11)	6331(17)	0288(14)	0415(26)	80(10)
C(12)	6142(16)	0576(17)	1579(24)	70(10)
C(13)	6944(16)	1157(13)	2218(23)	59(8)
C(14)	7629(17)	1227(13)	1449(20)	91(11)
C(15)	7250(20)	0690(17)	0334(22)	80(10)

<sup>a</sup>The estimated standard deviations in the parentheses are for the least significant digits.

<sup>b</sup>For anisotropically refined atoms,  $U_{iso} \equiv 10^3/3 \sum U_{ij} a_i^* a_j^* \vec{a}_i \cdot \vec{a}_j$ , where the temperature factors are defined as  $\exp(-2\pi^2 \sum h_i h_j a_i^* a_j^* U_{ij})$ .

Table 32. (continued)

---

Atom	x	y	z	U <sub>iso</sub>
C(21)	7171(14)	3785(16)	3589(16)	73(7)
C(22)	6370(18)	3382(15)	3948(15)	60(7)
C(23)	5557(14)	3953(16)	3951(16)	73(7)
C(24)	5855(16)	4709(13)	3594(18)	66(7)
C(25)	6852(15)	4606(12)	3370(19)	64(7)
C(31)	1954(16)	0344(16)	3941(21)	107(8)
C(32)	2543(18)	0540(15)	3152(20)	96(11)
C(33)	3390(18)	0001(15)	3079(22)	100(10)
C(34)	3325(18)	-0528(17)	3823(18)	80(10)
C(35)	2437(22)	-0316(17)	4355(19)	100(11)
C(41)	2022(17)	2795(16)	7891(23)	90(11)
C(42)	1426(14)	2181(20)	6964(20)	60(11)
C(43)	1597(26)	1239(17)	6912(33)	130(12)
C(44)	2299(27)	1272(27)	7808(40)	14(2)
C(45)	2561(20)	2234(20)	8413(18)	90(12)
C(51)	-0317(17)	4147(18)	2778(22)	80(10)
C(52)	0531(16)	3992(15)	3389(20)	54(8)
C(53)	0934(14)	4884(22)	4096(16)	100(11)
C(54)	0334(21)	5592(13)	3922(19)	100(12)
C(55)	-0439(16)	5136(20)	3108(25)	70(12)
C(61)	3037(19)	6940(14)	3090(21)	70(8)
C(62)	2119(18)	7130(13)	3554(16)	67(7)
C(63)	1490(17)	7400(13)	2781(23)	71(7)
C(64)	2020(20)	7376(13)	1839(17)	70(8)
C(65)	2977(18)	7092(15)	2030(23)	90(11)
B(1)	9421(29)	1713(28)	3916(36)	74(12)
F(1)	8786(13)	2408(12)	3926(16)	166(9)
F(2)	10038(13)	2015(12)	4870(16)	197(10)
F(3)	8908(13)	0921(12)	3861(16)	212(12)
F(4)	9949(13)	1525(12)	2984(16)	197(12)

---

Table 33. Anisotropic thermal parameters<sup>a</sup> ( $\times 10^3$ ) for 6

Atom	U <sub>11</sub>	U <sub>22</sub>	U <sub>33</sub>	U <sub>23</sub>	U <sub>13</sub>	U <sub>12</sub>
Ag(1)	67(1)	80(1)	91(1)	104(1)	54(1)	56(1)
Fe(1)	33(1)	39(1)	24(1)	01(1)	-18(1)	-09(1)
Fe(2)	31(1)	33(1)	34(1)	13(1)	-12(1)	-19(1)
Fe(3)	34(1)	25(1)	37(1)	10(1)	02(1)	02(1)
Fe(4)	41(2)	37(1)	38(1)	19(1)	12(1)	16(1)
Fe(5)	33(1)	40(1)	35(1)	15(1)	05(1)	-11(1)
Fe(6)	44(2)	36(1)	32(1)	26(1)	07(1)	-03(1)
S(1')	41(3)	50(3)	63(3)	10(3)	17(3)	-36(2)
S(2')	63(3)	36(2)	53(3)	39(2)	20(3)	28(2)
S(3')	35(3)	87(4)	148(6)	161(4)	20(3)	20(3)
O(1)	110(10)	110(10)	31(8)	52(9)	-80(8)	-40(8)
O(2)	140(20)	110(10)	120(10)	170(10)	-60(10)	60(10)
O(3)	54(9)	68(9)	80(10)	57(8)	-08(8)	-16(7)
O(4)	80(10)	100(10)	90(10)	40(10)	-56(9)	-90(10)
O(5)	280(30)	40(10)	60(10)	-10(8)	90(10)	10(10)
O(6)	160(20)	50(9)	53(9)	-25(7)	110(10)	-20(9)
O(7)	53(9)	90(10)	64(9)	66(8)	22(7)	-40(7)
O(8)	73(9)	66(8)	66(9)	72(7)	25(7)	69(7)
O(9)	60(10)	120(10)	60(10)	60(8)	-59(8)	23(9)
C(1')	40(10)	17(7)	31(9)	07(7)	-10(8)	-26(7)
C(2')	30(10)	21(8)	33(9)	02(7)	19(8)	-09(7)
C(3')	30(10)	50(10)	33(9)	23(8)	08(8)	-02(8)
C(1)	50(10)	50(10)	45(8)	16(9)	-19(9)	-36(9)
C(2)	50(10)	70(10)	72(9)	63(9)	-00(1)	02(1)
C(3)	30(10)	19(8)	55(8)	14(8)	-09(9)	-21(7)
C(4)	50(10)	70(10)	39(9)	42(9)	14(9)	30(10)
C(5)	100(20)	60(10)	40(10)	40(10)	00(10)	-60(10)
C(6)	100(20)	21(9)	60(10)	20(10)	30(10)	-26(9)
C(7)	60(10)	36(9)	28(8)	02(8)	09(8)	-20(8)
C(8)	40(10)	40(10)	47(8)	35(8)	21(8)	03(9)
C(9)	60(10)	60(10)	29(7)	09(8)	-02(8)	22(8)
C(11)	70(20)	30(10)	110(20)	-00(10)	-80(20)	00(10)
C(12)	80(20)	40(10)	110(20)	60(10)	20(20)	40(10)
C(13)	80(20)	70(10)	70(20)	81(8)	-00(10)	50(10)
C(14)	100(20)	80(10)	90(20)	43(9)	-60(20)	80(20)

<sup>a</sup>The estimated standard deviations in the parentheses are for the least significant digits. The anisotropic temperature factors are defined as  $\exp(-2\pi^2 \sum h_i h_j a_i^* a_j^* U_{ij})$ . Those numbers with e.s.d's which are multiples of 10 have significant digits only upto the second decimal place.

Table 33. (continued)

Atom	U <sub>11</sub>	U <sub>22</sub>	U <sub>33</sub>	U <sub>23</sub>	U <sub>13</sub>	U <sub>12</sub>
C(15)	90(20)	60(10)	80(20)	00(10)	20(10)	70(10)
C(21)	30(10)	90(20)	40(10)	-40(10)	-50(20)	-50(10)
C(22)	80(20)	60(10)	20(10)	-04(9)	-20(10)	-30(10)
C(23)	60(10)	70(10)	30(10)	-50(10)	10(10)	-20(10)
C(24)	70(20)	40(10)	60(10)	-20(10)	00(10)	00(10)
C(25)	80(20)	50(10)	60(10)	20(10)	-20(10)	-70(10)
C(31)	70(20)	60(10)	100(10)	-90(10)	-10(10)	-40(10)
C(32)	120(20)	90(20)	70(20)	60(20)	-150(20)	-160(20)
C(33)	80(20)	80(20)	70(20)	-60(10)	-30(1)	-20(10)
C(34)	110(20)	50(10)	70(20)	00(10)	-30(10)	00(10)
C(35)	170(30)	70(20)	60(20)	20(10)	20(20)	-160(20)
C(41)	80(20)	90(20)	80(20)	-20(20)	100(20)	10(20)
C(42)	30(10)	130(20)	140(20)	160(20)	90(10)	40(10)
C(43)	140(30)	90(20)	140(30)	-10(20)	240(20)	-90(20)
C(44)	260(50)	230(40)	300(50)	480(50)	470(40)	340(40)
C(45)	60(20)	250(40)	70(20)	170(20)	20(10)	40(20)
C(51)	30(10)	120(20)	70(20)	10(20)	10(10)	-90(10)
C(52)	60(10)	90(20)	80(20)	100(10)	50(20)	-20(10)
C(53)	100(20)	170(30)	20(10)	10(20)	50(10)	-100(20)
C(54)	170(30)	40(10)	130(30)	20(20)	240(20)	-10(20)
C(55)	60(20)	150(30)	140(30)	190(20)	140(20)	90(20)
C(61)	90(20)	30(10)	90(20)	30(10)	-30(10)	-40(10)
C(62)	100(20)	40(10)	43(10)	00(10)	-30(10)	-30(10)
C(63)	70(20)	30(10)	80(20)	-20(10)	10(10)	00(10)
C(64)	100(20)	50(10)	80(20)	60(10)	00(10)	-30(10)
C(65)	140(30)	70(20)	60(20)	10(10)	50(20)	-60(20)
B(1)	100(20)	100(20)	100(20)	120(20)	40(20)	120(20)
F(1)	170(20)	180(20)	110(10)	20(10)	-70(10)	180(10)
F(2)	170(20)	230(20)	130(10)	20(10)	-210(10)	120(20)
F(3)	330(30)	210(20)	190(20)	220(20)	-100(20)	-360(20)
F(4)	230(20)	270(30)	160(20)	120(20)	200(20)	200(20)

Table 34. Refined bond distances<sup>a</sup> (Å) for 6

Atoms	Distance	Atoms	Distance
Ag(1) - S(1')	2.517(5)	Fe(1) - Fe(2)	2.505(3)
Ag(1) - S(2')	2.482(6)	Fe(3) - Fe(4)	2.501(3)
Ag(1) - S(3')	2.496(7)	Fe(5) - Fe(6)	2.502(3)
Fe(1) - C(1)	1.77(2)	Fe(4) - C(4)	1.78(2)
Fe(2) - C(2)	1.77(2)	Fe(5) - C(5)	1.75(2)
Fe(3) - C(3)	1.72(2)	Fe(6) - C(6)	1.75(2)
Fe(1) - C(1')	1.90(1)	Fe(2) - C(1')	1.86(1)
Fe(3) - C(2')	1.87(1)	Fe(4) - C(2')	1.90(2)
Fe(5) - C(3')	1.85(2)	Fe(6) - C(3')	1.85(2)
Fe(1) - C(7)	1.90(2)	Fe(2) - C(7)	1.92(2)
Fe(3) - C(8)	1.93(2)	Fe(4) - C(8)	1.93(2)
Fe(5) - C(9)	1.90(2)	Fe(6) - C(9)	1.92(2)
Fe(1) - C(11)	2.07(1)	Fe(2) - C(21)	2.15(1)
Fe(1) - C(12)	2.11(2)	Fe(2) - C(22)	2.12(2)
Fe(1) - C(13)	2.16(2)	Fe(2) - C(23)	2.11(1)
Fe(1) - C(14)	2.15(2)	Fe(2) - C(24)	2.13(1)
Fe(1) - C(15)	2.09(2)	Fe(2) - C(25)	2.15(1)
Fe(3) - C(31)	2.06(1)	Fe(4) - C(41)	2.09(2)
Fe(3) - C(32)	2.08(2)	Fe(4) - C(42)	2.11(2)
Fe(3) - C(33)	2.13(2)	Fe(4) - C(43)	2.12(2)
Fe(3) - C(34)	2.15(2)	Fe(4) - C(44)	2.10(2)
Fe(3) - C(35)	2.10(2)	Fe(4) - C(45)	2.09(2)
Fe(5) - C(51)	2.11(2)	Fe(6) - C(61)	2.14(1)
Fe(5) - C(52)	2.11(2)	Fe(6) - C(62)	2.13(1)
Fe(5) - C(53)	2.11(2)	Fe(6) - C(63)	2.11(1)
Fe(5) - C(54)	2.11(2)	Fe(6) - C(64)	2.11(2)
Fe(5) - C(55)	2.11(2)	Fe(6) - C(65)	2.13(2)
S(1') - C(1')	1.61(2)	O(7) - C(7)	1.17(2)
S(2') - C(2')	1.61(2)	O(8) - C(8)	1.18(2)
S(3') - C(3')	1.64(2)	O(9) - C(9)	1.17(2)
O(1) - C(1)	1.15(2)	O(4) - C(4)	1.14(2)
O(2) - C(2)	1.14(3)	O(5) - C(5)	1.17(2)
O(3) - C(3)	1.12(2)	O(6) - C(6)	1.16(2)

<sup>a</sup>The estimated standard deviations in the parentheses are for the least significant digits.

Table 34. (continued)

Atoms	Distance	Atoms	Distance
C(11) - C(12)	1.42(3)	C(21) - C(22)	1.42(2)
C(12) - C(13)	1.42(2)	C(22) - C(23)	1.42(2)
C(13) - C(14)	1.42(3)	C(23) - C(24)	1.42(2)
C(14) - C(15)	1.42(2)	C(24) - C(25)	1.42(2)
C(15) - C(11)	1.42(3)	C(25) - C(21)	1.42(2)
C(31) - C(32)	1.42(3)	C(41) - C(42)	1.42(3)
C(32) - C(33)	1.42(2)	C(42) - C(43)	1.42(2)
C(33) - C(34)	1.42(4)	C(43) - C(44)	1.42(3)
C(34) - C(35)	1.42(2)	C(44) - C(45)	1.42(2)
C(35) - C(31)	1.42(3)	C(45) - C(41)	1.42(3)
C(51) - C(52)	1.42(2)	C(61) - C(62)	1.42(2)
C(52) - C(53)	1.42(3)	C(62) - C(63)	1.42(3)
C(53) - C(54)	1.42(3)	C(63) - C(64)	1.42(3)
C(54) - C(55)	1.42(2)	C(64) - C(65)	1.42(2)
C(55) - C(51)	1.42(3)	C(65) - C(61)	1.42(3)
B(1) - F(1)	1.37(2)	B(1) - F(3)	1.36(2)
B(1) - F(2)	1.36(2)	B(1) - F(4)	1.37(2)
Fe(1) - Cp(1) <sup>b</sup>	1.74(2)	Fe(2) - Cp(2)	1.76(1)
Fe(3) - Cp(3)	1.72(2)	Fe(4) - Cp(4)	1.72(2)
Fe(5) - Cp(5)	1.73(2)	Fe(6) - Cp(6)	1.75(1)

<sup>b</sup>Cp(n) stands for the centroid of the cyclopentadienyl ligand.

Table 35. Refined bond angles<sup>a</sup> (°) for 6

Atoms	Angle	Atoms	Angle
S(1') - Ag(1) - S(2')	126.6(2)	Ag(1) - S(1') - C(1')	116.6(5)
S(1') - Ag(1) - S(3')	109.9(2)	Ag(1) - S(2') - C(2')	113.4(6)
S(2') - Ag(1) - S(3')	118.2(2)	Ag(1) - S(3') - C(3')	114.4(7)
S(1') - C(1') - Fe(1)	133.7(8)	S(1') - C(1') - Fe(2)	142.8(8)
S(2') - C(2') - Fe(3)	143.0(10)	S(2') - C(2') - Fe(4)	133.5(8)
S(3') - C(3') - Fe(5)	140.0(10)	S(3') - C(3') - Fe(6)	135.0(10)
O(7) - C(7) - Fe(1)	139.0(10)	O(7) - C(7) - Fe(2)	139.0(10)
O(8) - C(8) - Fe(3)	138.0(10)	O(8) - C(8) - Fe(4)	141.0(10)
O(9) - C(9) - Fe(5)	140.0(20)	O(9) - C(9) - Fe(6)	138.0(20)
Fe(1) - C(1') - Fe(2)	83.5(6)	Fe(1) - C(7) - Fe(2)	81.9(8)
Fe(3) - C(2') - Fe(4)	83.2(7)	Fe(3) - C(8) - Fe(4)	80.9(7)
Fe(5) - C(3') - Fe(6)	85.3(7)	Fe(5) - C(9) - Fe(6)	81.9(7)
C(1) - Fe(1) - Fe(2)	99.9(5)	C(2) - Fe(2) - Fe(1)	99.0(6)
C(3) - Fe(3) - Fe(4)	99.6(6)	C(4) - Fe(4) - Fe(3)	101.5(5)
C(5) - Fe(5) - Fe(6)	100.5(8)	C(6) - Fe(6) - Fe(5)	100.4(7)
C(1') - Fe(1) - Fe(2)	47.7(4)	C(1') - Fe(2) - Fe(1)	48.8(4)
C(2') - Fe(3) - Fe(4)	48.9(5)	C(2') - Fe(4) - Fe(3)	48.0(4)
C(3') - Fe(5) - Fe(6)	47.3(6)	C(3') - Fe(6) - Fe(5)	47.4(5)
C(7) - Fe(1) - Fe(2)	49.3(5)	C(7) - Fe(2) - Fe(1)	48.8(5)
C(8) - Fe(3) - Fe(4)	49.5(5)	C(8) - Fe(4) - Fe(3)	49.6(5)
C(9) - Fe(5) - Fe(6)	49.5(5)	C(9) - Fe(6) - Fe(5)	48.6(6)
C(1') - Fe(1) - C(7)	95.5(7)	C(1') - Fe(2) - C(7)	96.2(6)
C(2') - Fe(3) - C(8)	96.5(6)	C(2') - Fe(4) - C(8)	95.7(7)
C(3') - Fe(5) - C(9)	95.9(8)	C(3') - Fe(6) - C(9)	95.0(8)
C(1) - Fe(1) - C(1')	89.0(7)	C(2) - Fe(2) - C(1')	89.5(8)
C(1) - Fe(1) - C(7)	91.7(8)	C(2) - Fe(2) - C(7)	89.7(8)
C(3) - Fe(3) - C(2')	89.7(7)	C(4) - Fe(4) - C(2')	89.4(8)
C(3) - Fe(3) - C(8)	88.3(8)	C(4) - Fe(4) - C(8)	91.4(7)
C(5) - Fe(5) - C(3')	90.6(8)	C(5) - Fe(6) - C(3')	90.6(8)
C(5) - Fe(5) - C(9)	92.8(9)	C(5) - Fe(6) - C(9)	92.8(9)

<sup>a</sup>The estimated standard deviations in the parentheses are for the least significant digits.

Table 35. (continued)

Atoms	Angle	Atoms	Angle
Fe(1) - C(1) - O(1)	176.6(16)	Fe(2) - C(2) - O(2)	178.0(17)
Fe(3) - C(3) - O(3)	177.8(14)	Fe(4) - C(4) - O(4)	174.4(17)
Fe(5) - C(5) - O(5)	175.6(19)	Fe(6) - C(6) - O(6)	177.9(17)
C(11) - C(12) - C(13)	108.0(19)	C(21) - C(22) - C(23)	108.0(16)
C(12) - C(13) - C(14)	108.0(18)	C(22) - C(23) - C(24)	108.0(16)
C(13) - C(14) - C(15)	108.0(18)	C(23) - C(24) - C(25)	108.0(16)
C(14) - C(15) - C(11)	108.0(19)	C(24) - C(25) - C(21)	108.0(16)
C(15) - C(11) - C(12)	108.0(19)	C(25) - C(21) - C(22)	108.0(16)
C(31) - C(32) - C(33)	108.0(18)	C(41) - C(42) - C(43)	108.0(20)
C(32) - C(33) - C(34)	108.0(18)	C(42) - C(43) - C(44)	108.0(20)
C(33) - C(34) - C(35)	108.0(19)	C(43) - C(44) - C(45)	108.0(20)
C(34) - C(35) - C(31)	108.0(19)	C(44) - C(45) - C(41)	108.0(20)
C(35) - C(31) - C(32)	108.0(18)	C(45) - C(41) - C(42)	108.0(20)
C(51) - C(52) - C(53)	108.0(18)	C(61) - C(62) - C(63)	108.0(17)
C(52) - C(53) - C(54)	108.0(18)	C(62) - C(63) - C(64)	108.0(18)
C(53) - C(54) - C(55)	108.0(19)	C(63) - C(64) - C(65)	108.0(18)
C(54) - C(55) - C(51)	108.0(20)	C(64) - C(65) - C(61)	108.0(18)
C(55) - C(51) - C(52)	108.0(19)	C(65) - C(61) - C(62)	108.0(18)
F(1) - B(1) - F(2)	109.0(10)	F(2) - B(1) - F(3)	111.0(20)
F(1) - B(1) - F(3)	109.0(10)	F(2) - B(1) - F(4)	109.0(10)
F(1) - B(1) - F(4)	109.0(20)	F(3) - B(1) - F(4)	109.0(10)
$\langle C(n) - Fe(n) - Cp(n) \rangle^b$	123.48, n = 1 to 6		
$\langle C(m) - Fe(n) - Cp(n) \rangle$	121.94, n = 1 to 6; m = 7 to 9		
$\langle C(m') - Fe(n) - Cp(n) \rangle$	125.41, m = 1 to 3; n = 1 to 6		
$\langle Fe(m) - Fe(n) - Cp(n) \rangle$	136.31, (n = 1,3,5; m = n+1); (n = 2,4,6; m = n-1)		
$\langle Fe(n) - Cp(n) - C(nm) \rangle$	90.00, n = 1 to 6; m = 1 to 5		
$\langle Cp(n) - Fe(n) - C(nm) \rangle$	34.84, n = 1 to 6; m = 1 to 5		
$\langle C(nm) - Fe(n) - C(np) \rangle$	39.24, n = 1 to 6; m, p = 1 to 5 <sup>c</sup>		

<sup>b</sup>Here Cp(n) corresponds to the centroid of the ligand Cp.

<sup>c</sup>m and p are cyclically adjacent to each other.



Table 36. Equations of least squares planes (in the triclinic coordinate system) and the interplanar angles in 6

Atom	Distance from Plane(Å)	Atom	Distance from Plane(Å)
Plane I fitting Ag(1)-S(1')-S(2')-S(3')			
$11.2018*X + 1.6328*Y + 5.5377*Z - 5.9446 = 0.0$			
Ag(1)	-0.2480	S(1')	0.0827
S(2')	0.0902	S(3')	0.0751
Plane II fitting Fe(1)-Fe(2)-C(1')-C(7)-S(1')-O(7)			
$5.8090*X - 7.3959*Y + 10.7205*Z - 3.2460 = 0.0$			
Fe(1)	0.1926	Fe(2)	0.1789
C(1')	0.0019	S(1')	-0.1629
C(7)	-0.0521	O(7)	-0.1584
Plane III fitting Fe(3)-Fe(4)-C(2')-C(8)-S(2')-O(8)			
$11.9810*X + 7.0209*Y - 1.3149*Z - 4.1908 = 0.0$			
Fe(3)	-0.2325	Fe(4)	-0.2507
C(2')	-0.0328	S(2')	0.2414
C(8)	0.0369	O(8)	0.2378
Plane IV fitting Fe(5)-Fe(6)-C(3')-C(9)-S(3')-O(9)			
$-3.0820*X + 5.7702*Y + 9.1600*Z - 4.5187 = 0.0$			
Fe(5)	0.1538	Fe(6)	0.1608
C(3')	0.0147	S(3')	-0.1457
C(9)	-0.0528	O(9)	-0.1308
Plane V fitting O(1)-C(1)-Fe(1)-Fe(2)-C(2)-O(2)			
$12.0454*X + 5.8644*Y - 5.6134*Z - 7.9687 = 0.0$			
O(1)	-0.0292	O(2)	0.0328
C(1)	0.0059	C(2)	-0.0119
Fe(1)	0.0337	Fe(2)	-0.0313
Plane VI fitting O(3)-C(3)-Fe(3)-Fe(4)-C(4)-O(4)			
$-6.0810*X + 12.3193*Y - 7.5328*Z + 4.4516 = 0.0$			
O(3)	-0.0481	O(4)	0.0669
C(3)	0.0096	C(4)	-0.0415
Fe(3)	0.0562	Fe(4)	-0.0432

Table 36. (continued)

Atom	Distance from Plane(Å)	Atom	Distance from Plane(Å)
Plane VII fitting O(5)-C(5)-Fe(5)-Fe(6)-C(6)-O(6)			
$10.8470*X - 6.6128*Y + 6.3681*Z + 0.6584 = 0.0$			
O(5)	0.0438	O(6)	-0.0139
C(5)	-0.0342	C(6)	-0.0157
Fe(5)	-0.0194	Fe(6)	0.0394
Plane VIII fitting C(11) through C(15)			
$-6.2543*X + 13.4353*Y - 4.3494*Z + 3.7534 = 0.0$			
Plane IX fitting C(21) through C(25)			
$2.6278*X + 3.6868*Y + 9.9979*Z - 6.8682 = 0.0$			
Plane X fitting C(31) through C(35)			
$5.5950*X + 7.9585*Y + 6.1534*Z - 3.7920 = 0.0$			
Plane XI fitting C(41) through C(45)			
$10.7203*X + 2.4134*Y - 8.4808*Z + 3.8506 = 0.0$			
Plane XII fitting C(51) through C(55)			
$-8.3473*X - 4.5077*Y + 10.4406*Z - 1.2955 = 0.0$			
Plane XIII fitting C(61) through C(65)			
$3.4677*X + 12.7607*Y + 1.6309*Z - 10.4128 = 0.0$			
Plane XIV fitting Fe(1)-Fe(2)-O(7)-C(7)			
$7.3999*X - 6.4572*Y + 9.9402*Z - 4.5125 = 0.0$			
Fe(1)	0.0077	Fe(2)	0.0076
O(7)	0.0189	C(7)	-0.0342
Plane XV fitting Fe(1)-Fe(2)-S(1')-C(1')			
$4.3262*X - 7.9717*Y + 11.2725*Z - 2.4611 = 0.0$			
Fe(1)	0.0037	Fe(2)	0.0045
S(1')	0.0072	C(1')	-0.0154
Plane XVI fitting Fe(3)-Fe(4)-O(8)-C(8)			
$10.7058*X + 9.2607*Y - 2.5321*Z - 3.1781 = 0.0$			
Fe(3)	-0.0020	Fe(4)	-0.0021
O(8)	-0.0050	C(8)	0.0091

Table 36. (continued)

Atom	Distance from Plane(Å)	Atom	Distance from Plane(Å)		
Plane XVII fitting Fe(3)-Fe(4)-S(2')-C(2')					
$12.7198*X + 4.9138*Y - 0.0785*Z - 4.583 = 0.0$					
Fe(3)	0.0039	Fe(4)	0.0032		
S(2')	0.0062	C(2')	-0.0133		
Plane XVIII fitting Fe(5)-Fe(6)-O(9)-C(9)					
$-4.3334*X + 6.5279*Y + 8.4280*Z - 4.7404 = 0.0$					
Fe(5)	0.0084	Fe(6)	0.0079		
O(9)	0.0202	C(9)	-0.0365		
Plane XIX fitting Fe(5)-Fe(6)-S(3')-C(3')					
$-1.9883*X + 4.9738*Y + 9.7380*Z - 4.5255 = 0.0$					
Fe(5)	0.0011	Fe(6)	0.0010		
S(3')	0.0017	C(3')	-0.0038		
<u>Interplanar Angles(°)</u>					
<u>Plane</u>	<u>Plane</u>	<u>Angle</u>	<u>Plane</u>	<u>Plane</u>	<u>Angle</u>
I	II	136.1	I	V	52.8
I	III	146.4	I	VI	61.4
I	IV	112.0	I	VII	32.7
II	V	88.1	XIV	XV	14.6
III	VI	87.7	XVI	XVII	19.7
IV	VII	86.7	XVIII	XIX	12.4
II	VIII	46.6	II	IX	46.6
III	X	45.7	III	XI	46.7
IV	XII	47.4	IV	XIII	47.1
VIII	IX	87.0	X	XI	87.7
XII	XIII	85.6			
<u>Torsional Angles (°)</u>					
<u>Atoms</u>	<u>Angle</u>	<u>Atoms</u>	<u>Angle</u>		
C(1')-S(1')-AG(1)-S(3')	37.9	C(1')-S(1')-AG(1)-S(2')	-115.6		
C(2')-S(2')-AG(1)-S(1')	-2.8	C(2')-S(2')-AG(1)-S(3')	-154.5		
C(3')-S(3')-AG(1)-S(2')	-82.1	C(3')-S(3')-AG(1)-S(1')	121.8		

furnishes some details about a few least squares planes. Figure 14 shows the ORTEP<sup>15</sup> drawing of 6 whereas Figure 15 shows the unit cell drawing (the Cp rings being omitted for clarity).

An x-ray structure determination of the major reaction product of the reaction mentioned earlier (see Introduction) clearly revealed that it is not the expected oxidation product, viz., the dithiocarbenium salt. On the other hand, it has revealed the structure of a hitherto unknown complex,  $[\text{AgL}_3]\text{BF}_4$ , where L stands for  $(\eta^5\text{-C}_5\text{H}_5)_2\text{Fe}_2(\text{CO})_3\text{CS}$ .

First we compare the structure of the ligand L in the complex with its reported structure in an uncomplexed state,<sup>73</sup> which we shall refer to as 'free L' in the following discussion. The Cp rings assume cis orientation as in the case of free L. The average Fe-Fe distance of 2.503 Å (see Table 34) is similar to that found in free L (2.505 Å) and is intermediate to that in cis- $[\text{CpFe}(\text{CO})_2]_2$ ,<sup>74</sup> 2.531 Å and that in cis- $[\text{CpFe}(\text{CO})(\text{CS})]_2$ ,<sup>75</sup> 2.482 Å. This lends supporting argument for the theory that the bonding between the two halves of the ligand is enhanced by the substitution of bridging thiocarbonyls for carbonyls. The iron to terminal carbonyl-carbon distances, 1.75 Å (ave.) are all shorter than the iron to bridging carbon distances, 1.89 Å (ave.) and these appear to be quite similar to those found in the literature.<sup>72,73,75</sup> The average C-S distance of 1.63 Å appears to be significantly longer than that in the free L, 1.60 Å, as one would expect (see later), and it is much larger than that found for terminal CS groups (1.51 - 1.54 Å).<sup>76</sup>

The iron to ring carbon distances range from 2.06 to 2.16 Å, with an average of 2.11 Å as in the case of free L. Such a variation is not surprising considering the large thermal parameters and the difficulty in refining the ring carbons. This could mean that there is considerable

freedom of rotary oscillations about the perpendiculars that go through the iron atoms.

As in the case of free L, the bridging groups in the ligand are bent away from the Cp rings via a folding along the Fe-Fe bond and the dihedral angles ( $14.6^\circ$ ,  $19.7^\circ$ ,  $12.4^\circ$ ; see Table 36, Planes XIV through XIX) differ, perhaps due to packing forces.

Finally other distances, angles and geometrical features in the ligand are strikingly similar to those in the free L.<sup>73</sup>

We now focus our attention on the environment about Ag(I) which like Hg(II), Cu(I) and Au(I) show a pronounced tendency to exhibit linear two fold coordination. However, because of relatively small energy differences among the filled d orbitals and the empty s and p orbitals ( $4d^{10}, 5s^0, 5p^0$  for Ag(I)) which lead to extensive hybridization of these orbitals, Ag(I) tends to exhibit a variety of coordination states,  $AgL_n^+$ , where n can be 1, 2, 3, 4 or 6. The coordination number n and hence the stability of  $AgL_n^+$  depend on the nature of the ligand and anions.

The geometry around Ag(I), in the present study, is a slightly distorted planar trigonal geometry. The silver to sulfur distances are close to each other, the average being  $2.498(6)$  Å (Table 34). The latter is intermediate to the Ag-S distance of  $2.42$  Å in digonal environment,<sup>77</sup> and to the average Ag-S distance of  $2.61$  Å in tetrahedral environment.<sup>78</sup> In one previously recorded case,<sup>79</sup> silver has been found to be coordinated by three sulfur atoms and the environment here is a highly distorted planar geometry as the Ag-S distances range from  $2.40$  to  $2.87$  Å while the S-Ag-S angles range from  $90$  to  $154^\circ$ . In the present study, we find that apart from the Ag-S distances being nearly equal, S-Ag-S angles do not deviate from the ideal trigonal angle by more than  $10^\circ$  (see Table

Figure 14. ORTEP drawing of  $[\text{Ag}\{(\eta^5\text{-C}_5\text{H}_5)_2\text{Fe}_2(\text{CO})_3\text{CS}\}_3]\text{BF}_4$  (6)  
Ring carbon atoms have been drawn arbitrarily as  
small spheres for clarity; hydrogen atoms are left  
out for clarity

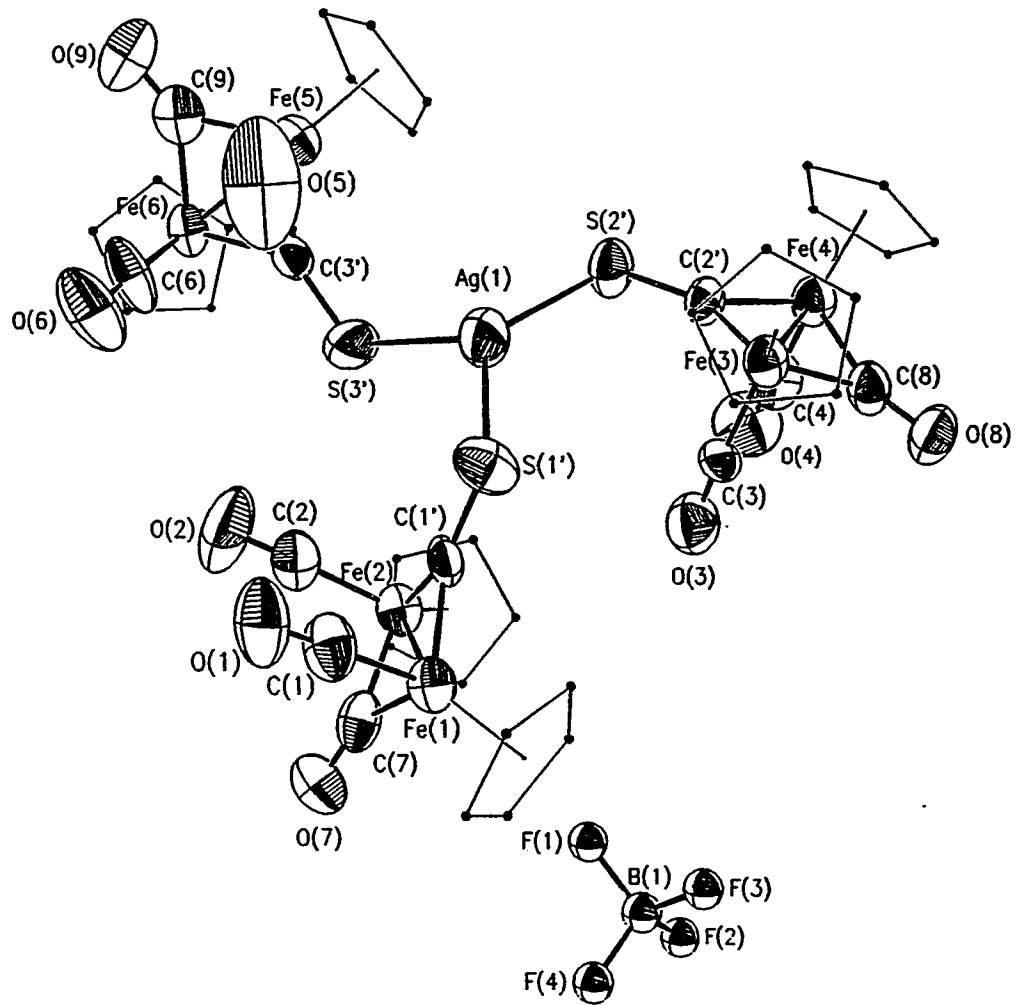
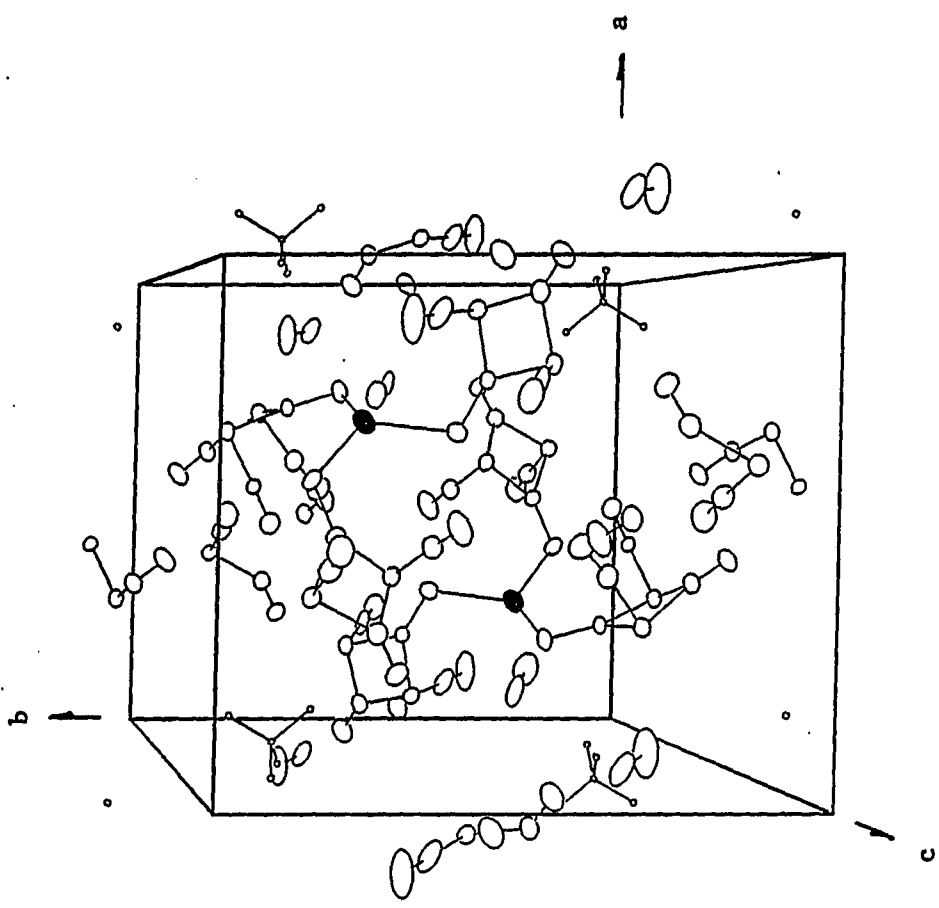


Figure 15. Unit cell drawing of  $[\text{Ag}\{(\eta^5\text{-C}_5\text{H}_5)_2\text{Fe}_2(\text{CO})_3\text{CS}\}_3]\text{BF}_4$  (6)  
Cp rings are left out for clarity; dark full ellipses  
represent silver atoms





35) and that the silver atom is calculated to be 0.33 Å from the plane of the sulfur atoms. Thus, to our knowledge, this is perhaps the first instance of silver atoms showing nearly trigonal geometry. Also, because of the nature of the ligand,  $\text{AgL}_3^+$  is discrete and not polymeric as in many Ag-S complexes.

We shall now look at the complex ion,  $\text{AgL}_3^+$  ion as a whole. The bonding interactions between sulfur atoms and silver explain why the C-S distances are a bit longer than those in the free L. The torsional angles in Table 36 together with Figure 14 reveal that the ligands are not arranged in any particular orientation either with respect to each other or relative to the  $\text{AgS}_3$  plane.

Packing arrangement seen in Figure 15 does not reveal anything particularly noteworthy except that the silver atoms line up nearly along the body diagonal through the origin of the unit cell.

### Conclusion

The fact that our crystal structure analysis revealed  $[\text{AgL}_3]\text{BF}_4$  as the major reaction product upon treating free L with  $\text{AgBF}_4$  does not necessarily mean that the expected dithiocarbenium,  $[\text{L-L}]^{2+}2\text{BF}_4^-$ , is not a reaction product. If metallic silver is really one of the reaction products as has been tacitly assumed, this would mean the formation of an oxidation product or products. This issue needs to be addressed by either suitably choosing the reaction conditions or by choosing a suitable oxidant. Finally, it would be interesting to see what kind of complexes form upon treating other thiocarbonyl complexes with  $\text{AgBF}_4$ .

## CRYSTAL STRUCTURE OF 1-ETHOXY SILATRANE (7)

## Introduction

In 1960 Finestone patented<sup>80</sup> the syntheses of two organosilicon compounds of a novel type. These compounds - later termed 'silatranes' - attracted the attention of many scientists due to the pentacovalency of silicon (currently described as hypervalent silicon) and the extraordinary biological activities of many derivatives, including ability to accelerate wound healing and to inhibit tumor growth.<sup>81</sup> More than 500 silatrane derivatives have been reported since 1960.

Five bonded silicon species have long been proposed as intermediates in the displacement reactions of silicon compounds, and there is strong evidence for penta coordinated silicon atoms in some stable organic and inorganic ions. The existence of pentacovalent silicon (with perfect trigonal bipyramidal geometry about Si) was not firmly established until 1967 when Hamilton *et al.*,<sup>82</sup> published their crystal structure work on the pentameric dimethylsilylamine. However the presence of an intramolecular trans-annular nitrogen to silicon coordinate bond, suggested as early as 1960, was not verified until 1968 when the first crystal structure study on 1-phenylsilatrane was reported by Turley and Boer.<sup>83</sup> A comprehensive review on the molecular geometry of silatranes appeared recently.<sup>84</sup>

Silatranes substituted in apical position, Y-Siln for brevity (with Y equal to OR, SR, OAr, Ar), have the ability to form onium ions. Thus it

would be of interest to correlate the strength of N-Si bond in the neutral molecules with that in the onium salts. With this goal in mind, Dr. Verkade's research group initiated the project by preparing 1-ethoxysilatronium trifluoroacetate. The single crystals of the onium salt and of the title compound were furnished by Dr. Verkade. The aim of the present study was then two fold: (i) To look at the effect of apical ethoxy group in the title compound upon the molecular geometry and in particular upon the length of N-Si dative bond. (ii) To compare the lengths of the N-Si bond of the onium salt with that of the title compound. But unfortunately the onium salt was so hygroscopic we have not found a suitable method to study this salt by the x-ray single crystal method. Thus we present below only the results for the title compound.

### Experimental

Data collection A colorless single crystal of the title compound, hereafter referred to as 7, with approximate dimensions of 0.8mm  $\times$  0.4mm  $\times$  0.25mm was mounted at the tip of a glass fiber and subsequently placed on a goniometer head. Fifteen reflections from a rotation photograph ( $15^\circ < 2\theta < 25^\circ$ ) were centered on a Syntex P2<sub>1</sub> automated four-circle diffractometer and indexed by the indexing program BLIND.<sup>7</sup> The resulting reduced cell and cell scalars revealed primitive monoclinic crystal symmetry. The intensity of one strong reflection was measured every 100 reflections during data collection to monitor any crystal decay. Four

Table 37. Crystal data for  $\text{SiO}_4\text{NC}_8\text{H}_{17}$  (7)

---

F.W.	: 219.31
Space Group	: $P2_1/n$
a, Å	: 10.956(4) <sup>a</sup>
b, Å	: 11.187(2)
c, Å	: 17.638(8)
$\beta$ , °	: 95.84(4)
V, Å <sup>3</sup>	: 2150.6(1.3)
$\rho_{\text{calc}}$ , g/cm <sup>3</sup>	: 1.355
Z	: 8
Temperature, °K	: 298
Diffractometer	: Syntex P2 <sub>1</sub>
Radiation, Å	: Mo $K_{\alpha}$
$\lambda$ , Å	: 0.70926
$\mu$ , cm <sup>-1</sup>	: 2.012
$2\theta_{\text{max}}$ , °	: 50.0
Number of reflections collected	: 7759 (four octants)
Number of reflections observed	: 1054
Min of $I/\sigma(I)$	: 3.0
Number of variables	: 313
Observations/Variables	: 3.4
R, % <sup>b</sup>	: 6.8
$R_{\omega}$ , %	: 8.3

---

<sup>a</sup>Estimated standard deviations shown in parentheses are for the least significant digits.

$$R = \frac{\sum ||F_o| - |F_c||}{\sum |F_o|}$$

$$R_{\omega} = [\sum \omega (|F_o| - |F_c|)^2 / \sum |F_o|^2]^{1/2}, \text{ where } \omega = 1/\sigma^2(F).$$

octants ( $h,k,l$ ;  $h,k,-l$  plus  $h,-k,l$ ;  $h,-k,-l$ ) of data were collected within a  $2\theta$  sphere of  $50^\circ$ . Crystal data are summarized in Table 37.

Reduction of x-ray intensity data      There was no noticeable change in intensity of the standard reflection throughout the data collection. There was no significant variation in the intensity of a reflection near  $\chi = 90^\circ$  as one would expect ( $\mu = 2.012 \text{ cm}^{-1}$ ). Thus the data were corrected for only Lorentz and polarization effects and the intensities of equivalent reflections were then averaged.

### Structure Determination and Refinement

The structure determination was begun with the determination of the space group: Systematic absences of  $h0l$  ( $h+1 = 2n+1$ ),  $0k0$  ( $k=2n+1$ ) uniquely defined the space group as the centrosymmetric space group  $P2_1/n$ . Since there are eight molecules per unit cell, the positions of all the atoms in two symmetry independent molecules had to be determined. The position of the two silicon atoms and eight of the oxygen atoms were obtained by the direct method program MULTAN\_80<sup>62</sup> which did not provide further information about the organic fragments. All the remaining non-hydrogen atoms were however found from successive structure factor and difference Fourier calculations. The positional and anisotropic thermal parameters for the non-hydrogen atoms were refined by a combination of block-matrix/full-matrix least-squares calculations.<sup>12</sup> The positional parameters of the hydrogen atoms were calculated and they were not

refined; the hydrogen atoms were all assigned an isotropic temperature factor of  $8.0 \text{ \AA}^2$ . The final conventional residual (R) was 6.8%.

The atomic scattering factors used were those from reference 13; that of silicon was modified for anomalous dispersion effects.<sup>14</sup>

### Discussion of the Structure

The results of the x-ray diffraction study on 7 are summarized in Tables 38-42. The final atomic positional and thermal parameters are listed in Tables 38 and 39 respectively, while the refined bond distances and bond angles are listed in Tables 40 and 41. Table 42 furnishes some details about selected least-squares planes and torsional angles. Figure 16 shows the ORTEP<sup>15</sup> drawing of the two molecules of 7 that make up one asymmetric unit (hydrogen atoms being excluded for clarity).

The most important structural feature of all silatrane molecules is the peculiar trans annular dative bond between nitrogen and silicon. The N→Si distance in all the silatranes studied thus far ranges from 2.02 to 2.42 Å<sup>85</sup> and this distance exceeds the 1.75 Å Si-N distance reported for tetrahedrally bonded silicon atoms in, e.g., Si<sub>3</sub>N<sub>4</sub><sup>86</sup> but is much shorter than the sum of the van der Waals radii (3.65 Å).<sup>18</sup> Thus the bonding about the silicon atoms in silatranes can be described in terms of a slightly distorted trigonal bipyramid (tbp for short) with Y-Si-O<sub>e</sub> angles ranging from 93 to 103° and O<sub>e</sub>-Si-O<sub>e</sub> angles ranging from 116 to 120 degree,<sup>87</sup> the subscript e signifying equatorial. Similar features are observed in our compound.

Table 38. Positional parameters<sup>a</sup> ( $\times 10^4$ ) for  $\text{SiO}_4\text{NC}_8\text{H}_{17}$  (7)

Atom	x	y	z	$U_{\text{iso}}^{\text{b}}$
Si(1)	1955(4)	0707(4)	3569(3)	53(2)
O(1)	3078(9)	1666(9)	3751(6)	72(5)
O(2)	0995(11)	0500(8)	4221(6)	71(5)
O(3)	1519(10)	0343(8)	2690(5)	66(5)
O(4)	2781(10)	-0532(8)	3735(6)	67(4)
N(1)	0887(14)	2275(11)	3292(10)	68(7)
C(1)	2878(19)	2900(18)	3781(13)	101(10)
C(2)	1784(24)	3240(15)	3326(17)	144(15)
C(3)	-0017(18)	1239(16)	4289(10)	91(9)
C(4)	0118(23)	2352(17)	3846(17)	140(13)
C(5)	0861(17)	1099(17)	2172(9)	75(8)
C(6)	0340(25)	2067(23)	2545(15)	161(14)
C(7)	3414(21)	-0788(18)	4459(12)	121(11)
C(8)	4286(21)	-1625(17)	4500(12)	123(11)
Si(2)	1519(4)	-5918(4)	6663(2)	50(2)
O(5)	2337(9)	-6956(9)	6274(6)	80(5)
O(6)	1871(9)	-5550(9)	7565(6)	75(5)
O(7)	0119(9)	-5642(8)	6254(5)	61(4)
O(8)	2217(9)	-4745(7)	6336(6)	59(4)
N(2)	0611(14)	-7408(10)	7152(8)	61(6)
C(9)	2260(18)	-8184(15)	6449(13)	108(10)
C(10)	1038(18)	-8453(14)	6745(12)	95(9)
C(11)	1302(19)	-6120(20)	8169(10)	105(10)
C(12)	1030(17)	-7390(18)	7942(11)	90(9)
C(13)	-0857(15)	-6488(14)	6267(10)	71(8)
C(14)	-0707(16)	-7180(14)	6981(11)	71(8)
C(15)	2325(16)	-4566(14)	5571(10)	70(8)
C(16)	3578(18)	-4743(16)	5364(9)	97(7)
H(11)	363	343	370	101
H(12)	266	315	438	101
H(21)	205	333	271	101
H(22)	139	408	341	101
H(31)	-18	133	487	101
H(32)	-84	78	401	101
H(41)	61	297	432	101
H(42)	-72	277	372	101

<sup>a</sup>The estimated standard deviations in the parentheses are for the least significant digits. Parameters for hydrogen atoms are multiplied by  $10^3$ .

<sup>b</sup>For anisotropically refined atoms,  $U_{\text{iso}} \equiv 10^3/3 \sum U_{ij} a_i^* a_j^* \vec{a}_i \cdot \vec{a}_j$ , where the temperature factors are defined as  $\exp(-2\pi^2 \sum h_i h_j a_i^* a_j^* U_{ij})$ .



Table 38. (continued)

---

Atom	x	y	z	U <sub>iso</sub>
H(51)	16	57	183	101
H(52)	142	147	177	101
H(61)	-66	177	255	101
H(62)	29	280	219	101
H(71)	266	-122	479	101
H(72)	364	-3	475	101
H(81)	512	-124	449	101
H(82)	423	-215	499	101
H(83)	410	-222	401	101
H(91)	301	-842	687	101
H(92)	242	-869	595	101
H(101)	108	-924	708	101
H(102)	37	-864	626	101
H(111)	40	-570	823	101
H(112)	179	-608	870	101
H(121)	36	-776	826	101
H(122)	185	-788	806	101
H(131)	-83	-706	579	101
H(132)	-169	-601	620	101
H(141)	-124	-798	690	101
H(142)	-110	-668	741	101
H(151)	202	-368	540	101
H(152)	170	-516	523	101
H(161)	402	-387	538	101
H(162)	409	-526	579	101
H(163)	360	-510	484	101

---

Table 39. Anisotropic thermal parameters<sup>a</sup> ( $\times 10^3$ ) for SiO<sub>4</sub>NC<sub>8</sub>H<sub>17</sub> (7)

Atom	U <sub>11</sub>	U <sub>22</sub>	U <sub>33</sub>	U <sub>23</sub>	U <sub>13</sub>	U <sub>12</sub>
Si(1)	55(3)	44(3)	60(3)	-04(3)	03(3)	-01(3)
O(1)	53(8)	50(7)	112(9)	-22(7)	04(7)	-02(6)
O(2)	79(9)	62(7)	73(8)	10(6)	21(7)	-03(7)
O(3)	93(9)	59(7)	46(7)	-05(6)	00(6)	15(7)
O(4)	81(8)	50(6)	67(8)	-05(6)	-08(7)	15(6)
N(1)	72(12)	46(9)	93(13)	13(9)	48(11)	24(9)
C(1)	40(14)	73(15)	193(22)	-49(14)	32(14)	-14(11)
C(2)	101(20)	20(11)	326(36)	19(15)	94(23)	-12(13)
C(3)	105(17)	84(15)	95(14)	-11(12)	62(13)	23(13)
C(4)	131(22)	75(15)	227(30)	59(17)	75(22)	59(15)
C(5)	81(14)	79(15)	66(14)	-04(11)	11(11)	16(12)
C(6)	213(31)	161(22)	94(20)	17(18)	-60(20)	90(21)
C(7)	141(21)	108(17)	103(17)	-13(15)	-44(15)	45(17)
C(8)	132(23)	102(16)	123(18)	-17(14)	-48(16)	48(16)
Si(2)	54(3)	37(3)	60(3)	-01(2)	07(3)	-05(3)
O(5)	56(8)	51(7)	138(11)	00(7)	41(8)	-04(6)
O(6)	89(10)	72(8)	62(8)	-03(6)	01(7)	-36(7)
O(7)	56(8)	53(7)	72(7)	20(6)	-01(6)	05(6)
O(8)	75(8)	42(6)	63(8)	06(5)	24(7)	-20(6)
N(2)	72(13)	33(8)	74(12)	08(7)	-09(9)	-19(8)
C(9)	75(16)	37(11)	221(23)	-03(13)	56(16)	04(11)
C(10)	68(15)	39(11)	180(20)	15(12)	17(14)	-11(10)
C(11)	126(19)	133(18)	53(12)	18(13)	-14(12)	-67(16)
C(12)	67(15)	117(17)	83(16)	48(13)	-15(12)	-27(13)
C(13)	43(12)	62(12)	105(15)	04(11)	-13(11)	-09(10)
C(14)	38(13)	70(12)	102(15)	28(11)	-04(11)	00(10)
C(15)	72(15)	79(13)	64(12)	14(10)	23(11)	-05(10)
C(16)	88	126(17)	81(13)	-09(12)	35(12)	-13(13)

<sup>a</sup>The estimated standard deviations in the parentheses are for the least significant digits. The anisotropic temperature factors are defined as  $\exp(-2\pi^2 \sum h_j a_j^* U_{ij})$ .

Table 40. Refined bond distances<sup>a</sup> (Å) for SiO<sub>4</sub>NC<sub>8</sub>H<sub>17</sub> (7)

Atoms	Distance	Atoms	Distance
Si(1) - N(1)	2.138(15)	Si(2) - N(2)	2.165(14)
Si(1) - O(1)	1.639(11)	Si(2) - O(5)	1.659(11)
Si(1) - O(2)	1.652(11)	Si(2) - O(6)	1.650(11)
Si(1) - O(3)	1.628(11)	Si(2) - O(7)	1.656(10)
Si(1) - O(4)	1.665(10)	Si(2) - O(8)	1.651(10)
O(1) - C(1)	1.399(23)	O(5) - C(9)	1.413(21)
O(2) - C(3)	1.398(21)	O(6) - C(11)	1.437(22)
O(3) - C(5)	1.391(20)	O(7) - C(13)	1.430(18)
O(4) - C(7)	1.419(23)	O(8) - C(15)	1.381(18)
N(1) - C(2)	1.457(28)	N(2) - C(10)	1.472(22)
N(1) - C(4)	1.356(28)	N(2) - C(12)	1.422(23)
N(1) - C(6)	1.410(29)	N(2) - C(14)	1.467(21)
C(1) - C(2)	1.425(32)	C(9) - C(10)	1.516(26)
C(3) - C(4)	1.485(30)	C(11) - C(12)	1.497(27)
C(5) - C(6)	1.418(31)	C(13) - C(14)	1.473(23)
C(7) - C(8)	1.333(29)	C(15) - C(16)	1.469(24)

<sup>a</sup>The estimated standard deviations in the parentheses are for the least significant digits.

Table 41. Refined bond angles<sup>a</sup> (°) for SiO<sub>4</sub>NC<sub>8</sub>H<sub>17</sub> (7)

Atoms	Angle	Atoms	Angle
O(1) - Si(1) - O(2)	118.3( 6)	O(5) - Si(2) - O(6)	119.4( 5)
O(1) - Si(1) - O(3)	119.5( 5)	O(5) - Si(2) - O(7)	117.7( 5)
O(2) - Si(1) - O(3)	118.8( 5)	O(6) - Si(2) - O(7)	119.3( 5)
O(4) - Si(1) - O(1)	97.3( 5)	O(8) - Si(2) - O(5)	97.0( 5)
O(4) - Si(1) - O(2)	97.7( 5)	O(8) - Si(2) - O(6)	93.9( 5)
O(4) - Si(1) - O(3)	93.4( 5)	O(8) - Si(2) - O(7)	98.1( 5)
N(1) - Si(1) - O(1)	83.7( 5)	N(2) - Si(2) - O(5)	85.1( 5)
N(1) - Si(1) - O(2)	84.4( 5)	N(2) - Si(2) - O(6)	83.1( 5)
N(1) - Si(1) - O(3)	83.5( 5)	N(2) - Si(2) - O(7)	82.8( 5)
N(1) - Si(1) - O(4)	176.4( 6)	N(2) - Si(2) - O(8)	177.3( 5)
Si(1) - O(1) - C(1)	122.4(11)	Si(2) - O(5) - C(9)	122.9(10)
Si(1) - O(2) - C(3)	122.9(10)	Si(2) - O(6) - C(11)	121.8(10)
Si(1) - O(3) - C(5)	123.8(10)	Si(2) - O(7) - C(13)	122.0( 9)
Si(1) - O(4) - C(7)	122.2(10)	Si(2) - O(8) - C(15)	123.1( 9)
Si(1) - N(1) - C(2)	104.3(12)	Si(2) - N(2) - C(10)	103.6(10)
Si(1) - N(1) - C(4)	104.6(13)	Si(2) - N(2) - C(12)	105.2(10)
Si(1) - N(1) - C(6)	104.4(13)	Si(2) - N(2) - C(14)	105.4(10)
C(2) - N(1) - C(4)	112.9(17)	C(10) - N(2) - C(12)	113.7(13)
C(2) - N(1) - C(6)	112.4(17)	C(10) - N(2) - C(14)	113.1(13)
C(4) - N(1) - C(6)	116.6(18)	C(12) - N(2) - C(14)	114.4(13)
O(1) - C(1) - C(2)	111.6(17)	O(5) - C(9) - C(10)	110.0(15)
O(2) - C(3) - C(4)	109.2(15)	O(6) - C(11) - C(12)	108.2(15)
O(3) - C(5) - C(6)	111.5(16)	O(7) - C(13) - C(14)	110.1(13)
O(4) - C(7) - C(8)	118.2(18)	O(8) - C(15) - C(16)	113.5(13)
N(1) - C(2) - C(1)	110.5(19)	N(2) - C(10) - C(9)	110.3(14)
N(1) - C(4) - C(3)	115.4(19)	N(2) - C(12) - C(11)	108.2(15)
N(1) - C(6) - C(5)	114.0(20)	N(2) - C(14) - C(13)	106.8(13)

<sup>a</sup>The estimated standard deviations in the parentheses are for the least significant digits.

Table 42. Equations of selected least squares planes (in the monoclinic coordinate system), interplanar angles and torsional angles in  $\text{SiO}_4\text{NC}_8\text{H}_{17}$  (7)

Atom	Distance from Plane(Å)	Atom	Distance from Plane(Å) <sup>a</sup>
Plane I fitting Si(1)-O(1)-O(2)-O(3)			
$-5.7910*X + 9.1691*Y - 2.9289*Z + 1.3974 = 0.0$			
Si(1)	-0.1317	O(1)	0.0439
O(2)	0.0433	O(3)	0.0445
Plane II fitting N(1)-Si(1)-O(1)-C(1)			
$-3.7895*X - 0.0420*Y + 17.0841*Z - 5.3062 = 0.0$			
N(1)	-0.0280	Si(1)	0.0478
O(1)	-0.0707	C(1)	0.0509
C(2)	-0.3146*		
Plane III fitting N(1)-Si(1)-O(2)-C(3)			
$5.5985*X + 5.9575*Y + 10.9224*Z - 5.4352 = 0.0$			
N(1)	0.0120	Si(1)	-0.0205
O(2)	0.0302	C(3)	-0.0217
C(4)	0.2324*		
Plane IV fitting N(1)-Si(1)-O(3)-C(5)			
$9.3787*X + 5.0567*Y - 5.9365*Z - 0.0442 = 0.0$			
N(1)	-0.0164	Si(1)	0.0284
O(3)	-0.0423	C(5)	0.0303
C(6)	-0.1912*		
Plane V fitting Si(1)-O(4)-C(7)-C(8)-O(3)-C(5)-C(6)-N(1)			
$8.9540*X + 5.6843*Y - 6.2363*Z + 0.0540 = 0.0$			
Si(1)	-0.0191	O(4)	-0.0875
C(7)	-0.1174	C(8)	0.1621
O(3)	-0.0678	N(1)	0.0881
C(5)	0.0957	C(6)	-0.0541

<sup>a</sup>The distances marked with a \* are those of the atoms not included in the calculation of the planes.

Table 42. (continued)

Atom	Distance from Plane(Å)	Atom	Distance from Plane(Å)
Plane VI fitting Si(2)-O(5)-O(6)-O(7)			
$5.2766*X + 8.7898*Y - 7.6759*Z + 9.6514 = 0.0$			
Si(2)	0.1368	O(5)	-0.0453
O(6)	-0.0463	O(7)	-0.0453
Plane VII fitting N(2)-Si(2)-O(5)-C(9)			
$6.3374*X + 0.8176*Y + 13.2174*Z - 9.2530 = 0.0$			
N(2)	-0.0188	Si(2)	0.0329
O(5)	-0.0485	C(9)	0.0345
C(10)	-0.3719*		
Plane VIII fitting N(2)-Si(2)-O(6)-C(11)			
$9.1414*X - 6.0358*Y + 0.4819*Z - 5.3397 = 0.0$			
N(2)	0.0345	Si(2)	-0.0583
O(6)	0.0855	C(11)	-0.0617
C(12)	0.4450*		
Plane IX fitting N(2)-Si(2)-O(7)-C(13)			
$-3.7961*X + 6.2570*Y + 13.8357*Z - 4.9950 = 0.0$			
N(2)	0.0329	Si(2)	-0.0553
O(7)	0.0816	C(13)	-0.0592
C(14)	0.4391*		
Plane X fitting Si(2)-O(8)-C(15)-O(6)-C(11)-N(2)			
$9.3362*X - 5.7784*Y - 0.0573*Z - 4.7964 = 0.0$			
Si(2)	0.0031	O(8)	-0.0208
C(15)	-0.0195	O(6)	0.1146
C(11)	-0.0909	N(2)	0.0135
C(16)	1.2539*		

## Interplanar Angles(°)

<u>Plane</u>	<u>Plane</u>	<u>Angle</u>	<u>Plane</u>	<u>Plane</u>	<u>Angle</u>
I	II	88.42	VI	VII	88.82
I	III	89.01	VI	VIII	86.22
I	IV	88.48	VI	IX	88.87
I	V	92.55	VI	X	88.40
II	III	117.02	VII	VIII	122.33

Table 42. (continued)

<u>Plane</u>	<u>Plane</u>	<u>Angle</u>	<u>Plane</u>	<u>Plane</u>	<u>Angle</u>
II	IV	122.21	VII	IX	116.89
III	IV	120.59	VIII	IX	120.39
II	V	122.66	VII	X	121.56
III	V	120.32	IX	X	121.40
IV	V	4.09	VIII	X	2.35
Torsional Angles (°)					
<u>Atoms</u>	<u>Atoms</u>	<u>Angle</u>	<u>Atoms</u>	<u>Atoms</u>	<u>Angle</u>
Si(1)-O(1)-C(1)-C(2)	Si(2)-O(5)-C(9)-C(10)	-26.3	Si(2)-O(6)-C(11)-C(12)	C(13)	23.4
Si(1)-O(2)-C(3)-C(4)	Si(2)-O(7)-C(13)-C(14)	-14.7	Si(2)-O(7)-C(13)-C(14)	C(15)	32.7
Si(1)-O(3)-C(5)-C(6)	Si(2)-O(8)-C(15)-C(16)	-15.9			32.7
Si(1)-O(4)-C(7)-C(8)		-164.5			-108.1
O(1)-Si(1)-O(4)-C(7)	O(5)-Si(2)-O(8)-C(15)	61.5	O(7)-Si(2)-O(8)-C(15)		55.3
O(2)-Si(1)-O(4)-C(7)	O(6)-Si(2)-O(8)-C(15)	-58.5			-64.1
O(3)-Si(1)-O(4)-C(7)		-178.2			175.6
O(4)-Si(1)-O(1)-C(1)	O(8)-Si(2)-O(5)-C(9)	-172.8	O(8)-Si(2)-O(6)-C(11)		170.8
O(4)-Si(1)-O(2)-C(3)	O(8)-Si(2)-O(6)-C(11)	-173.2			167.3
O(4)-Si(1)-O(3)-C(5)	O(8)-Si(2)-O(7)-C(13)	-173.2			171.5

The average N→Si distance of 2.152 Å observed in 7 is intermediate between that found in 1-chlorosilatrane (2.02 Å) and that in 1-ethylsilatrane (2.21 Å) and it is comparable to that in 1-chloromethyl- and 1-phenylsilatranes (2.12 and 2.15 Å respectively). This lends supporting evidence for the Lewis acid-base theory that explains the length (and hence the strength) of the N→Si dative bond in silatranes. The silicon atom when surrounded by electron withdrawing oxygen atoms in a t<sub>bp</sub> environment becomes partially positive and as a Lewis acid readily interacts with the proper Lewis base, i.e., the lone pair of electrons on nitrogen atom. Thus electron withdrawing apical substituents (e.g., Cl in 1-chlorosilatrane) enhance Si←N bond strength (shorter Si←N bond) while electron releasing groups (e.g., ethyl group in 1-ethylsilatrane) lower the Si←N bond strength (longer Si←N bond). The ethoxy group in 7 is, (like 1-chloromethyl or 1-phenyl groups) intermediate between the above two extremes with respect to the inductive electronic effects and thus the Si←N bond strength in 7 is intermediate to these two extremes.

The extent of distortion of the t<sub>bp</sub> conformation of silatrane molecules has been explained on the basis of electronic and steric requirements. In the molecule of triethanolamine<sup>88</sup> (precursor of silatranes) a claw-shaped structure consisting of three chains is achieved, the C-O and C-N bonds being nearly in the gauche position. The unshared pair of electrons on N is oriented inside the cage of the claw. Thus any electronic or size effects imposed by substituents on the triethanolamine would be expected to distort the claw-shape thereby affecting the t<sub>bp</sub> geometry about silicon. Similarly the electronic effects together with the bulkiness of the Y group would be expected to affect the t<sub>bp</sub> geometry in silatranes.

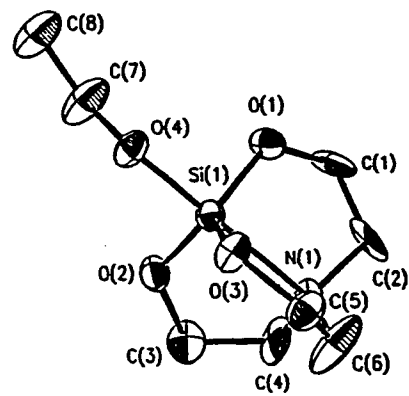
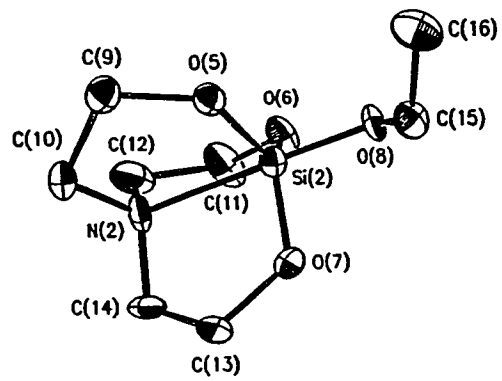


In the case of 7 there is no size effect to consider and thus the overall electron withdrawing effect of the ethoxy group determines the Si-N bond strength and hence the extent of distortion of tbp geometry. The O(4)-Si(1)-O(n) (n = 1,2,3) and O(8)-Si(2)-O(m) (m = 5,6,7) angles range from 93.4 to 98.1° (ave. 96.2°). The N(1)-Si(1)-O(n) (n = 1,2,3) and N(2)-Si(2)-O(m) (m = 5,6,7) angles range from 82.8 to 85.1° (ave. 83.8°). The N(1)-Si(1)-O(4) and N(2)-Si(2)-O(8) angles (176.4 and 177.3° respectively) are close to being 180° (see Table 41). The silicon atoms are above the respective equatorial-oxygen-atoms-planes (and toward the respective ethoxy groups) by an average distance of 0.18 Å. The nitrogen atoms are below the respective equatorial-oxygen-atoms-planes by an average distance of 1.97 Å and this is approximately similar ( $2.0 \pm 0.05$  Å) in all the known silatranes. Thus the N→Si distance in silatranes is mainly determined by the electronic effects of the substituent Y and of the substituents on the triethanolamine portion (when there are no steric effects to consider). It is interesting to note that the N→Si bond distance in the pentameric dimethylsilylamine was found to be 1.98 Å.<sup>82</sup>

A careful examination of the five-atom heterocycles forming the silatrane skeleton revealed that they are in an envelope conformation with O<sub>e</sub>, Si, N and C (the latter attached to O<sub>e</sub>) lying in the plane. The carbon atoms attached to N form the 'corner' of the envelope; these carbon atoms are at distances that range from 0.191 to 0.445 Å from the respective planes just mentioned (Planes II, III, IV and VII, VIII, IX; see Table 42). Similar feature was seen in other silatranes.

Figure 16 shows that the orientation of the ethoxy groups in the two molecules (making up the asymmetric unit) are different. In the first molecule (with Si(1)), the torsional angle of -164.5° for Si(1)-O(4)-

**Figure 16. ORTEP drawing of two 1-ethoxysilatrane (7)  
molecules constituting one asymmetric unit.  
Hydrogen atoms have been omitted for clarity**



C(7)-C(8) suggests that the Si(1)-O(4) and C(7)-C(8) bonds are nearly in the anti position with respect to one another. These four atoms together with O(3), C(5), C(6) and N(1) atoms nearly fall in a plane (Plane V; see Table 42). In the second molecule (with Si(2)), the torsional angle of  $-108.1^\circ$  for Si(2)-O(8)-C(15)-C(16) suggests that this unit adopts a staggered conformation with respect to O(8)-C(15) bond. The existence of these two conformations are likely due to differences in packing forces in the crystal.

Molecular packing in the crystal is expected to be dominated by dipole-dipole interactions (dipolar axis along the N $\rightarrow$ Si bonds) and no unusually closer intermolecular contact distances were observed.

### Conclusion

The crystal and molecular structure of 7 has been presented. The trans annular dative bond between N and Si in 7 is nearly as short (strong) as it is in 1-chloromethyl- and 1-phenylsilatranes. Although we were not able to carry out the x-ray experiment on an onium salt of 7 because of its highly hygroscopic nature, we venture to predict that the N $\rightarrow$ Si bond in these salts should be shorter (stronger) than the thus far reported strongest (and hence shortest) N $\rightarrow$ Si dative bond in 1-chlorosilatrane; in fact it is likely to be as strong as the one in the pentameric dimethylsilylamine.<sup>82</sup>

## APPENDIX: LOW TEMPERATURE APPARATUS FOR SINGLE CRYSTAL DATA COLLECTION

In many X-ray experiments one is required to collect high quality intensity data from crystals which have been cooled to a temperature as low as  $-100^{\circ}\text{C}$ . This may be necessary to study a low temperature phase of the substance or merely to reduce the thermal motion of its constituent atoms. Cooling of crystals on a four-circle diffractometer that is not already equipped with suitable cooling devices requires designing and building such special parts which when assembled and used solve many problems associated with data collection at low temperature. We designed and built these special parts for the DATEX diffractometer which can be used otherwise to collect room temperature data only.

Figure 17 is a schematic diagram of a four-circle, single crystal diffractometer such as the one we use (DATEX). Right on top of the  $\chi$ -circle are mounted two stepping motors (not shown in Figure 17) which drive the  $\chi$ - and the  $\phi$ -angles to any desired locations. The presence of these motors allow little room for clamping any delivery system that can deliver cold gas onto the crystal. Thus we built a Dewared delivery system such as the one seen in Figure 18 that can deliver cold nitrogen gas. The Dewared tube is clamped over the X-ray tube and thus it does not interfere with any angular motions of the  $\chi$ -circle and the tip of the Dewared tube is well above the diffraction plane.

Initially we tried using a glove bag to cover the entire  $\chi$ -circle in order to prevent frost formation on and about the crystal. Even though there was no significant reduction of intensity for a chosen reflection, the glove bag arrangement did not provide the flexibility we were

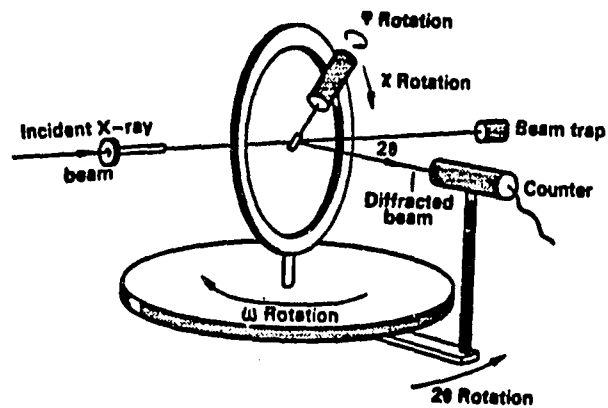


Figure 17. Typical four-circle diffractometer; the counter rotates about the  $2\theta$  axis in one plane, and the crystal is oriented about the three axes  $\phi$ ,  $\chi$ , and  $\omega$  so that the incident and reflected beams lie in the horizontal ( $2\theta$ ) plane

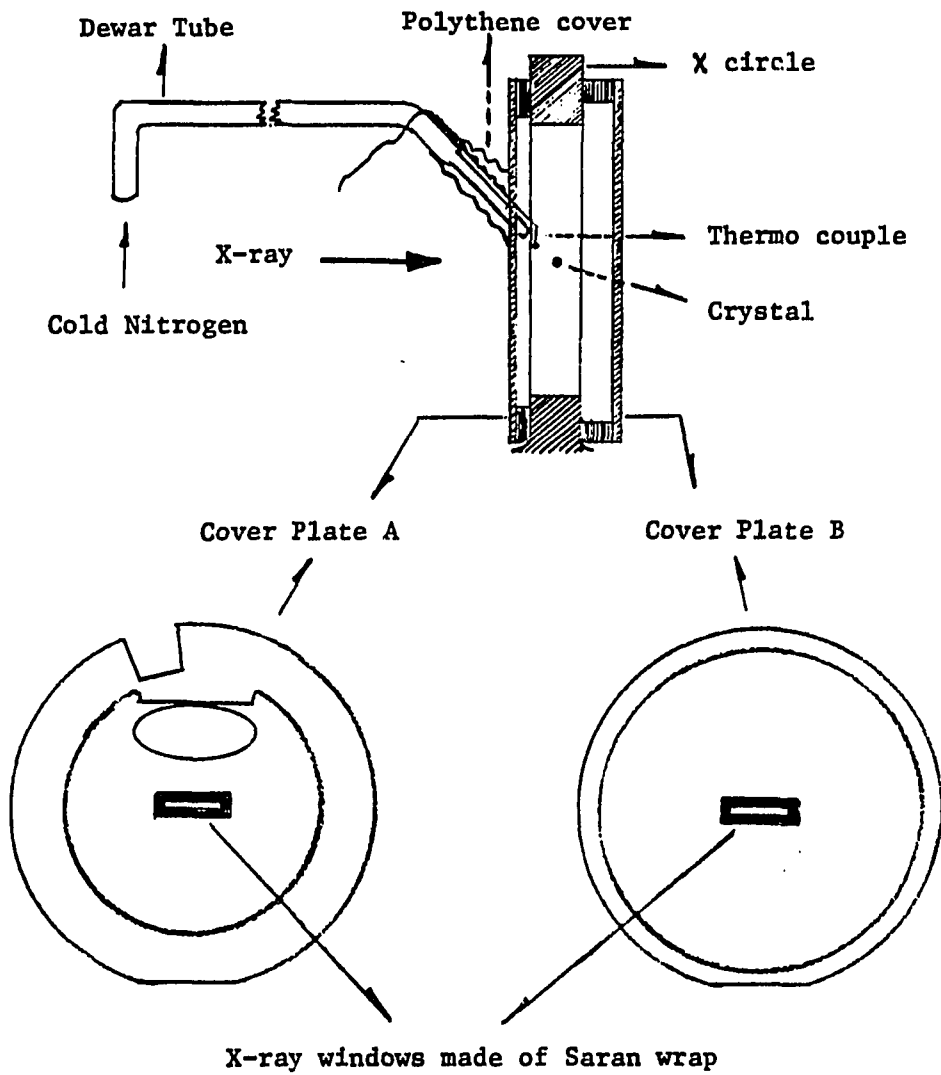


Figure 18. Schematic diagram showing the low temperature setup designed for DATEX diffractometer

looking for. For instance, the bulging glove bag altered the position of the delivery nozzle when the  $\omega$  angle was greater than  $15^\circ$  or so. The bag was even expected to trigger the limit switches in place on the detector, thereby shutting the instrument off. Thus we built the parts seen in Figure 18. The circular cover plates A and B are made of plexiglass. These plates have annular rings of suitable thickness stuck onto them so that (when assembled as shown in Figure 18) the  $\phi$ -mount moves around the  $\chi$ -circle freely,  $\chi$ -angle limits being  $\pm 100^\circ$ . The coverplates can be taped onto the  $\chi$ -circle. Rectangular slots cut out at the center of these plates and covered with Saran plastic wrap serve as "windows" for the incident/diffracted X-rays. The length of these slots is such that the data collection may not be carried out beyond  $50^\circ$  in  $2\theta$ . Through the elliptical slot in cover plate A is introduced the Dewared tube. A conical polythene cover is taped around the elliptical slot (excepting the top side of the slot to allow the nitrogen gas to escape); the thermocouple wire can be introduced through the conical polythene cover and the tip of the thermocouple can be conveniently held midway between the crystal and the tip of the Dewared tube.

One must observe the following precautions when using our low temperature apparatus. We recommend that the optical centering of the crystal be done before assembling the cover plates. Cover plate B must be installed without hitting the telescope mounted on the  $\chi$ -circle; a few strips of card board need to be placed beneath this plate so that  $\phi$ -mount slides around the  $\chi$ -circle unhindered. The clamps holding the Dewared tube must be tightened so that the tip of the tube points at the crystal all the time during data collection. From time to time during data collection one needs to carefully wipe off the water that condenses



on the outer faces of the cover plates. It is our experience that very little water condenses on the Saran wrap "windows". Use of a small fan blowing air onto the cover plate B minimizes ice build up below the Saran wrap "window".

With our low temperature setup we have completely overcome frost formation on and around the crystal. The current Dewared delivery tube is too long (nearly 6') and this is perhaps the reason we have been limited to a low temperature of only about  $-53^{\circ}\text{C}$  at the maximum rate of boiling of liquid nitrogen. By suitably redesigning the Dewared delivery tube one is expected to have a better control over the temperature near the crystal.

## REFERENCES

1. Osborn, R. S.; Rogers, D. Acta Crystallogr. 1975, B31, 359.
2. Polyakova, I. N.; Starikova, Z. A.; Parusnikov, B. V.; Krasavin, I. A.; Dobryakova, G. N.; Zhadanov, B. V. J. Struct. Chem. 1984, 25(5), 752.
3. Markuszewski, R.; Diehl, H. Talanta 1980, 27, 937.
4. Dubost, J. -P.; Leger, J. -M.; Colleter, J. -C.; Levillain, P.; Fompeydie, D. C. R. Acad. Sci., Paris 1981, 292, 965.
5. Cody, V. Endocrine Research 1985, 11, 211.
6. Rohrbangh, W. J.; Jacobson, R. A. Inorg. Chem. 1974, 13, 2535.
7. Jacobson, R. A. J. Appl. Crystallogr. 1976, 9, 115.
8. Howels, E. R.; Philips, D. C.; Rogers, D. Acta Crystallogr. 1950, 3, 210.
9. Karcher, B. A. Ph.D. Thesis, Iowa State University, 1980.
10. Lawton, S. L.; Jacobson, R. A. Inorg. Chem. 1968, 7, 2124.
11. Hubbard, C. R.; Quicksal, C. O.; Jacobson, R. A. 'The Fast Fourier Algorithm and the programs ALFF, ALFFDP, ALFFPROJ, ALFFT, and FRIEDEL', U.S. Atomic Energy Commission Report IS-2625, Iowa State University and Institute for Atomic Research, Ames, Iowa, 1971.
12. Lapp, R. L.; Jacobson, R. A. 'ALLS: Generalized Crystallographic Least Squares Program', U. S. DOE Report IS-4708, 1979.
13. Cromer, D. T.; Waber, J. T. 'International Tables for X-ray Crystallography', Kynoch Press: Birmingham, England, 1974, Vol. IV, Table 2.2a, 71.
14. Cromer, D. T. 'International Tables for X-ray Crystallography',

- Kynoch Press: Birmingham, England, 1974, Vol. IV, Table 2.3.1, 149.
15. Johnson, C. A. 'ORTEP-II: A Fortran Thermal-Ellipsoid Plot Program for Crystal Structure Illustration', U.S. Atomic Energy Commission Report ORNL-3794 (2nd revision with supplemental instruction), Oak Ridge National Laboratory, Oak Ridge, Tenn., 1970.
  16. Rogers, D.; Williams, D. J.; Thomas, R. J. Chem. Soc. (D) 1971, 393.
  17. Kennard, O. 'International Tables for X-ray Crystallography', Kynoch Press: Birmingham, England, 1962, Vol. III, Table 4.2.5, 276.
  18. Bondi, A. J. Phys. Chem. 1964, 68, 441.
  19. Larock, R. C. 'Organomercury Compounds in Organic Synthesis', Springer Verlag: New York, 1985.
  20. Larock, R. C.; Riefling, B. Tetrahedron Lett. 1976, 4661.
  21. Larock, R. C.; Riefling, B.; Fellows, C. A. J. Org. Chem. 1978, 43, 131.
  22. Richardson, Jr., J. W. Ph.D. Thesis, Iowa State University, 1984.
  23. Larock, R. C.; Burns, L. D.; Varaprath, S.; Russel, C. E.; Richardson, Jr., J. W.; Janakiraman, M. N.; Jacobson, R. A. Organometallics 1987, 6, 1780.
  24. Richardson, Jr., J. W.; Jacobson, R. A. 'Patterson and Pattersons', Oxford University Press: Oxford, England, 1987, 311-317.
  25. Grdenic, D. Quarterly Reviews 1965, 303.
  26. Davis, J. E. D.; Long, D. A. J. Chem. Soc. A 1968, 2564.
  27. Deacon, G. B. Rev. Pure Appl. Chem. 1963, 13, 189.
  28. Kistenmacher, T. J.; Rossi, M.; Chiang, C. C.; Van Duyne, R. P.; Siedle, A. R. Inorg. Chem. 1980, 19, 3604.
  29. Bats, J. W.; Fuess, M.; Daoud, A. Acta Crystallogr. 1980, B36, 2150.
  30. Goggin, P. L.; King, P.; McEwan, D. M.; Taylor, G. E.; Woodward, P.;

- Sangstrom, M. J. Chem. Soc. Dalton Trans. 1982, 875.
31. Zhilaeva, E. I.; Lyubovskaya, R. N.; Khidekel, M. L.; Shibaeva, R. P.; Rozenberg, L. P.; Simonov, M. A.; Neiland, O. Ya.; Bite, D. D. B. Dokl. Akad. Nauk SSSR 1980, 250, 868.
  32. Ferguson, G.; Jeffreys, J. A. D.; Sim, G. A. J. Chem. Soc. B 1966, 454.
  33. Mason, R.; Robertson, G. B.; Rushholm, G. A. Acta Crystallogr. 1974, B30, 894.
  34. Halfpenny, J.; Small, R. W. H. Acta Crystallogr. 1979, B35, 1239.
  35. Atwood, J. L.; Canada, L. G.; Lau, A. N. K.; Ludwick, A. G.; Ludwick, L. M. J. Chem. Soc. Dalton 1978, 1573.
  36. Alcock, N. W.; Curson, E. H.; Merron, N.; Moore, P. J. Chem. Soc. Dalton 1979, 1987.
  37. Authier-Martin, M.; Beauchamp, A. L. Can. J. Chem. 1975, 53, 2345.
  38. Barr, R. M.; Goldstein, M.; Mairs, T. N. D.; MacPartlin, M.; Markwell, M. J. J. Chem. Soc. Chem. Commun. 1974, 221.
  39. Biscarini, P.; Fusina, L.; Nivellini, G.; Pelizzi, G. J. Chem. Soc. Dalton 1981, 1024.
  40. Bell, N. A.; Goldstein, M.; Jones, T.; Nowell, I. W. Inorg. Chimica Acta 1980, 43, 87.
  41. Skirica, M.; Grdenic, D. Cryst. Struct. Commun. 1982, 11, 1299.
  42. Mohana Rao, J. K.; Rajaram, R. K. Z. Kristallogr. 1982, 160, 219.
  43. Gerken, V. A.; Pakhomov, V. I.; Sonin, A. S.; Marchenko, E. I.; Nepomnyashchaya, V. I. Kristallografia 1967, 12, 607.
  44. Fedorov, P. M.; Pakhomov, V. I. Koord. Khim. 1975, 1, 1140.
  45. Nyqvist, L.; Johansson, G. Acta Chim. Scand. 1971, 25, 1615.

46. White, J. G. Acta Crystallogr. 1963, 16, 397.
47. Fenn, R. H. Acta Crystallogr. 1966, 20, 20.
48. Biscarini, P.; Fusina, L.; Nivellini, G.; Pellizzi, G.  
J. Chem. Soc. Dalton 1977, 664.
49. Ondik, H.; Smith, D. 'International Tables for X-ray  
Crystallography', Kynoch Press: Birmingham, England, 1962, 261.
50. Bondoli, G.; Clemente, D. A.; Sindellari, L.; Tondello, E.  
J. Chem. Soc. Dalton 1975, 449.
51. Brotherton, P. D.; Healy, P. C.; Raston, C. L.; White, A. H.  
J. Chem. Soc. Dalton 1973, 334.
52. Hubert, J.; Beauchamp, A. L.; Rivest, R. Canad. J. Chem. 1975, 53,  
3383.
53. Carty, A. J.; Marker, A.; Gatehouse, B. M. J. Organometallic Chem.  
1975, C31, 88.
54. Aurivillius, K.; Stalhandske, C. Acta Crystallogr. 1974, B30, 1907.
55. Bowden, F. L.; Gites, R. Coord. Chem. Rec. 1976, 20, 81.
56. Stang, P. J.; White, M. R. Organometallics 1983, 2, 720.
57. Angus, Jr., R. O.; Johnson, R. P. J. Org. Chem. 1984, 49, 2880.
58. Moore, W. R.; Ozretich, T. M. Tetrahedron Lett. 1967, 3205.
59. Zoch, H. -G.; Szeimies, G.; Romer, R.; Schmitt, R. Angew. Chem.,  
Int. Ed. Engl. 1981, 20, 877.
60. Schluter, A. -D.; Belzner, J.; Heywang, V.; Sceimies, G.  
Tetrahedron Lett. 1980, 24, 891.
61. For a review of structural limitation in cyclic cumuleves, see:  
Johnson, R. P. In 'Molecular Structure and Energetics'; Greenberg,  
A., Liebman, J., Eds.; VCH Publishers: Deersfield Beach, FL, 1986,  
Vol. 3, 85.

62. Main, P.; Fise, S. J.; Hull, S. E.; Leissinger, L.; Germain, G.; Declercq, J. P.; Woolfson, M. M. 'MULTAN\_80: A system of computer programs for the automatic solution of crystal structures from X-ray diffraction data,' University of York, 1980.
63. Angus, Jr., R. O.; Janakiraman, M. N.; Jacobson, R. A.; Johnson, R. P. Organometallics 1987, 6, 1909.
64. Hagelee, L.; West, R.; Calabrese, J.; Normall, J. J. Am. Chem. Soc. 1979, 101, 4888.
65. Bright, D.; Mills, O. S. J. Chem. Soc. A 1971, 1979.
66. (a) Berkovitch, Y. Z.; Leiserowitz, L. J. Am. Chem. Soc. 1975, 97, 5627.  
(b) Irngartinger, H.; Jager, H. -V. Angew. Chem., Int. Ed. Engl. 1976, 15, 562.
67. Baird, M. C.; Wilkinson, G. Chem. Commun. 1966, 267.
68. Broadhurst, P. V. Polyhedron 1985, 4, 1801.
69. Kim, S. Ph.D. Thesis, Iowa State University, 1986.
70. Blankespoor, R. L.; Doyle, M. P.; Hedstrand, D. M.; Tamblyn, W. H.; Van Dyke, D. A.; J. Am. Chem. Soc. 1981, 103, 7096.
71. Sheldric, G. M. "SHELXS-86", Institute for Anorganische Chemieder Universitaf, Gottingen, F. R. G., 1986.
72. Sheldric, G. M. "SHELX-76: A Program for Crystal Structure determination", University Chemical Laboratory, Cambridge, England, 1976.
73. Beckman, D. E.; Jacobson, R. A. J. Organometallic Chem. 1979, 179, 187.
74. Bryan, R. F.; Greene, P. T. J. Chem. Soc. A 1970, 3068.
75. Dunker, J. W.; Finer, J. S.; Clardy, J.; Angelic, R. J.

- J. Organometallic Chem. 1976, C49, 114.
76. Butler, I. S.; Fenster, A. E. J. Organometallic Chem. 1974, 66, 161.
77. Ondik, H.; Smith, D. "International Tables for X-ray Crystallography" Kynoch Press: Birmingham, England, 1962, Vol. III Table 4.11, 260.
78. Udupa, M. R.; Krebs, B. Inorg. Chem. Acta 1973, 7, 271.
79. Hong, S.; Olin, A.; Herse, R. Acta Chem. Scand. 1975, A29, 583.
80. Finestone, A. B. US 2,953,545 1960; Chem. Abstr. 1961, 4045.
81. "Organosilicon and Biorganosilicon Chemistry", Sakurai, H.; Editor, John Wiley & Sons, Inc.: Somerset, N. J., 1985.
82. Hamilton, W. C.; Rudman, R.; Goldfarb, T. D.; Novic, S. J. Am. Chem. Soc. 1967, 89, 5157.
83. Turley, J. W.; Boer, F. P. J. Am. Chem. Soc. 1968, 90, 4026.
84. Hencsei, P.; Parkanyi, L. Reviews on Silicon, Germanium, Tin and Lead Compounds 1985, 8, 191-218.
85. Tandura, S. N.; Voronkov, M. G.; Alekseev, N. V. Topics in Current Chemistry 1986, 131, 99.
86. Leapman, R. D. Microbeam Analysis 1982, III.
87. Voronkov, M. G.; Dyakov, V. M.; Kirpichenko, S. V. J. Organometallic Chem 1982, 233, 1-147.
88. Brodalla, D.; Mootz, D. Angew Chem., Int. Ed. Engl. 1981, 20, 791.

## ACKNOWLEDGEMENTS

It is a great pleasure to acknowledge Professor Robert A. Jacobson for being such a good and kind supervisor to me, for sharing his expertise in crystallography, and for his careful reading and correction of this thesis. I am particularly grateful to him because I believe that I started learning through him to be a fair minded and open minded human being.

I would like to thank the former group members Jim Benson, Jim Richardson, Suelein Wang and Kim Sangsoo who helped me a great deal with the techniques in crystallography and to the current group members Yingzhong Su, Tom Hendrixson and Lance Miller.

I wish to thank Drs. Neckers, Larock, Johnson, Angelici and Verkade for providing interesting crystallographic problems.

I would like to thank Brenda, Marlene, Barbara and all my former and current group members for being nice to me and for making me feel at home.

Special thanks are due to my parents, who were so hesitant to see me leaving for a far away land, for their love and blessings.

Finally, I thank my wife Devaki for helping me with typing the most-difficult-to-type reference section and above all for her love, support and understanding.